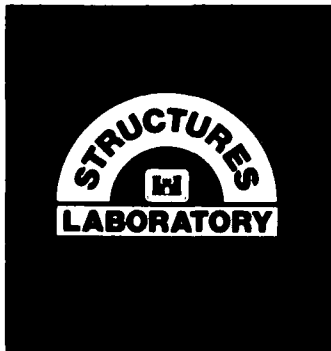
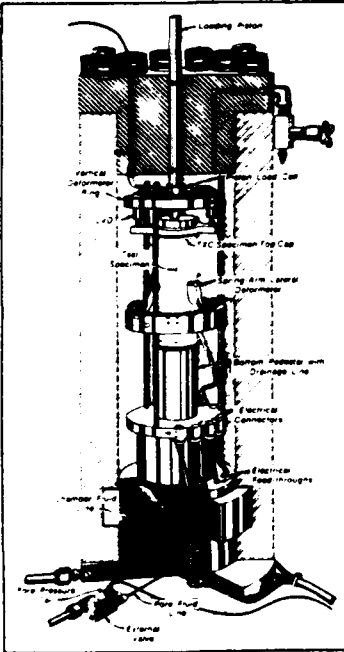
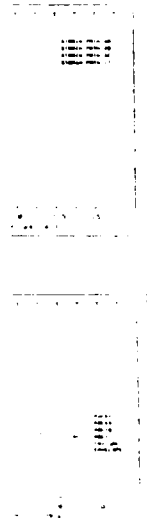




US Army Corps
of Engineers

AD-A171 468



TECHNICAL REPORT SL-86-24

2

AXISYMMETRIC STRAIN PATH TESTS ON NELLIS BASELINE SAND

by

Stephen A. Akers

Structures Laboratory

DEPARTMENT OF THE ARMY
Waterways Experiment Station, Corps of Engineers
PO Box 631, Vicksburg, Mississippi 39180-0631



September 1986

Final Report

Approved For Public Release: Distribution Unlimited

DTIC FILE COPY

DTIC
ELECTRONIC
SEP 2 1986

Prepared for Defense Nuclear Agency
Washington, DC 20305

Under DNA Task Code Y99QAXSB, Work Unit 00019

86 9 2 050
86 9 2 050

Destroy this report when no longer needed. Do not return
it to the originator.

The findings in this report are not to be construed as an official
Department of the Army position unless so designated
by other authorized documents.

The contents of this report are not to be used for
advertising, publication, or promotional purposes.
Citation of trade names does not constitute an
official endorsement or approval of the use of
such commercial products.

Unclassified
SECURITY CLASSIFICATION OF THIS PAGE

AD-A171468

REPORT DOCUMENTATION PAGE				Form Approved OMB No 0704-0188 Exp Date Jun 30 1986	
1a REPORT SECURITY CLASSIFICATION Unclassified		1b RESTRICTIVE MARKINGS			
2a SECURITY CLASSIFICATION AUTHORITY		3 DISTRIBUTION/AVAILABILITY OF REPORT Approved for public release; distribution unlimited.			
2b DECLASSIFICATION/DOWNGRADING SCHEDULE		5 MONITORING ORGANIZATION REPORT NUMBER(S)			
4 PERFORMING ORGANIZATION REPORT NUMBER(S) Technical Report SL-86-24		7a. NAME OF MONITORING ORGANIZATION			
6a. NAME OF PERFORMING ORGANIZATION USAEWES Structures Laboratory		6b. OFFICE SYMBOL (If applicable) WESSD		7b. ADDRESS (City, State, and ZIP Code)	
6c. ADDRESS (City, State, and ZIP Code) PO Box 631 Vicksburg, MS 39180-0631		9. PROCUREMENT INSTRUMENT IDENTIFICATION NUMBER			
8a. NAME OF FUNDING /SPONSORING ORGANIZATION Defense Nuclear Agency		8b. OFFICE SYMBOL (If applicable)		10. SOURCE OF FUNDING NUMBERS See reverse	
8c. ADDRESS (City, State, and ZIP Code) Washington, DC 20305		PROGRAM ELEMENT NO.	PROJECT NO.	TASK NO.	WORK UNIT ACCESSION NO.
11. TITLE (Include Security Classification) Axisymmetric Strain Path Tests on Nellis Baseline Sand					
12. PERSONAL AUTHOR(S) Akers, Stephen A.					
13a. TYPE OF REPORT Final report		13b. TIME COVERED FROM _____ TO _____		14. DATE OF REPORT (Year, Month, Day) September 1986	15. PAGE COUNT 135
16. SUPPLEMENTARY NOTATION This report was originally published as a draft report to the sponsor in October 1983.					
17. COSATI CODES			18. SUBJECT TERMS (Continue on reverse if necessary and identify by block number)		
FIELD	GROUP	SUB-GROUP	Laboratory tests Strain path tests		
			Remolded specimens Stress path tests		
			Sand with clay		
19. ABSTRACT (Continue on reverse if necessary and identify by block number)					
<p>This report documents the results of a laboratory testing program conducted by the US Army Engineer Waterways Experiment Station (WES) in which the responses of cylindrical specimens of Nellis baseline (NB) sand were measured under imposed axisymmetric strain path loadings. Two strain path shapes (designated as shapes 2 and 3) were investigated, each having three levels of strain magnitude (A, B, and C) for a total of six strain paths.</p> <p>It was found that a unique stress path was produced by following a given strain path. This was true for all of the six strain paths investigated. All of the strain path tests which followed shape 3 reached a point of continuing strain with little change in the applied stresses. These specimens appeared to be yielding or flowing as the stress path moved along a failure envelope.</p> <p>Reverse strain path tests (tests which followed a stress path generated by a previous</p>					
20 DISTRIBUTION/AVAILABILITY OF ABSTRACT <input checked="" type="checkbox"/> UNCLASSIFIED/UNLIMITED <input type="checkbox"/> SAME AS RPT <input type="checkbox"/> OTIC USERS				21 ABSTRACT SECURITY CLASSIFICATION Unclassified	
22a NAME OF RESPONSIBLE INDIVIDUAL			22b TELEPHONE (Include Area Code)		22c OFFICE SYMBOL

10. SOURCE OF FUNDING NUMBERS (Continued).

DNA Task Code Y99QAXSB, Work Unit 00019, "Test Equipment and Techniques"

19. ABSTRACT (Continued).

strain path test) proved that a unique strain path was not necessarily produced by following a given stress path. When stress paths developed by strain path shape 3 were followed, several different strain paths were produced. The resulting strain magnitudes were directly dependent upon the length of time the stress path spent moving along the failure envelope.

Results of a series of strain-rate tests indicated that the NB sand exhibited an 18 percent increase in peak stress difference when loading times were decreased from 133 to 4 minutes. These times represent the practical bounds for the WES manually controlled test system. To achieve faster strain rates, an automated system is needed.

PREFACE

The Geomechanics Division (GD), Structures Laboratory (SL), of the U.S. Army Engineer Waterways Experiment Station (WES) was funded by the Defense Nuclear Agency (DNA) to conduct a series of strain path tests on remolded specimens of Nellis Baseline sand. This research work was conducted during the period April 1983 through August 1983 and was funded under DNA Task Code Y99QAXSB, Work Unit 00019, "Test Equipment and Techniques."

The laboratory work was performed and this report was prepared by Mr. Stephen A. Akers under the general direction of Dr. J. G. Jackson, Jr., Chief, GD, and Mr. J. Q. Ehrgott, Chief, Operations Group, GD. Mr. A. E. Jackson, Jr., provided technical assistance during the test program and during the preparation of this report. Numerous technicians and aides assisted in the testing program. This report was transmitted to the sponsor in October 1983.

COL Tilford C. Creel, CE, was the Commander and Director of WES during this investigation. The previous Director of WES was COL Allen F. Grum, USA. The present Commander and Director of WES is COL Dwayne G. Lee, CE. During this investigation, Mr. Fred R. Brown was Technical Director. The present Technical Director is Dr. Robert W. Whalin. Mr. Bryant Mather is Chief, SL.



Approved For	<input checked="" type="checkbox"/>
DTIC	<input type="checkbox"/>
Code	<input type="checkbox"/>
Classification	<input type="checkbox"/>
Exemption Codes	
Author/Editor	
Reviewer	
DTIC	

AI

CONTENTS

	<u>Page</u>
PREFACE.....	1
CONVERSION FACTORS, NON-SI TO SI (METRIC) UNITS OF MEASUREMENT.....	3
CHAPTER 1 INTRODUCTION.....	4
1.1 BACKGROUND.....	4
1.2 PURPOSE AND SCOPE.....	5
CHAPTER 2 LABORATORY TESTS.....	9
2.1 COMPOSITION AND INDEX PROPERTIES FOR NELLIS BASELINE SAND.....	9
2.2 TEST EQUIPMENT.....	10
2.2.1 Test Chamber, Loader, and Pressure Console.....	10
2.2.2 Instrumentation.....	11
2.2.3 Data Acquisition.....	12
2.3 TEST SPECIMEN PREPARATION.....	12
2.4 DATA PROCESSING.....	13
2.5 HYDROSTATIC COMPRESSION (HC) TESTS.....	14
2.6 TRIAXIAL COMPRESSION (TXC) TESTS.....	15
2.7 STRAIN PATH (SP) TESTS.....	17
2.7.1 Test Procedures.....	17
2.7.2 Strain Path 3 Tests.....	19
2.7.3 Strain Path 2 Tests.....	20
2.7.4 Reverse Strain Path Tests.....	20
2.7.5 Strain-Rate Tests.....	21
CHAPTER 3 DATA ANALYSIS.....	32
3.1 HC TESTS.....	32
3.2 TXC TESTS.....	33
3.3 PHASE I SP TESTS.....	34
3.3.1. SP 3 Tests.....	34
3.3.2. SP 2 Tests.....	36
3.4 PHASE II SP TESTS.....	37
3.4.1 Reverse SP Tests.....	38
3.4.2 Strain-Rate Tests.....	39
CHAPTER 4 CONCLUSIONS AND RECOMMENDATIONS.....	67
4.1 CONCLUSIONS.....	67
4.2 RECOMMENDATIONS.....	68
REFERENCES.....	69
PLATES 1-62	

CONVERSION FACTORS, NON-SI TO SI (METRIC)
UNITS OF MEASUREMENT

Non-SI units of measurement used in this report can be converted to SI (metric) units as follows:

<u>Multiply</u>	<u>By</u>	<u>To Obtain</u>
degrees (angle)	0.01745329	radians
feet	0.3048	metres
gallons (US liquid)	3.785412	cubic decimetres (litres)
inches	2.54	centimetres
kips (force)	4.448222	kilonewtons
kips (force) per square inch	6.894757	megapascals
megatons (nuclear equivalent of TNT)	4.184	petajoules
pounds (force) per square inch	6.894757	kilopascals
pounds (mass)	0.4535924	kilograms
pounds (mass) per cubic foot	16.01846	kilograms per cubic metre

AXISYMMETRIC STRAIN PATH TESTS ON NELLIS BASELINE SAND

CHAPTER 1

INTRODUCTION

1.1 BACKGROUND

In recent years, a new approach has arisen to address predictions of ground motions resulting from the intense transient loadings produced by high-explosive (HE) and nuclear (NE) events. Based on analyses of HE and NE field event data and of ground shock calculation output, it was postulated that strain paths, or the paths traced in strain space by material elements as they deform, have shapes and magnitudes that are primarily functions of burst geometry and that are somewhat independent of the explosive source and of the medium in which or on which the explosion occurs (References 1-3). Furthermore, it has been suggested that more accurate ground shock calculations could be made if material response models were fit to stress-strain data resulting from tests along these specific strain paths rather than the data resulting from tests conducted under more conventional stress and strain boundary conditions.

The Defense Nuclear Agency (DNA) has supported efforts to define these strain paths and to acquire material response data from both field and laboratory strain path tests. The Geomechanics Division of the Structures Laboratory at the U. S. Army Engineer Waterways Experiment Station (WES), Terra Tek Research, and the University of Colorado were tasked to conduct strain path tests on remolded specimens of Nellis Baseline (NB) sand (see Section 2.1 for a description of this material). The test specimens were to have the same pretest water content and wet density. An initial prestress of 6.9 MPa was to be applied to the test specimens before conducting the strain path (SP) tests. Thus, the three laboratories would conduct tests on theoretically identical test specimens.

The University of Colorado conducted its tests in a three-dimensional (3D) triaxial test device in which the applied stresses on each of the three principal planes can be independently controlled. With its 3D equipment, the University was able to follow all three of the proposed strain path shapes (Figure 1.1). However, the laboratories at WES and Terra Tek were limited by

equipment constraints in that only axisymmetric tests on cylindrical specimens using modified triaxial compression test devices could be conducted. Therefore, only two strain path shapes were tested by WES and Terra Tek. These two shapes, identified in Figure 1.1 as strain path shapes 2 and 3, were primarily axisymmetric. When the strains deviated from axisymmetric conditions, the average of the intermediate and minor principal strains was followed.

The WES strain path test program eventually developed into two parts, identified herein as Phases I and II. The purpose of the Phase I test program was to duplicate and, in some cases, expand the test matrix conducted by Ko and Meier at the University of Colorado (Reference 4). The strain path names and some of the actual procedures developed by Ko and Meier were used by WES. WES, however, was able to conduct the tests to larger strain magnitudes. At the end of the Phase I test program, 43 tests had been completed, of which 25 were strain path tests. A summary of these tests is presented in Table 1.1.

The Phase I tests raised several questions which WES felt compelled to answer. The first question addressed "the uniqueness of stress and strain." Most soils are assumed to be stress path dependent, i.e., if tested to the same point via different stress paths, then different strains should result. However, if a single stress path was followed, one would expect a unique relationship between stress and strain. Trulio (Reference 1) suggests that this is not necessarily true; one would only observe a unique stress-strain relationship by following a common strain path. This was investigated at WES by reversing the strain path process, i.e., by following a stress path developed from one or more strain path tests. Nine of these reverse tests were conducted in the second phase of the test program (see Table 1.1).

The Phase II test program was continued by investigating strain-rate effects. A single strain path was followed in several tests; times required to follow that path ranged between 4 and 133 minutes. Five successful tests were conducted, completing the second phase of the test program (see Table 1.1).

1.2 PURPOSE AND SCOPE

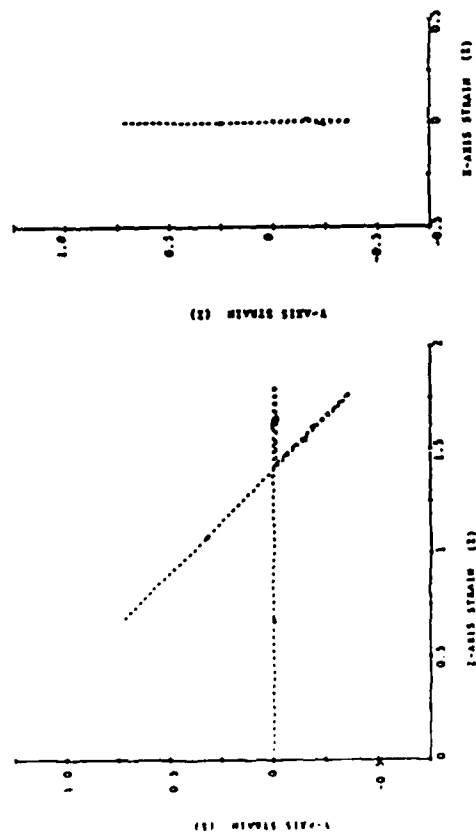
The purpose of this report is to document the WES FY 83 strain path test program conducted on remolded specimens of Nellis Baseline sand. This report (a) describes the test equipment, (b) documents the test procedures, (c) presents the test data, and (d) presents an analysis of the test results.

Chapter 2 covers items (a) through (c); the analysis, item (d) above, is presented in Chapter 3. Chapter 4 presents conclusions and provides recommendations for further testing.

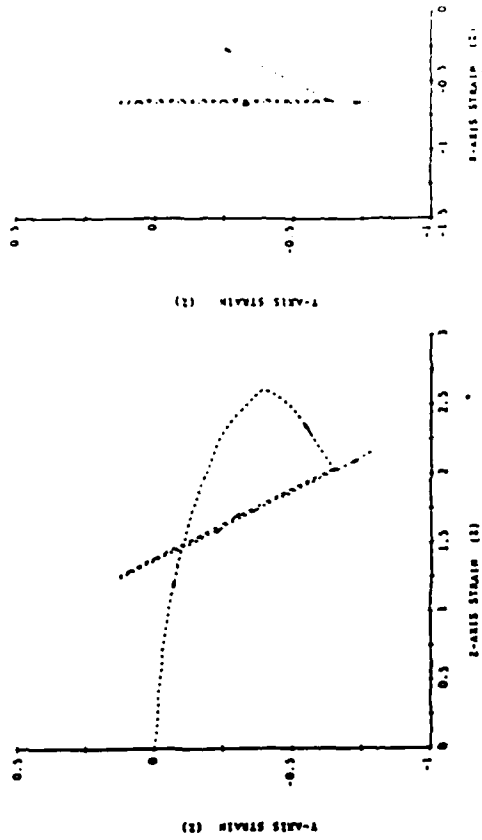
Table 1.1 Completed Test Program

<u>Test Type</u>	<u>Number of Tests</u>
<u>Phase I: Planned Investigation</u>	
Hydrostatic compression (HC)	10
Triaxial compression (TXC)	5
Strain path (SP) 3A	7
Strain path (SP) 3B	3
Strain path (SP) 3C	3
Strain path (SP) 2A	5
Strain path (SP) 2B	4
Strain path (SP) 2C	3
Tests from which no valuable data were obtained	<u>3</u>
TOTAL	43
<u>Phase II: Special Investigation</u>	
Reverse strain path test SP2C	4
Reverse strain path test SP3B	5
Strain rate test SP3A	5
Other tests (HC)	2
Tests from which no valuable data were obtained	<u>1</u>
TOTAL	17

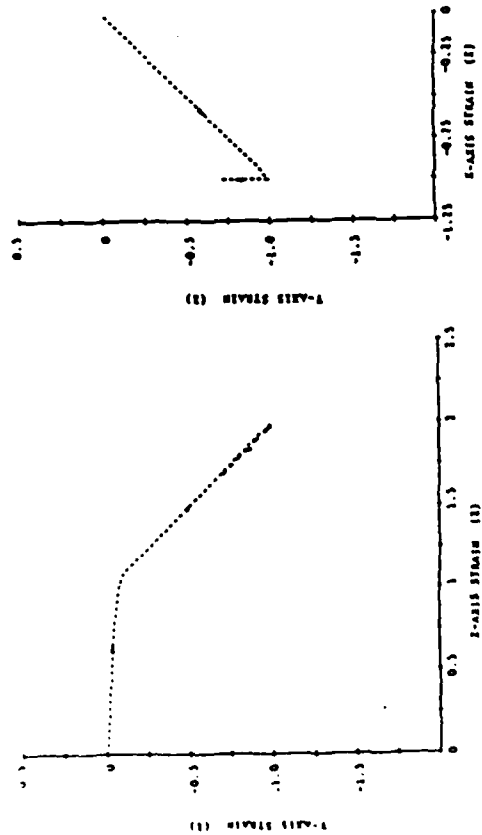
a. STRAIN PATH 1



b. STRAIN PATH 2



c. STRAIN PATH 3



NOTE: COMPRESSION IS POSITIVE.

Figure 1.1 Shapes of strain paths 1, 2, and 3 (from Reference 4).

CHAPTER 2
LABORATORY TESTS

2.1 COMPOSITION AND INDEX PROPERTIES
FOR NELLIS BASELINE SAND

The NB sand used in this test program was reconstructed from soil materials found within Ralston Valley, Nevada. The reconstruction process involved separating the host material according to grain size and recombining the parts to obtain a specified gradation. This new gradation approximated that of soils typically found in the southeastern part of Ralston Valley within the confines of Nellis Air Force Base.

Four separate batches of NB sand were reconstructed by different personnel at different times over an 8-month period. Ideally, the four batches should have had identical gradations and physical properties. To establish the variability or lack thereof among these four batches of soil, eight representative samples were taken and tested to determine their grain-size distributions, specific gravities, and Atterberg limits. The results of these tests are summarized in Table 2.1. The table also lists the mean and standard deviation values for the percentages of material passing each sieve size and the mean values of liquid and plastic limits, plasticity index, and specific gravity.

All four batches of NB sand were classified by the Unified Soil Classification System (Reference 5) as brown sand with clay (SW-SC). Two empirical gradation parameters, the coefficient of uniformity C_u and the coefficient of curvature C_c , were calculated to have average values of 13.2 and 1.0, respectively.

From each batch of air-dried NB sand, smaller amounts of material were taken and mixed with water to obtain a desired water content of approximately 6 percent. These materials were placed in plastic bags, sealed, and then placed in numbered cans for shipment and/or storage.

Test specimens for the WES strain path tests were constructed of material obtained from cans numbered 18, 24, 26, 29, and 30. The soil in can 18 was taken from batch 2 materials, whereas the soil in the remaining cans was mixed from batch 3 materials. Table 2.1 shows that the soil in can 18 contained slightly more fines and had a higher plasticity index than the soil in the

other four cans. These differences, although apparently insignificant, caused some variations in the responses of specimens prepared from can 18 material (described in Chapter 4). However, the variability in this material is minimal in light of the variability normally observed in undisturbed soil specimens.

The height, diameter, and weight of each test specimen were recorded prior to testing. Posttest water contents were also obtained for each test specimen except for those contaminated by oil due to membrane leakage. Based on these data and a specific gravity of 2.62, values of dry density, void ratio, degree of saturation, and volumes of air, water, and solids were calculated. These values are listed in Table 2.2 along with data plate numbers, the type of test conducted, and the can number from which specimen material was obtained.

2.2 TEST EQUIPMENT

The equipment used in this test program is not typically found in geotechnical laboratories. Therefore, a brief description of this equipment is provided.

2.2.1 Test Chamber, Loader, and Pressure Console

The chamber used in this test program was designed for static high-pressure and high-load applications--approximately 70 MPa and 44.5 kN, respectively. It can be used to conduct drained or undrained hydrostatic compression (HC), triaxial compression (TXC), triaxial extension (TXE), or uniaxial strain (UX) tests. The chamber also has pore pressure and back pressure saturation capabilities. The test specimens in this experimental program were partially saturated with degrees of saturation between 25 and 33 percent. All tests were conducted under undrained conditions; i.e., the air and water were not allowed to drain from the specimen.

A pressure console supplied a regulated fluid pressure to the chamber using hydraulic oil as a confining fluid. This console has low, intermediate, and high pressure ranges (0-0.69 MPa, 0-14 MPa, and 0-70 MPa, respectively), using house air, bottled nitrogen, and a hydraulic pump, respectively, as pressure sources. Bottled nitrogen was used for all tests reported herein with the exception of the high-pressure HC tests.

A strain-controlled compression testing machine was used to displace the loading piston and, thus, axially deform the test specimens. The loader has a capacity of 89 kN under stepwise variable deformation rates between 0.0005 and 50 mm/min. It can be used to both load and unload test specimens at a constant deformation rate.

2.2.2 Instrumentation

Within the test chamber, two vertical deformeters and one lateral deformer were used to measure specimen deformations. The three deformeters were fixed in space relative to the base of the test specimen. The lateral deformer was positioned to measure the midheight lateral movements of the specimen. Two linear variable differential transducers (LVDT's) mounted 180 degrees apart in a vertical orientation measured the vertical displacement of the specimen top cap. These LVDT's have a maximum range of 8.9 mm.

Two different lateral deformeters were used in the test program to monitor lateral displacements. One deformer had three LVDT's mounted 120 degrees apart in a horizontal orientation. The LVDT cores were spring-loaded and contacted the rubber membrane inclosing the test specimen (see Section 2.3). The output of the individual LVDT's was electrically summed to produce a single output. The maximum range of this deformer was ± 1 -mm change in diameter.

The second lateral deformer had four strain-gage-mounted spring-steel arms located 90 degrees apart around an aluminum ring. These arms contacted the sides of the specimen (inclosed in the rubber membrane) and deflected as the specimen deformed. The individual outputs from each arm were electrically summed to produce one output from the gage. The maximum range of this gage was ± 5 -mm change in diameter.

A filmpot was used when vertical deformations exceeded the calibrated range of the two vertical deformeters. The filmpot was located outside of the test chamber and measured the displacement of the axial loading piston relative to the chamber. It provided an indirect measurement of the specimen's vertical deformation only when the test specimen was deformed with the loading piston. Some engineering judgment was required to determine when the piston was in contact with the specimen and, thus, when the filmpot could be used for vertical measurements.

Vertical loads were measured by a load cell mounted on the end of the loading piston. Since the load cell was contained within the test chamber, no corrections for piston friction were necessary. The load cell had a capacity of 44.5 kN.

Two different pressure cells were used to measure the fluid pressure within the test chamber. A 14-MPa pressure cell was used in all of the tests except for the high-pressure HC tests. For these high pressure tests, a 70-MPa pressure cell was used.

2.2.3 Data Acquisition

A programmable data acquisition system was used to measure, convert, output, and store test data. The system components included a controller, voltmeter, scanner, and X-Y plotter. The analog signals of the six transducers (three for vertical deflection, one for lateral deflection, one for load, and one for pressure) were monitored by the system at a selected time interval. These signals were digitized by the voltmeter, converted to displacements, forces, or pressures by the controller, and then output to a CRT screen and paper printer and stored on magnetic tape.

During the SP tests, the controller also calculated vertical and lateral stresses and strains. These variables were then plotted on the X-Y plotter as lateral strain versus vertical strain and as vertical stress versus lateral stress. The plotter was stationed next to the pressure console and loader and enabled the engineer conducting the test to observe the real time stress and strain paths. The system was also used to reprocess and plot all of the test data. The strain path tests could not have been conducted if this system were not available.

2.3 TEST SPECIMEN PREPARATION

In this test program, all specimens were constructed by jacking the soil material into a steel mold. This process produced consistent, high-quality specimens. All test specimens were constructed and tested sequentially, usually the same day.

Each test specimen was constructed in five 2.54-cm-high lifts, with each lift compacted to the desired density of 1.9 g/cc. Material for each lift was weighed, spooned into the steel mold, and jacked to the correct height. Before placing the next lift, the surface was scarified to ensure adequate

bonding between lifts. After five lifts were compacted, the specimen was jacked out of the mold, weighed, and measured. The specimen was then encased in two 0.64-mm-thick rubber membranes with a top cap and bottom pedestal. The membranes were sealed to the end caps with rubber bands and covered with a synthetic rubber coating. This coating prevented the degradation of the membranes by the hydraulic oil. The average height and diameter of the specimens were 12.8 and 5.4 cm, respectively.

At this point, the specimen was set into the bottom section of the test chamber and the vertical and lateral deformeters were put in place around the specimen. Each of the three deformeters was offset to ensure that the displacements would be within its calibrated range. The top of the test chamber was secured, the chamber filled with oil, the piston seated onto the specimen top cap, and the amplifiers of the six transducers were zeroed. From this point in time, all pressures, displacements, and loads were measured.

Starting with test specimen NBSP17, the loads required to compact each lift of a test specimen were measured with a 31-kN-capacity proving ring. In some cases, the capacity of the proving ring was approached and the remaining lift or lifts were compacted without the proving ring. These measurements gave the first clue that the soil material in can 18 was different from that in the other cans. For specimens prepared from can 18 material, the measured loads were significantly lower than specimens prepared from materials in the other cans.

2.4 DATA PROCESSING

For this report, all compressive stresses and strains are positive. All strains were calculated as engineering strains using the pretest specimen height and diameter. Axial strains were calculated from the average displacements of the two vertical deformeters. For tests in which displacements approached the maximum calibrated range of the internally-mounted vertical deformeters, the displacements were measured by the filmpot. Lateral displacements were measured with one of the two lateral deformeters.

The actual measurement of lateral deformations at the specimen midheight permits the calculation of an accurate specimen cross-sectional area. The cross-sectional area at any time during the test is calculated as

$$A = A_0 (1 - \epsilon_r)^2$$

where A_0 is the original pretest specimen area and ϵ_r is the calculated lateral strain. No corrections were made to account for membrane deflection.* The measured piston load was divided by the specimen cross-sectional area to calculate principal stress difference.

Volumetric strains were calculated from deformer measurements, assuming either a uniform cylinder or truncated cone deformed specimen shape. The uniform cylinder approximation assumes the specimen deforms as a right circular cylinder. The current diameter of the specimen (i.e., the original diameter minus the change in diameter) is assumed to exist over the entire length of the specimen. The truncated cone approximation assumes the current diameter is measured at the specimen's midheight and that it changes linearly to the original pretest diameter at the ends of the specimen. All second-order terms were included in the calculations of volumetric strain. The uniform shape assumption approximates the true volumetric strains more accurately during hydrostatic compression and at small axial strains during shear. The truncated cone assumption approximates the true volumetric strains more accurately during shear at larger axial strains, i.e., $\epsilon_a > 7-8$ percent. The true volumetric strains are somewhere intermediate between these two calculated values (Reference 6).

Data measurements were started at a zero stress-zero strain state and were continued until the end of the desired loading. Most of the figures presented herein include the imposed stresses and strains that occurred during hydrostatic compression. The only exceptions are the strain path plots in which the vertical and lateral strains during hydrostatic compression were zeroed out. The strain path was initiated when the vertical stress exceeded the lateral stress.

2.5 HYDROSTATIC COMPRESSION (HC) TESTS

Each test conducted in this test program was subjected to an HC loading, either entirely or as a first step to a subsequent shear loading. In an HC

* Previous measurements have shown that two 0.64-mm-thick membranes deflect only 0.0013 mm at a pressure of 7 MPa, or about 0.02 percent lateral strain.

test, the specimen is subjected to a uniform fluid loading that produces both vertical and lateral deformations. In this test program, the fluid pressure was gradually increased or decreased to the desired stress levels. The measured pressures and displacements were converted to values of mean normal stress and volumetric strain (see Section 2.4). The slope of the mean normal stress versus volumetric strain curve at any point is the bulk modulus K of the material at that point. The data may also be presented as mean normal stress versus both lateral and vertical strains. From this plot one can discern the isotropic or anisotropic response of the material.

HC data were obtained from 12 tests conducted in Phases I and II. Seven of the twelve tests were planned HC tests. The remaining five tests were planned as either SP or TXC tests, but the only meaningful data obtained were the HC data.

Starting with test NBSP26 and continuing through the entire test program until test NBSP58, an unloading-reloading cycle was incorporated into the hydrostatic loading. The pressure was unloaded at 0.75 MPa down to 0.14 MPa and then increased to the desired stress level. This cycle was designed to simulate the Ko and Meier data (Reference 7). Due to equipment limitations, this cycle could not be incorporated into the loading history of the high pressure HC tests.

For each of the 12 HC tests, the data were plotted as mean normal stress versus volumetric strain (cone and uniform) and are presented in Plates 1-12. For the HC tests conducted to pressures greater than 7 MPa, the test data were also plotted as mean normal stress versus both vertical and lateral strain; these plots are presented in Plates 13-19.

Table 2.3 is presented to inform the reader about problems encountered, observations made, and thought processes involved in conducting these tests. This table lists the test number and data plate numbers, identifies the type of test conducted, and lists pertinent test notes for each of the 60 test specimens constructed. For example, if the notes indicate that the membrane leaked during hydrostatic loading, the reader should understand that no strain path or TX shear data are available.

2.6 TRIAXIAL COMPRESSION (TXC) TESTS

All TXC tests conducted in this test program were unconsolidated-undrained tests. Theoretically, if the test specimen cannot drain, it cannot

be consolidated. However, these test specimens were not saturated, so they did compact during the application of confining pressure (see Section 2.5).

In general, a TXC test is hydrostatically loaded to some desired stress level prior to shear loading. Upon obtaining this stress level, the lateral stress is held constant, and the vertical stress is increased. If desired, unloading and reloading cycles can be included in the test. During the test, the vertical and lateral deformations, axial loads, and confining pressures are recorded. From these measurements, values of principal stress difference, mean normal stress, axial strain, lateral strain, principal strain difference, and volumetric strain can be calculated.

A TXC test provides data necessary to establish strength properties of a given material. The test data can be plotted as principal stress difference versus axial strain, in which case the slope of the curve is the Young's modulus E . The test data can also be plotted as principal stress difference versus principal strain difference, the slope of which is twice the shear modulus G .

In general, the principal stress difference at failure is a function of the initial confining pressure imposed upon the test specimen. At WES, failure is defined as either the peak value of stress difference or the stress difference at 15 percent axial strain during shear, whichever occurs first (Reference 8). A failure relationship, usually referred to as the failure envelope, may be developed by plotting principal stress difference at failure versus mean normal stress at failure. Several tests at different initial confining pressures are needed to develop this relationship.

Five TXC tests were conducted in this test program. Each test specimen was hydrostatically loaded to 6.9 MPa and then axially loaded to either 15 percent axial strain or until the maximum capacity of the load cell was reached. Test NBSP26 was the only exception to the above. During this test, the filmpot was disabled. Therefore, the test was conducted to the maximum calibrated range of the two internally-mounted vertical deformeters.

The five TXC tests were conducted using the spring-arm lateral deformer. Each of the tests was conducted at a constant strain rate and had at least one unload-reload cycle. Table 2.3 contains further test notes related to the TXC tests.

The data from these five TXC tests are presented as 4-corner plots in Plates 20-24. These plots permit the stress-strain state at any time during

the test to be determined. Proceeding clockwise from the upper left corner, the plots are (a) principal stress difference versus mean normal stress, (b) principal stress difference versus principal strain difference (solid line) and principal stress difference versus total axial strain (dashed line), (c) volumetric strain versus principal strain difference for the uniform (solid line) and truncated cone (dashed line) assumed shapes, and (d) volumetric strain versus mean normal stress for both shape assumptions. The start of the test, the end of the test, and the beginning of shear are identified on each data plate by the symbols A, E, and B, respectively.

2.7 STRAIN PATH (SP) TESTS

As described in the introduction, the strain path test program developed into two parts, Phase I and Phase II. Forty-three tests were conducted in the Phase I test program, twenty-five of which were strain path tests. Two strain path shapes were investigated (2 and 3), each having three levels of strain magnitude (A, B, and C) for a total of six strain paths. These six paths are presented in Figures 2.1 and 2.2. At least three replications per individual strain path were conducted.

Seventeen tests were conducted in the Phase II test program, fourteen of which were completed as strain path tests. This second phase of testing addressed the question of "the uniqueness of stress and strain." Having found in the Phase I tests that following a single strain path generated a unique stress path, WES conducted tests NBSP44-54 to investigate the reverse process; i.e., if a single stress path was followed, would a unique strain path be generated?

For a similar reason, tests NBSP55-60 were conducted to see if strain rate affected the output stress path. These five tests were conducted at four different strain rates.

The strain path test program is documented in more detail in the following subsections. The subsections present or describe changes in test procedures required by the SP 3 tests, the SP 2 tests, the reverse tests, and the strain-rate tests.

2.7.1 Test Procedures

Specimens for the SP tests, like the TXC tests, were all subjected to an initial 6.9-MPa hydrostatic loading. Beginning with test NBSP26, an

unload-reload cycle was incorporated into the hydrostatic loading (see Section 2.5). The HC portion of the test took approximately 5 to 6 minutes. In general, the actual SP test was completed in approximately 30 minutes. In specific cases a different time was required. These times are documented in the appropriate subsection below. Of course, the time and the strain magnitudes dictated the strain rates. In most tests, the strain rate was kept constant during the loading (increasing vertical strain), then stepped up slightly during the unloading (decreasing vertical strain).

At the end of hydrostatic loading (i.e., when 6.9 MPa was reached), several procedures were performed. First, the loading piston was again placed in contact with the top cap. During hydrostatic loading, the test specimen underwent vertical deformation while the loading piston remained stationary. Second, the data acquisition system was instructed to rezero the lateral and vertical strains and to plot all subsequent stresses and strains in the form of stress and strain paths. After this, the loader was started at the desired deformation rate, deforming the specimen in the vertical direction.

The intent now was to control the test such that the resulting strain path plotted directly on top of the preselected (i.e., the intended) strain path. After each scan of the data acquisition system, the resulting stress and strain increments were plotted. A typical plot of the output stress and strain path data is illustrated in Figure 2.3. Figure 2.3a is the strain path plot for test NBSPl2 plotted over the intended path 3A. Figure 2.3b is the corresponding stress path, starting from the end of hydrostatic loading when the vertical and lateral stresses were approximately 6.9 MPa (1 ksi).

The vertical strains were controlled primarily by the loader. Thus, one was assured of increasing vertical strains if the loader was compressing the test specimen. The lateral strains were controlled by manually adjusting the confining pressure, i.e., the pressure was increased to get positive lateral strains and decreased to get negative lateral strains. To reverse the direction of vertical strain, the loader had to be stopped, reversed, and then restarted. At this point, the strain rate was usually increased by a factor of 1-1/2 to 2.

Several important observations were made during the early part of the test program and, in some cases, these observations changed subsequent test procedures. The most important change involved switching from the spring-arm lateral deformer to the LVDT lateral deformer. As illustrated in

Figure 2.4, the spring-arm lateral deformer gave a very noisy, erratic signal at these small strains. It also measured large (relative to the total strain path) negative lateral strains at the start of the SP test. The LVDT lateral deformer had much better resolution at these small strains and the problem of large initial negative lateral strains was omitted.

The introduction of the LVDT lateral deformer enabled another potential problem to be found. With approximately one quarter of the tests completed, it was observed that the lateral strains were increasing after the 6.9-MPa stress level had been obtained. In other words, the test specimens were creeping in the lateral direction, causing the strain paths to move up relative to the intended strain paths. This required additional confining pressure to be relieved before the strain path was brought back onto the intended path. This problem was solved by allowing enough time to lapse between the end of hydrostatic loading and the start of the SP test so that the lateral strains could reach equilibrium.

Vertical specimen creep was observed during the reversal of strain directions. Even though the loader was physically unloading the test specimen, the vertical strains were observed to increase. It is possible that this occurred because the creep strain rate was greater than the unloading strain rate.

One final item that should be emphasized is the data acquisition process. The use of 5-second scan intervals and 500 data points per test helped to produce the high-quality results reported herein. In most cases, the 5-second scanning rate prevented the engineer from getting too far off the intended strain path. The 500 data points provided more than enough resolution in the real-time strain path and in the data plots. Changes in test procedures required to perform the reverse and strain-rate tests are described later.

2.7.2 Strain Path 3 Tests

The first strain path test attempted was test NBSP07, which followed the SP 3A strain path shape. This test was prematurely terminated by a power failure (see Table 2.3). This and the next three tests must be considered trial tests. During these tests, the engineer obtained a "feel" for the equipment, i.e., how much to increase or decrease the pressure in order to move the strain path, when to start unloading the test specimen, and when to

increase or decrease the strain rate. Test NBSP11 was the first test in which good control was maintained.

Test NBSP10 was the first test to use the LVDT lateral deformer; the spring-arm lateral deformer had been used in the three previous tests. The data in Figure 2.4 illustrates the improvement in control brought about by switching to the LVDT lateral deformer.

Thirteen tests were conducted following strain path shape 3 with seven tests following SP 3A (including the four trial tests), three tests following SP 3C, and three tests following SP 3B. The tests were numbered and are presented in chronological order. The data from these tests are presented in Plates 25-36. Table 2.3 contains pertinent test notes.

In the plates, a modified version of the TXC 4-corner plot is used to present the strain path test results. The plot of volumetric strain versus mean normal stress (lower left corner) was replaced with a plot of the strain paths. Both the intended strain path (dashed line) and the actual test strain path (solid line) are presented in this plot. The start and end of the test and the start of the strain path loading are identified on the plates by the symbols A, E, and B, respectively. Note that the lower left plot (i.e., the strain path plot) starts at point B.

Corresponding points on the 4-corner plots, i.e., the filled-in symbols, are numbered in chronological order and were selected to identify points of interest in the test. These points provide an indication of the change in stress required to produce a corresponding change in strain. In the upper right corner plot, corresponding points on each curve are horizontally across from each other. In the lower right corner plot, the corresponding points on the two curves are vertically above or below each other.

2.7.3 Strain Path 2 Tests

Twelve tests were conducted following the strain path shape 2 with five tests following SP 2A, three following SP 2C, and four following SP 2B; test NBSP23 was the first attempt to follow SP 2A. The data from these 12 tests are presented in Plates 37-48. Modified 4-corner plots were again used to present the data. Table 2.3 contains pertinent test notes.

2.7.4 Reverse Strain Path Tests

The second phase of this test program was designed to investigate the uniqueness of stress and strain. To this end, reverse strain path tests were

conducted to prove or disprove the statement: "if a single stress path is followed, then a unique strain path will be obtained." These tests were conducted by following either a single stress path or an average stress path which had been generated from several strain path tests.

Nine tests were successfully completed in this part of the test program. The first reverse test, NBSP44, followed a stress path generated from the results of three tests which followed SP 3B. The stress paths from these three tests (NBSP20, 21, and 22) were analyzed collectively and an interpreted "average" stress path was produced. In a similar manner, the stress path in test NBSP46 was generated and followed using the data from three SP 2C tests, i.e., NBSP33, 34, and 35. The data from these two tests are presented in Plates 49 and 50. On the data plates for the reverse tests, the expected strain path, i.e., the strain path used to generate the stress path, is presented in the lower left corner.

The results from tests NBSP44 and 46 were disappointing. It was thought that the resulting strain paths would be much closer to the expected strain paths. The differences were finally attributed to the slight variations in material response observed between test specimens remolded from material obtained from different cans (see Section 2.1). To solve this problem, a single strain path test was conducted, after which the reverse tests were performed. All these latter tests were conducted on material obtained from the same can.

Test NBSP47 was conducted following SP 2C. Its stress path was digitized, and it in turn was followed in tests NBSP48 and 49. The data from these three tests are presented in Plates 51-53. In a similar manner, test NBSP51 was conducted following SP 3B. The stress path from this test was then digitized and followed in tests NBSP52, 53, and 54. The data from the latter four tests, presented in Plates 54-57, disproved the statement presented in the introduction of this subsection. These test results are described and analyzed further in Section 3.4.1.

2.7.5 Strain-Rate Tests

The strain-rate tests were conducted in order to investigate the effects of strain rate on the measured stress paths. Five tests were successfully completed at four different deformation rates while following SP 3A. The test specimens were first hydrostatically loaded in the usual time (5-6

minutes) and then deformed at a constant deformation rate to the point of strain reversal. After reversing the strain direction, the deformation rate was either increased or left the same. The times required to complete the five tests NBSP55, 56, 57, 59, and 60 were 30, 12, 5, 4, and 133 minutes, respectively. The results from these tests are presented in Plates 58-62 and are described and analyzed further in Section 3.4.2.

Table 2.1 Gradation and Index Test Results for Nellis Baseline Sand

Sample No.	Batch No.	Percent Finer By Weight											Liquid Limit LL	Plastic Limit PL	Plasticity Index PI	Specific Gravity G _s	
		#4	#6	#10	#16	#20	#30	#40	#50	#70	#100	#140					#200
1	1	98.3	91.4	77.6	63.8	55.3	47.5	39.7	32.3	24.6	17.3	11.9	9.7	23	14	9	2.62
2	1	97.7	89.4	74.9	59.9	51.5	43.9	36.7	29.9	23.1	16.6	11.1	10.1	21	14	7	2.62
3	1	97.6	89.0	74.3	60.3	51.7	44.2	36.7	30.1	23.5	17.5	12.8	11.0	22	14	8	2.62
4	2	98.8	88.7	72.5	58.1	50.1	42.1	34.2	27.7	20.8	15.6	12.1	11.0	25	13	12	2.62
5	3	99.1	81.3	60.9	50.3	43.9	37.5	31.6	23.4	16.8	10.5	7.5	7.0	22	15	7	2.61
6	3	99.1	84.4	67.1	57.1	50.3	44.0	36.6	27.1	19.4	12.0	8.5	8.0	20	16	4	2.60
8	4	99.3	92.7	78.9	67.1	58.8	50.6	42.8	35.1	26.3	17.2	12.3	11.2	19	12	7	2.62
9	4	99.7	90.8	73.2	60.3	51.4	42.7	35.1	27.7	19.9	12.2	9.3	8.6	21	14	7	2.62
	Mean	98.7	88.5	72.4	59.6	51.6	44.1	36.7	29.2	21.8	14.9	10.7	9.6	22	14	8	2.62
	Standard Deviation	0.8	3.8	5.9	4.9	4.3	3.8	3.4	3.6	3.1	2.8	2.0	1.6				

$D_{10} = 0.085$ $C_u = 13.2$
 $D_{30} = 0.305$ $C_c = 1.0$
 $D_{60} = 1.12$

NOTE: The materials in can 18 originated from batch 2. The materials in cans 24, 26, 29, and 30 originated from batch 3.

Table 2.2 Test Specimen Composition Properties

Test No.	Plate No.	Type of Test	Can No.	Wet Density γ_s , g/cc	Water Content w , %	Dry Density γ_d , g/cc	Void Ratio e	Degree of Saturation S_r , %	Volumes of		
									Air V_a , %	Solids V_s , %	Water V_w , %
NBSP01	1, 13	HC	30	1.857	*	---	---	---	---	---	---
NBSP02	2, 14	HC	30	1.877	5.45	1.780	0.472	30.3	22.4	67.9	9.7
NBSP03	---	NG	30	1.872	*	---	---	---	---	---	---
NBSP04	3, 15	HC	30	1.881	4.41	1.802	0.454	25.4	23.3	68.8	7.9
NBSP05	20	TXC	30	1.886	4.38	1.807	0.450	25.5	23.1	69.0	7.9
NBSP06	21	TXC	18	1.897	5.55	1.797	0.458	31.8	21.4	68.6	10.0
NBSP07	25	SP3A	30	1.898	5.44	1.800	0.455	31.3	21.5	68.7	9.8
NBSP08	---	NG	30	1.904	5.43	1.806	0.451	31.6	21.3	68.9	9.8
NBSP09	26	SP3A	30	1.914	5.43	1.815	0.443	32.1	20.9	69.3	9.8
NBSP10	27	SP3A	30	1.907	5.56	1.807	0.450	32.4	21.0	69.0	10.0
NBSP11	28	SP3A	30	1.892	5.40	1.795	0.460	30.8	21.8	68.5	9.7
NBSP12	29	SP3A	30	1.895	5.41	1.798	0.457	31.0	21.7	68.6	9.7
NBSP13	30	SP3A	30	1.905	5.41	1.807	0.450	31.5	21.2	69.0	9.8
NBSP14	31	SP3C	18	1.907	4.25	1.829	0.432	25.8	22.4	69.8	7.8
NBSP15	32	SP3C	18	1.904	4.06	1.830	0.432	24.6	22.7	69.8	7.5
NBSP16	33	SP3C	18	1.915	5.61	1.813	0.445	33.0	20.6	69.2	10.2
NBSP17	4	HC	18	1.905	*	---	---	---	---	---	---
NBSP18	---	NG	18	1.920	5.39	1.822	0.438	32.2	20.6	69.5	9.9
NBSP19	5	HC	18	1.912	*	---	---	---	---	---	---
NBSP20	34	SP3B	18	1.915	5.63	1.813	0.445	33.1	20.6	69.2	10.2
NBSP21	35	SP3B	18	1.908	5.45	1.809	0.448	31.9	21.1	69.1	9.8
NBSP22	36	SP3B	18	1.912	5.35	1.815	0.444	31.6	21.0	69.3	9.7
NBSP23	37	SP2A	18	1.906	5.46	1.807	0.450	31.8	21.2	69.0	9.8
NBSP24	38	SP2A	18	1.917	5.52	1.817	0.442	32.7	20.6	69.3	10.1
NBSP25	39	SP2A	18	1.906	5.54	1.806	0.451	32.2	21.1	68.9	10.0
NBSP26	22	TXC	18	1.894	5.57	1.794	0.460	31.7	21.5	68.5	10.0
NBSP27	23	TXC	18	1.896	5.64	1.795	0.460	32.1	21.4	68.5	10.1
NBSP28	6, 16	HC	18	1.902	5.53	1.802	0.454	31.9	21.2	68.8	10.0
NBSP29	---	NG	18	1.896	*	---	---	---	---	---	---
NBSP30	7, 17	HC	18	1.892	*	---	---	---	---	---	---

* Membrane leaked; no posttest water content was obtained.

(Continued)

Table 2.2 (Concluded)

Test No.	Plate No.	Type of Test	Can No.	Wet Density γ_s , g/cc	Water Content w , %	Dry Density γ_d , g/cc	Void Ratio e	Degree of Saturation S_r , %	Volume of		
									Air V_a , %	Solids V_s , %	Water V_w , %
NBSP31	40	SP2A	24	1.901	5.31	1.805	0.451	30.8	21.5	68.9	9.6
NBSP32	41	SP2A	29	1.896	5.34	1.800	0.456	30.7	21.7	68.7	9.6
NBSP33	42	SP2C	29	1.888	5.38	1.792	0.462	30.5	22.0	68.4	9.6
NBSP34	43	SP2C	29	1.886	5.31	1.791	0.463	30.1	22.1	68.4	9.5
NBSP35	44	SP2C	29	1.898	5.41	1.801	0.455	31.1	21.5	68.7	9.8
NBSP36	8	HC	29	1.893	5.15	1.800	0.455	29.6	22.0	68.7	9.3
NBSP37	45	SP2B	29	1.892	5.34	1.796	0.459	30.5	21.9	68.6	9.5
NBSP38	46	SP2B	29	1.898	5.39	1.801	0.455	31.1	21.6	68.7	9.7
NBSP39	47	SP2B	29	1.902	5.46	1.804	0.453	31.6	21.3	68.8	9.9
NBSP40	48	SP2B	29	1.893	5.33	1.797	0.458	30.5	21.8	68.6	9.6
NBSP41	9, 18	HC	29	1.893	5.43	1.796	0.459	31.0	21.7	68.5	9.8
NBSP42	10, 19	HC	29	1.889	5.42	1.792	0.462	30.7	21.9	68.4	9.7
NBSP43	24	TXC	29	1.897	5.41	1.800	0.456	31.1	21.6	68.7	9.7
NBSP44	49	SP3B**	24	1.891	5.23	1.797	0.458	29.9	22.0	68.6	9.4
NBSP45	---	HC	24	1.895	5.24	1.801	0.455	30.2	21.8	68.7	9.5
NBSP46	50	SP2C**	24	1.908	5.38	1.811	0.447	31.5	21.2	69.1	9.7
NBSP47	51	SP2C	24	1.900	5.30	1.804	0.452	30.7	21.6	68.9	9.5
NBSP48	52	SP2C**	24	1.891	5.25	1.797	0.458	30.0	22.0	68.6	9.4
NBSP49	53	SP2C*	24	1.901	5.15	1.808	0.449	30.0	21.7	69.0	9.3
NBSP50	11	HC	24	1.894	5.30	1.799	0.457	30.4	21.8	68.7	9.5
NBSP51	54	SP3B	24	1.897	5.24	1.803	0.453	30.3	21.8	68.8	9.4
NBSP52	55	SP3B	24	1.901	5.08	1.809	0.448	29.7	21.8	69.1	9.1
NBSP53	56	SP3B	24	1.901	5.01	1.810	0.447	29.3	21.8	69.1	9.1
NBSP54	57	SP3B	24	1.895	5.10	1.803	0.453	29.5	22.0	68.8	9.2
NBSP55	58	SP3A†	26	1.891	5.07	1.800	0.456	29.1	22.2	68.7	9.1
NBSP56	59	SP3A†	26	1.895	5.06	1.804	0.453	29.3	22.0	68.8	9.2
NBSP57	60	SP3A†	26	1.901	4.88	1.812	0.445	28.7	22.0	69.2	8.8
NBSP58	12	HC	26	1.895	*	---	---	---	---	---	---
NBSP59	61	SP3A†	26	1.900	5.13	1.807	0.450	29.9	21.7	69.0	9.3
NBSP60	62	SP3A†	26	1.894	5.01	1.804	0.453	29.0	22.1	68.8	9.1

* Membrane leaked; no posttest water content was obtained.

** Reverse tests.

† Strain-rate tests.

Table 2.3 Test Notes

Test No.	Place No.	Type of Test*	Test Notes
NBSP01	1, 13	HC	Membrane leaked at 10.7 MPa. Spring-arm lateral deformer used.
NBSP02	2, 14	HC	Pressure cycled at 13.8 and 27.6 MPa; unloaded to 3.4 MPa.
NBSP03	---	HC(NG)	Membrane leaked at 3.8 MPa.
NBSP04	3, 15	HC	Pressure cycled at 13.8 and 27.6 MPa; unloaded to 3.4 MPa.
NBSP05	20	TXC	Deformation rate too high at the start of test. Decreased after three readings (15 seconds). Load cycled twice.
NBSP06	21	TXC	Load cycled at a vertical stress of 13.8 MPa.
NBSP07	25	SP3A	First strain path test attempted. Test terminated due to power failure. Spring-arm lateral deformer used.
NBSP08	---	SP3A(NG)	No valuable data recorded.
NBSP09	26	SP3A	First completed strain path test.
NBSP10	27	SP3A	Changed to LVDT lateral deformer. Power failure terminated test.
NBSP11	28	SP3A	Data acquisition system hung up. Test terminated.
NBSP12	29	SP3A	First completed test with LVDT lateral deformer.
NBSP13	30	SP3A	Good test.
NBSP14	31	SP3C	First attempt at SP3C. Film pot used to calculate axial strains.
NBSP15	32	SP3C	Good test.
NBSP16	33	SP3C	Good test.
NBSP17	4	SP3B(HC)	Measured loads during specimen construction. Membrane leaked at the start of SP. HC data available.
NBSP18	---	SP3B(NG)	Broken wire in lateral deformer; test terminated.
NBSP19	5	SP3B(HC)	Membrane leaked at the end of HC. HC data available.
NBSP20	34	SP3B	Loading piston not in contact with top cap when strains rezeroed. During the time required to seat piston, specimen crept in lateral direction.
NBSP21	35	SP3B	Good test.
NBSP22	36	SP3B	Waited for lateral creep to equalize. Excellent test.
NBSP23	37	SP2A	Good test. End of test on HC line.
NBSP24	38	SP2A	Data acquisition system locked up for 15 minutes at the start of the SP. Specimen crept laterally during this time. Test completed.
NBSP25	39	SP2A	Good test. Material from can 18.
NBSP26	22	TXC	First test to have HC cycle at 0.7 MPa. Broken wire in film pot; used vertical deformers for shear, thus limiting axial strains to approximately 7 percent.
NBSP27	23	TXC	Load cycled at a vertical stress of 13.8 MPa.
NBSP28	6, 16	HC	Pressure cycled at 21.5 MPa. No low pressure cycle.
NBSP29	---	HC(NG)	Membrane leaked; no valuable data obtained.
NBSP30	7, 17	HC	Membrane leaked at 24.1 MPa.

* Identifies the intended type of test. (HC) indicates that only HC data were obtained. (NG) indicates no valuable test data were obtained.

(Continued)

Table 2.3 (Concluded)

Test No.	Plate No.	Type of Test*	Test Notes
NBSP31	40	SP2A	Good test. Material from can 24.
NBSP32	41	SP2A	Good test. Material from can 29.
NBSP33	42	SP2C	Good test.
NBSP34	43	SP2C	Good test.
NBSP35	44	SP2C	Good test.
NBSP36	8	SP2B(HC)	Broken wire on film pot. HC data available.
NBSP37	45	SP2B	Completed 500 scans before the end of test. Good test. Used film pot to calculate axial strains.
NBSP38	46	SP2B	Good test. Film pot used.
NBSP39	47	SP2B	Good test. Film pot used.
NBSP40	48	SP2B	Good test. Changed to vertical deformaters; can see difference at end of test.
NBSP41	9, 18	HC	HC to 41.4 MPa with cycle at 20.6 MPa.
NBSP42	10, 19	HC	Repeat of NBSP41. Excellent repeatability.
NBSP43	24	TXC	Load cycled at a vertical stress of 27.6 MPa.
NBSP44	49	SP3B**	First reverse test attempted. Average stress path from tests NBSP20, 21, and 22. Strain path different.
NBSP45	---	SP2C**(NG)	No lateral deformer measurements recorded. Test terminated.
NBSP46	50	SP2C**	Used average stress path from tests NBSP33, 34, and 35. Strain path different.
NBSP47	51	SP2C	Material from can 24. Will use this stress path as an input to subsequent reverse tests.
NBSP48	52	SP2C**	Good test. Strain path very close to SP2C.
NBSP49	53	SP2C**	Good test. Strain path very close to SP2C.
NBSP50	11	SP3B(HC)	Confining pressure exceeded 6.9 MPa; went up to 9.3 MPa. HC data available.
NBSP51	54	SP3B	Good test. Recognized period in test during which specimen strained at constant stress (constant stress "zone"). Used stress path as an input to subsequent reverse tests.
NBSP52	55	SP3B**	Realized that the time spent in constant stress "zone" would determine the magnitude of resulting strains. Good test.
NBSP53	56	SP3B**	Proceeded through constant stress zone as quickly as possible (approximately 0.8 minutes). Good test.
NBSP54	57	SP3B**	Proceeded through constant stress zone as slowly as possible (approximately 9.7 minutes). Good test.
NBSP55†	58	SP3A	First strain-rate test. Covered SP in conventional time of 30 minutes.
NBSP56†	59	SP3A	Covered SP in 12 minutes.
NBSP57†	60	SP3A	Covered SP in 5 minutes.
NBSP58†	12	SP3A(HC)	Membrane leaked. HC data available.
NBSP59	61	SP3A	Covered SP in 4 minutes.
NBSP60†	62	SP3A	Covered SP in 133 minutes.

* Identifies the intended type of test. (HC) indicates that only HC data were obtained. (NG) indicates no valuable test data were obtained.

** Reverse tests.

† Strain-rate tests.

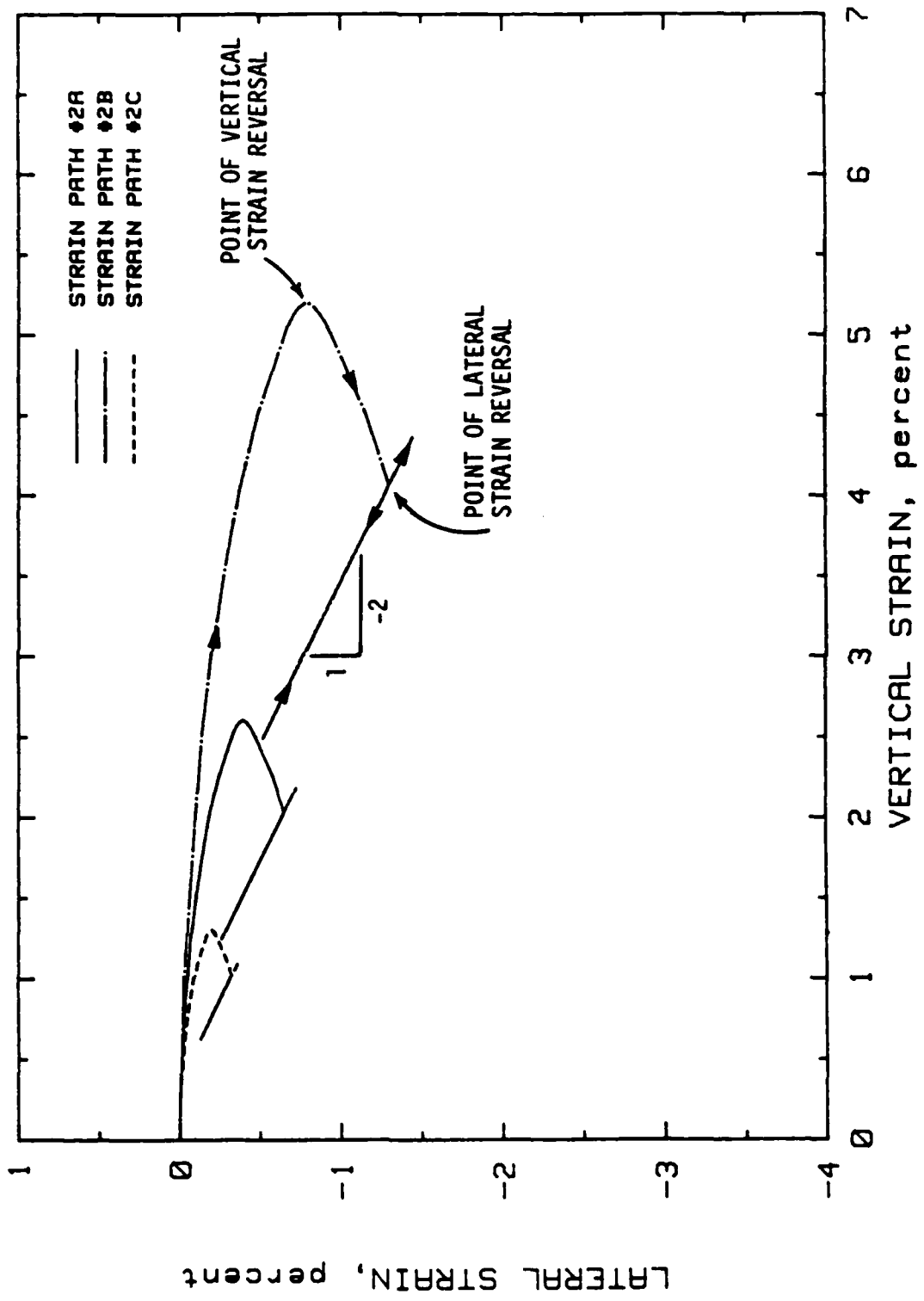


Figure 2.1 Comparison plot of strain paths 2A, 2B, and 2C.

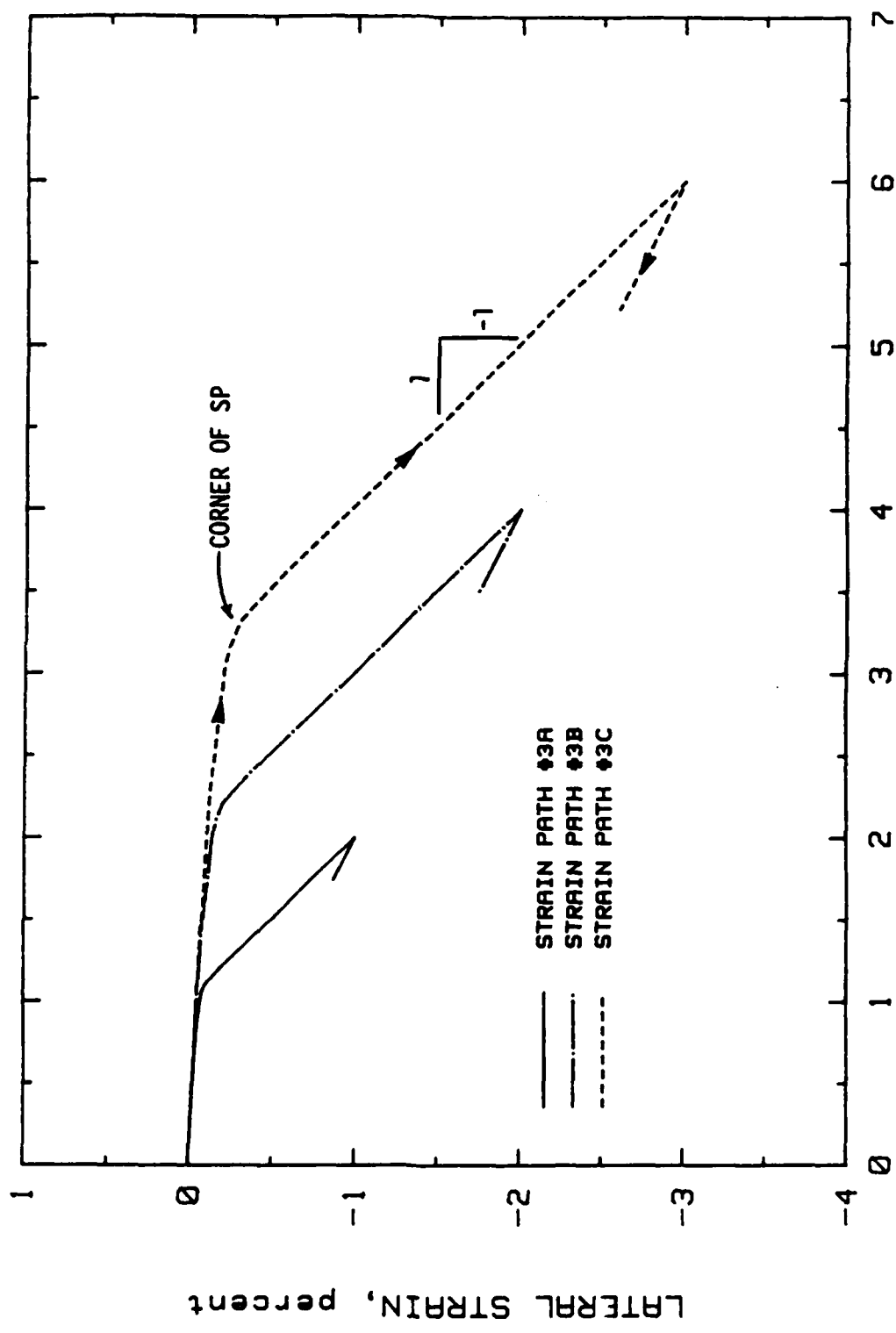
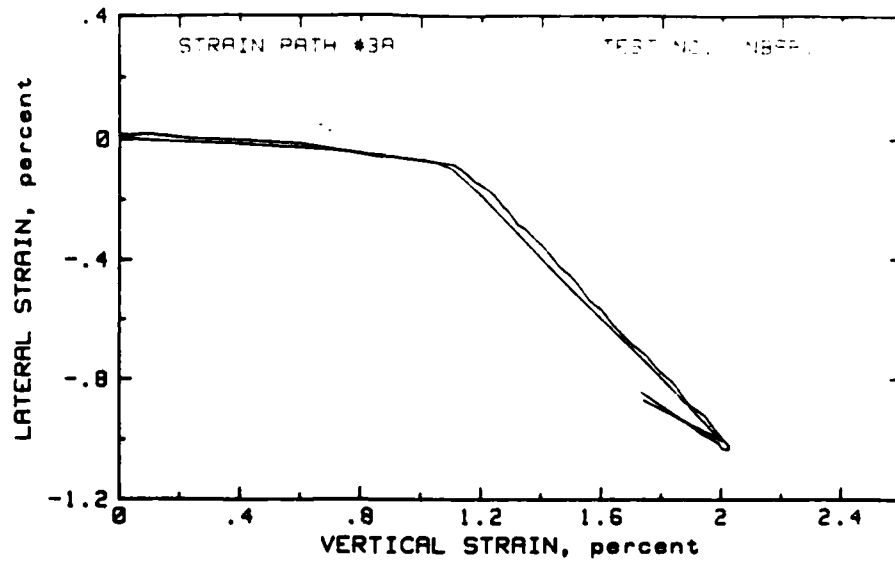
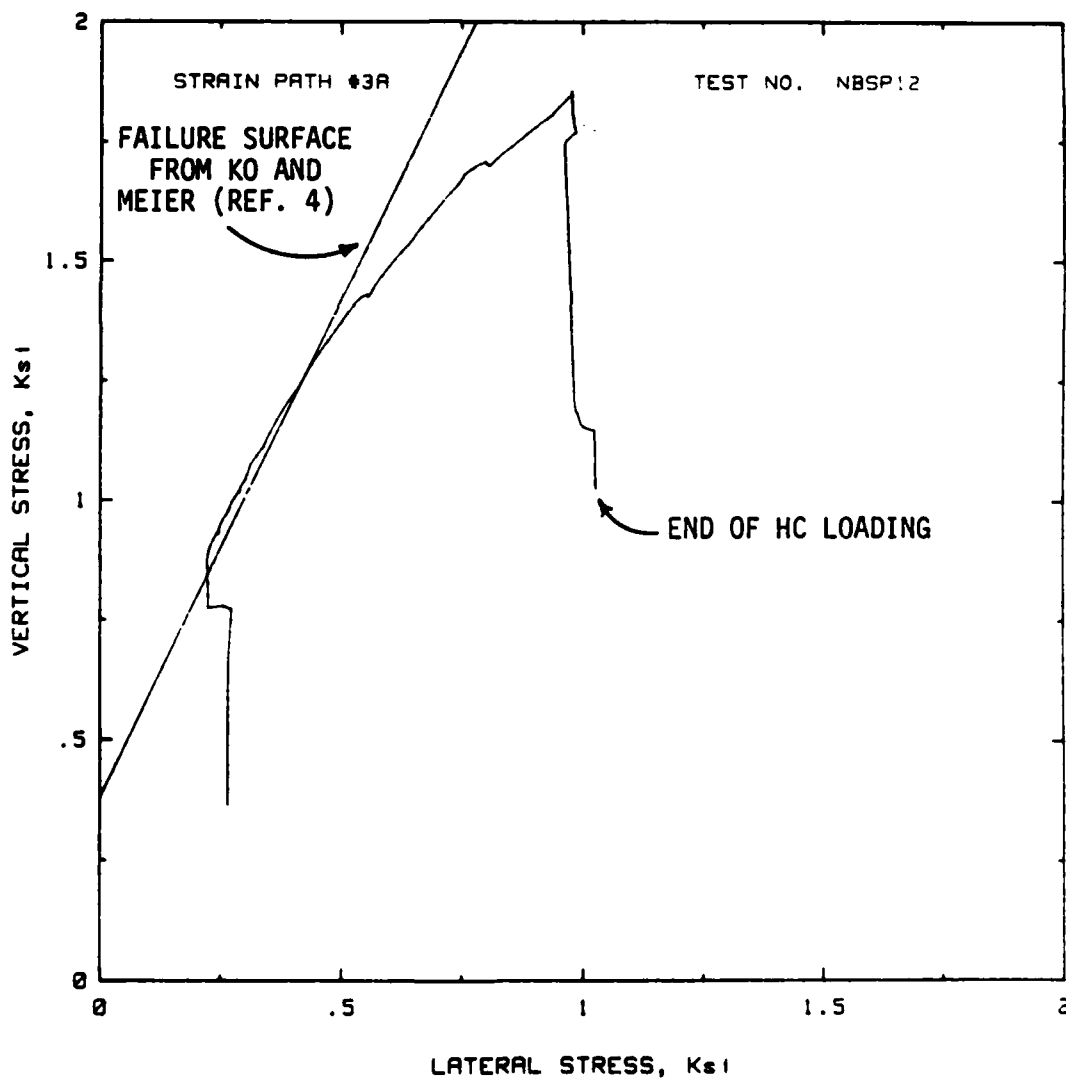


Figure 2.2 Comparison plot of strain paths 3A, 3B, and 3C.



a. STRAIN PATH



b. STRESS PATH

Figure 2.3 Typical real time plots of strain path data.

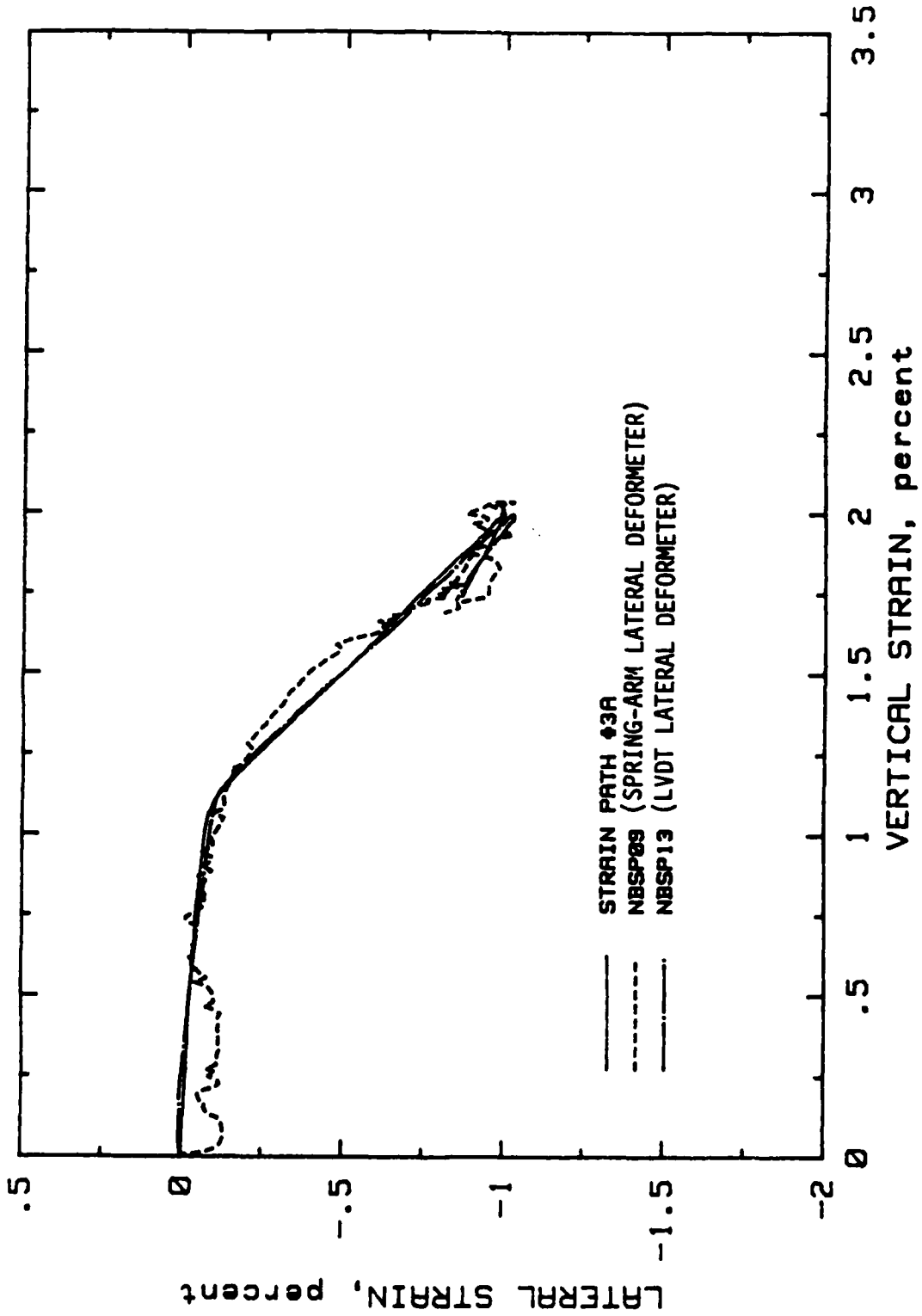


Figure 2.4 Comparison of strain paths resulting from the use of spring-arm and LVDT lateral deformers.

CHAPTER 3

DATA ANALYSIS

The purpose of this chapter is to provide an analysis of the test data presented in Chapter 2. The Phase I test data are analyzed first, including the HC, TXC, strain path 3, and strain path 2 test results. An analysis of the reverse strain path and strain-rate tests concludes this chapter.

3.1 HC TESTS

HC data up to 6.9-MPa pressure were obtained from every successfully completed test. This stress level was the desired initial prestress for every TXC and SP test. As illustrated in Figure 3.1, all of the test specimens, with the exception of those from can 18, exhibited similar volumetric responses between 1 and 6.9 MPa; the test specimens from can 18 had a softer response. To generate this figure, the mean volumetric strain was calculated at several stress levels for the material obtained from cans 18, 24, 26, 29, and 30. For each material, these mean values were plotted and a smooth curve was drawn through the points. The mean response of the material from can 18 is obviously different. The other four materials have parallel response curves. In fact, if they were rezeroed at 1 MPa, they would probably lie on top of each other.

The variations in volumetric response were not a function of pretest specimen water content or density. To show this, Table 3.1 lists the mean and standard deviation values for water content, wet density, and dry density for specimens prepared from each of the five cans of material. The can numbers are listed in the order in which they were used, starting with the first can opened. The water content of the can 18 material is within the range of the other water contents. However, the densities of the specimens prepared from can 18 materials are higher than those prepared from the other cans. If the materials from the various cans were the same, this higher density should have produced a stiffer volumetric response curve, not a softer curve. Also recall that the measured loads during specimen construction were smaller for the can 18 materials. It is concluded, therefore, that the differences in the volumetric response of specimens prepared from the can 18 material were not due to water content or density variations, but were the result of gradation

differences. The additional fines in the can 18 material apparently produced the variation in material response. These differences in gradation, however, are small compared to the variations normally encountered in undisturbed soil samples obtained from a specific site.

Seven high-pressure (>6.9 -MPa) HC tests were conducted on test specimens constructed from three different cans of material, i.e., cans 30, 18, and 29. The volumetric response data from these seven tests are plotted in Figure 3.2. The data essentially fall into two groups. Specimens NBSP28 and NBSP30 (can 18 material) had the softest responses, as was the case in the low-pressure HC tests. The remaining tests, with the exception of NBSP04, group together. The unloading responses, however, were similar for all of the high-pressure HC tests.

In Plates 13-19, plots of mean normal stress versus vertical and lateral strains are presented for the seven high-pressure HC tests. Notice that the test specimens were all slightly anisotropic, with the lateral strains larger than the vertical strains. Vertical strains were found to be less variable than the lateral strains. As an example, the vertical and lateral strains for three tests are plotted in Figure 3.3. Note that the vertical strain data plot very close together, while the lateral strain data are scattered over a wider range. This behavior may be the result of the specimen construction process, e.g., using a steel mold, or the result of some other specimen variable such as density or grain size.

3.2 TXC TESTS

Five TXC tests were conducted on specimens constructed from three different cans of material, i.e., cans 30, 18, and 29. The data from these tests are presented in Plates 20-24. Each test specimen was prestressed to 6.9 MPa during its HC phase.

The stress-strain responses from the five tests are compared in Figure 3.4. All of the specimens constructed from the can 18 material (NBSP06, NBSP26, and NBSP27) had stress-strain curves which overlaid each other. Thus, for the same material, the repeatability was excellent. The other two specimens (NBSP05 and NBSP43) had only slightly stiffer stress-strain responses.

TXC data from three different test specimens, each constructed from a different can of material, are compared in Figure 3.5. The only significant difference observed in these data is the volumetric response of specimen

NBSP27 (bottom two plots in Figure 3.5). The major portion of that difference was produced during HC (between points A to B). The volumetric response during shear, from B to E, appears to be similar for all three test specimens. This would suggest that the volumetric strain response of this material is a function of both the imposed mean normal stresses and the imposed shear stresses.

3.3 PHASE I SP TESTS

Twenty-five SP tests were conducted during the first phase of this test program. Two strain path shapes were investigated (3 and 2), each having three levels of strain magnitude (A, B, and C) for a total of six strain paths. To provide some indication of test control and specimen repeatability, at least three replications per individual strain path were conducted. In the following two subsections, an analysis of the SP test data from the two strain path shapes, 3 and 2, is presented.

3.3.1 SP 3 Tests

Thirteen SP 3 tests were described in Section 2.7.2 and the data presented in Plates 25-36. The first four SP tests (NBSP07, NBSP08, NBSP09, and NBSP10) should be considered trial tests. During these tests, several adjustments were made to the equipment and procedures (see Section 2.7.1) before the necessary test control was obtained. The most significant change and the one which proved to be the most beneficial was the change from the spring-arm lateral deformer to the LVDT lateral deformer. Figure 3.6 is presented to illustrate the improved control and higher quality test data brought about by this change. Test NBSP09 was conducted using the spring-arm lateral deformer. The strain path from this test exhibits drastic movements off of the desired strain path. Test NBSP13 was conducted with the LVDT lateral deformer, and its strain path plots directly on top of the desired path. The data from this latter test are very smooth and consistent, exhibiting no drastic changes or fluctuations.

Excluding the four trial tests, the test data for each of the three strain paths (3A, 3B, and 3C) were very consistent and show excellent repeatability. To illustrate this, a comparison plot was generated for each of the three paths. These plots are presented in Figures 3.7-3.9. Figure 3.10 is

presented to illustrate the differences between the three strain paths. In reviewing these four figures, two significant observations were made.

First, the initial slope of the stress path, from point B to the peak stress, changed with increasing vertical strain magnitude (see upper left plot in Figure 3.10). All of the tests had an initial TXC stress path (3:1 slope). For SP 3A, this slope continued up to the peak stress. For SP 3B, the tests reached a point on the strain path (before reaching the corner on the strain path) when the confining pressure had to be increased. This moved the stress path to the right of a 3:1 slope. For the SP 3C tests, the required increase in confining pressure was greater than for the SP 3B tests. This behavior can be explained if one considers the two paths illustrated in Figure 3.11. Note that the assumed TXC path falls below the SP 3 path during the initial loading, i.e., between B and the corner of the strain path. In order to bring the TXC path up to the intended strain path, the applied confining pressure must be increased. By increasing the confining pressure, one moves the stress path to the right of a 3:1 slope. Figure 3.12 shows the strain paths from two TXC tests, NBSP05 and NBSP43, plotted with the SP 3 paths. This figure clearly indicates that the TXC strain paths fall below the intended paths during the initial loading.

The second observation made in reviewing Figures 3.7-3.10 was that all of the SP 3 tests were observed to reach a point of continuing strain with little change in the applied stresses. The test specimens tended to "yield" or "flow" as the stress path moved along a "failure" envelope. Figure 3.13 shows the proximity of three stress paths (tests NBSP13, SP 3A; NBSP22, SP 3B; and NBSP15, SP 3C) to a failure envelope developed from conventional TXC data (Reference 9). In each test, the stress path reached the failure envelope as the strain path moved around the corner and onto the -1:1 slope. Figure 3.14 better illustrates this behavior. In this figure, the strain path from test NBSP22 had just passed the corner at point 1, then proceeded down the -1:1 slope to point 2. At point 2, the stress-strain curve flattened out and the vertical strain increased at either a constant or near constant level of principal stress difference to point 3. From point 2 to point 3, the stress path was moving along the failure envelope. Notice the movement along the strain path from point 2 to 3 and the corresponding movement along the stress path. This observation of yielding resulted in the planning of the reverse strain path tests.

3.3.2 SP 2 Tests

Twelve SP 2 tests were described in Section 2.7.3 and the data presented in Plates 37-48. The test data for each of the three strain paths (2A, 2B, and 2C) were very consistent and showed excellent repeatability. A comparison plot was generated for each of the three paths; these plots are presented in Figures 3.15-3.17. Figure 3.18 illustrates the differences in responses between these three strain paths. Several significant observations were made in reviewing the data in these four figures.

First, the amount of recoverable vertical and lateral strain relative to the total strain path was inversely related to the vertical strain magnitude, i.e., the smaller the vertical strains, the larger the recoverable strains relative to the total strain path. Each SP 2 test specimen was able to unload from the point of peak vertical strain to the point of lateral strain reversal. From this latter point, the strain paths followed a -2:1 slope, with increasing lateral strain and decreasing vertical strain. The three sets of SP 2 tests followed this portion of the strain path to different final points. The SP 2A tests (Figure 3.15) went past the point of lateral strain reversal, then terminated (point E). At the point of lateral strain reversal, the stress paths were above the HC line; at the end of the tests, the stress paths had reached the HC line at which point the strain path could no longer be followed. The SP 2B tests (Figure 3.16), which had the largest strain magnitudes, behaved differently. At the point of lateral strain reversal, the stress paths had already reached the HC line (see upper left plot in Figure 3.16). Two of these tests (NBSP39 and NBSP40) terminated at this point, while the other two tests (NBSP37 and NBSP38) exhibited large recoverable vertical strains. Test NBSP40 was the only test among the four in which the vertically-oriented LVDT deformeters were used to measure vertical strain; the other three tests used the external film pot. The large recoverable vertical strains observed in tests NBSP37 and NBSP38 may have been piston movement and not true specimen deformation. Therefore, more confidence should be placed in the unloading data from test NBSP40. The SP 2C tests (Figure 3.17), which had the smallest strain magnitudes, exhibited significant recoverable vertical strains. The strain paths terminated approximately half way up the -2:1 slope. LVDT deformeters were used in all of these tests to measure vertical strain. Note also that at the point of lateral strain reversal, the stress

paths were significantly above the HC line. Thus, changing the magnitudes of the strains in the strain paths altered both the stress path shapes and the stress levels associated with specific points on the strain path.

The second observation associated with the strain path 2 tests was the variation in response caused by differences in material (can number). Figure 3.19 presents results of tests conducted on three specimens constructed from three different cans of material. Note the HC response (points A to B) of test NBSP23. This test specimen was prepared from can 18 material. It had larger volumetric strains and larger negative values of principal strain difference at point B than the other two test specimens. In addition, it exhibited a smaller value of peak stress difference than the other two specimens. Comparing tests NBSP31 and NBSP32, the very small variations in response could be a function of either material differences or data scatter. The point to be made is that small variations in material characteristics can have significant effects upon response. The strain path tests appear to be more sensitive to these material differences than the TXC tests.

The third observation related to the strain path 2 tests concerned the initial slope of the stress path from point B to the peak stress. For the SP 2B tests (Figure 3.16), it was necessary to increase the confining pressure and therefore move the stress path to the right of a 3:1 slope during the initial loading from point B to the point of vertical strain reversal. Similar behavior was observed in the SP 3C tests described in the previous section. Figure 3.20 illustrates that typical TXC strain paths plot below the SP 2 paths and that the largest divergence exists between the TXC path and SP 2B. Therefore, the largest increase in pressure would be required to bring the TXC path up to the SP 2B path.

Finally, the proximity of the SP 2 stress paths to the failure envelope is shown in Figure 3.21. Unlike the SP 3 tests, these stress paths always remained below the failure envelope. This observation is important when considering the reverse strain path tests.

3.4 PHASE II SP TESTS

In the first phase of testing, WES demonstrated its ability to follow a given strain path and conduct the tests with excellent repeatability. However, the question of stress-strain uniqueness still remained to be answered. It was therefore decided to conduct several reverse strain path tests under

the assumption that there exists a unique relationship between stress and strain if one follows the same stress path, i.e., if the stress path measured during strain path test "X" were followed during test "Y", then the resulting strain path from test "Y" should match that of test "X". The fact that repeated TXC tests on one material produced similar stress-strain curves and similar volumetric responses indicated that such a relationship might exist.

The strain-rate tests completed the second phase of the test program. WES demonstrated in the first phase of testing that a unique stress path was obtained from a single strain path. However, each set of SP tests was conducted at one deformation rate. The strain-rate tests were conducted to investigate the effects of different strain rates on material response.

3.4.1 Reverse SP Tests

Nine reverse SP tests were described in Section 2.7.4 and the data presented in Plates 49-57. After recognizing that all of the test specimens should be constructed from the same material, tests NBSP47, NBSP48, and NBSP49 were conducted. The data from these tests are plotted in Figure 3.22. Remember that test NBSP47 provided the input stress path to tests NBSP48 and NBSP49. In reviewing Figure 3.22, first note that WES was able to follow the input stress path from test NBSP47 very closely. Although there is variability in the strain path data, one could reasonably suggest that there exists a unique stress-strain relationship for these reverse SP tests. However, it is uncertain whether this statement can be applied to SP 2A or SP 2B.

For SP 3B, there was no unique relationship between stress and strain. Figure 3.23 shows data from four tests; test NBSP51 provided the input stress path which was followed during tests NBSP52, 53, and 54. The changes in strain path response were produced by increasing the rate of change in confining pressure as the stress path moved along the failure envelope between the points 1 and 2 on the stress path. In all tests the vertical deformation rate was the same. During test NBSP54, the operator decreased the confining pressure between points 1 and 2 as slowly as possible (~9.7 min) and yet still remained on the stress path. During test NBSP53, the confining pressure was decreased as quickly as possible (~0.8 min). Test NBSP52 was conducted with a rate of change in confining pressure that was intermediate between the previous two tests (~5.6 min). From these results, it is obvious that time is

an important factor, at least between points 1 and 2. The longer the stress path rides the failure envelope, the larger the strains. To further demonstrate the importance of time, Figure 3.24 is presented. This figure shows the stress-strain-time histories of tests NBSP51-54. Notice that up to a time of 22-23 minutes, the stresses and strains are nearly identical for all four tests. Not until the stress path reaches the failure envelope do the curves diverge.

3.4.2 Strain-Rate Tests

The five strain-rate tests were described in Section 2.7.5 and the data presented in Plates 58-62. In order to investigate the effects of strain rate on "stress-strain uniqueness", tests on Nellis Baseline sand were conducted at four different strain rates while following strain path 3A. The times required to complete the entire strain path for each test were: NBSP55, 30 min; NBSP56, 12 min; NBSP57, 5 min; NBSP59, 4 min; and NBSP60, 133 min. The test data are plotted in Figure 3.25. The stress-strain curves exhibit a slight increase in peak stress with increasing loading rate. After reaching the points of peak stress, the stress paths converge to a common point on the failure envelope (labeled point "1" in Figure 3.25), then show very similar unloading paths.

Figure 3.26 shows the stress-strain curves for these five tests rezeroed at point B. There is an 18 percent increase in peak stress difference between test NBSP60 (133 minutes) and test NBSP59 (4 minutes). This 18 percent increase is not attributed to data scatter; there is a consistent increase in the peak stress levels with decreasing test times. If an 18 percent increase is observed over a range of times between 4 and 133 minutes, one should expect an even greater increase in stress level for SP tests conducted in the millisecond and submillisecond regimes.

Table 3.1 Summary of Test Specimen Density and Water Content Data

Can No.	Number of Specimens	Wet Density g/cc		Water Content %		Dry Density g/cc	
		Mean	Std Dev	Mean	Std Dev	Mean	Std Dev
30	10	1.895	0.011	5.23	0.44	1.802	0.009
18	14	1.907	0.008	5.32	0.50	1.811	0.012
29	12	1.894	0.005	5.36	0.08	1.798	0.004
24	12	1.898	0.005	5.22	0.11	1.804	0.005
26	5	1.896	0.004	5.03	0.09	1.805	0.004

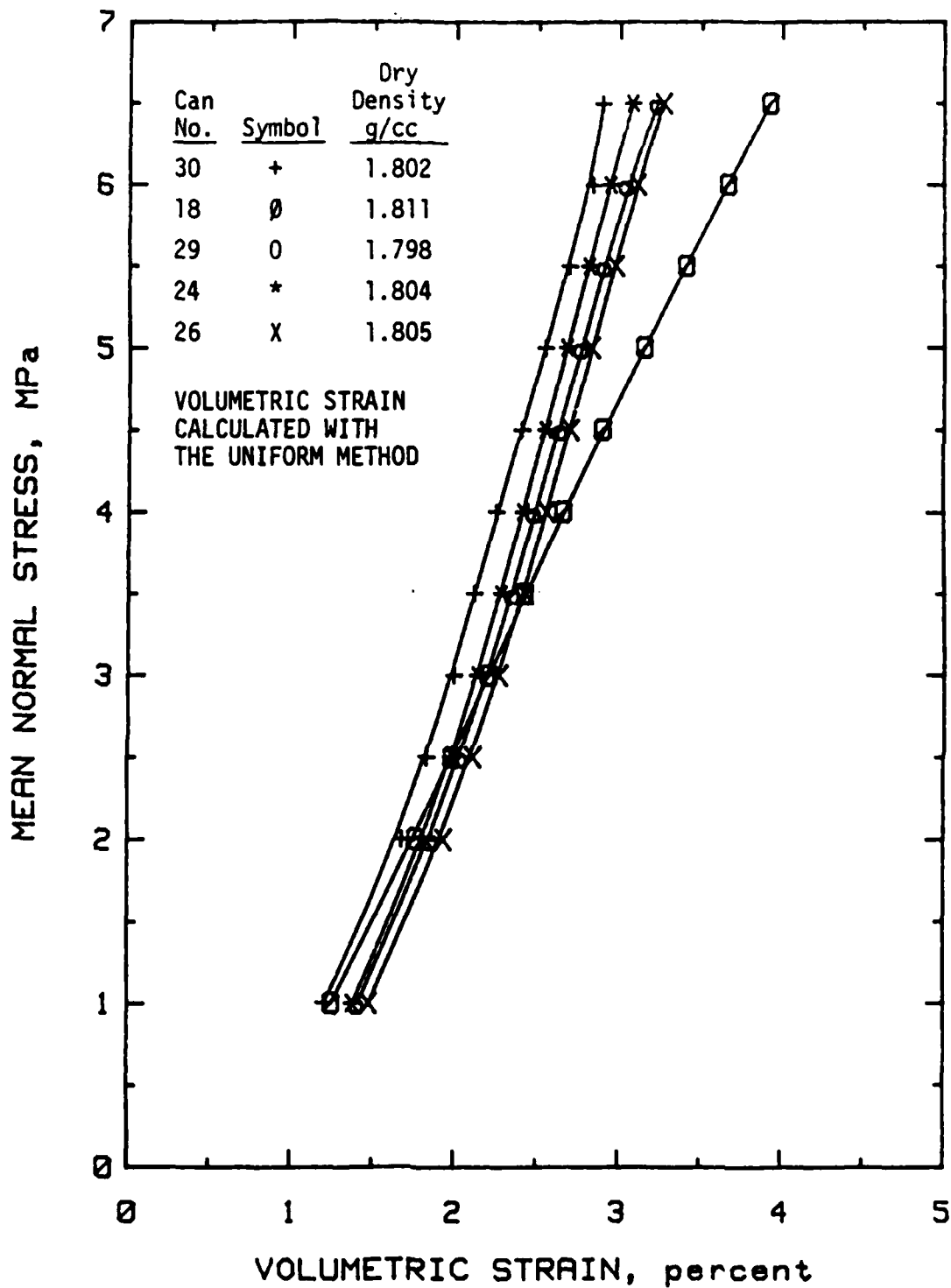


Figure 3.1 Mean hydrostatic compression volumetric responses for Nellis Baseline sand

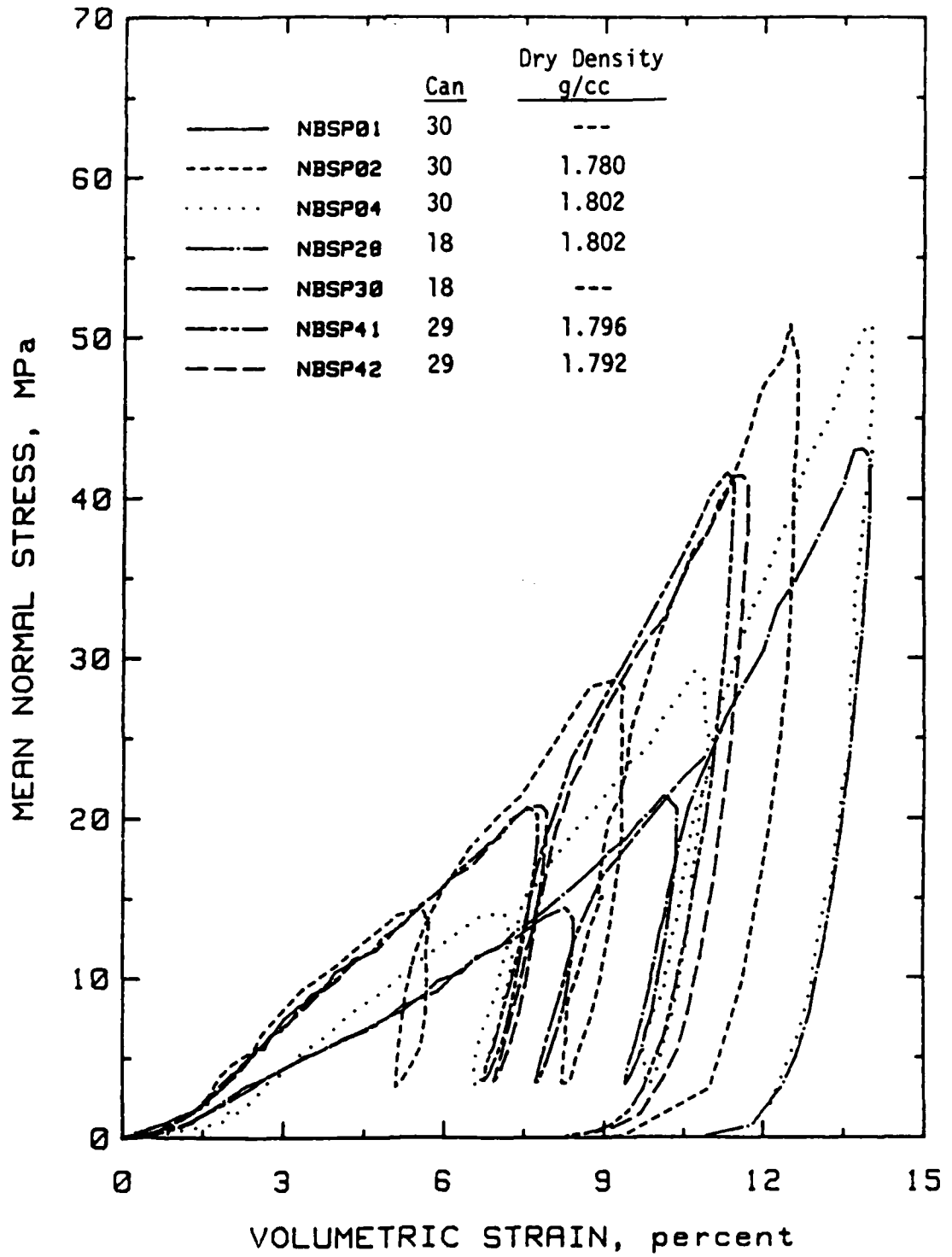


Figure 3.2 Static high-pressure hydrostatic compression test results.

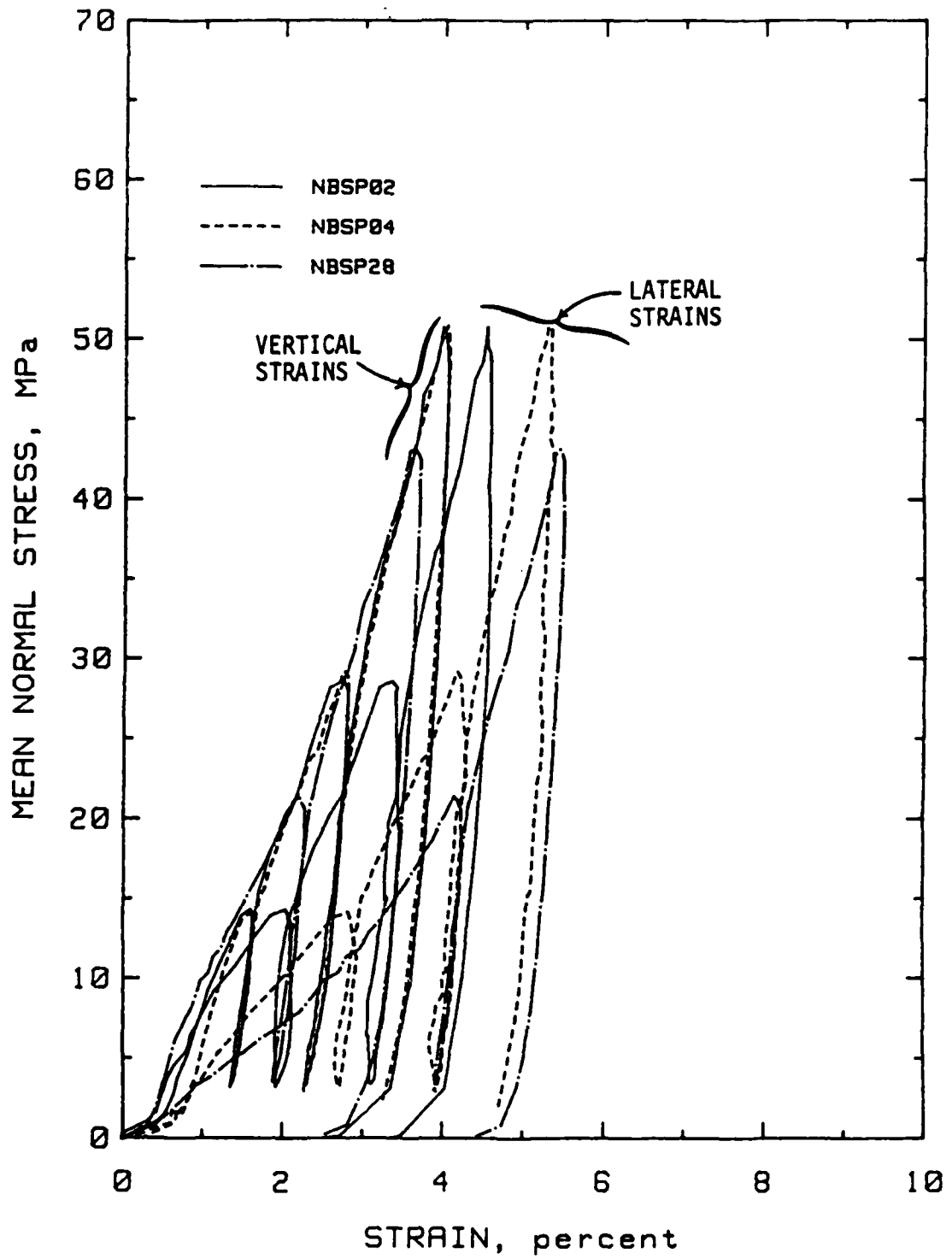


Figure 3.3 Comparison plot of vertical and lateral strains during static hydrostatic compression.

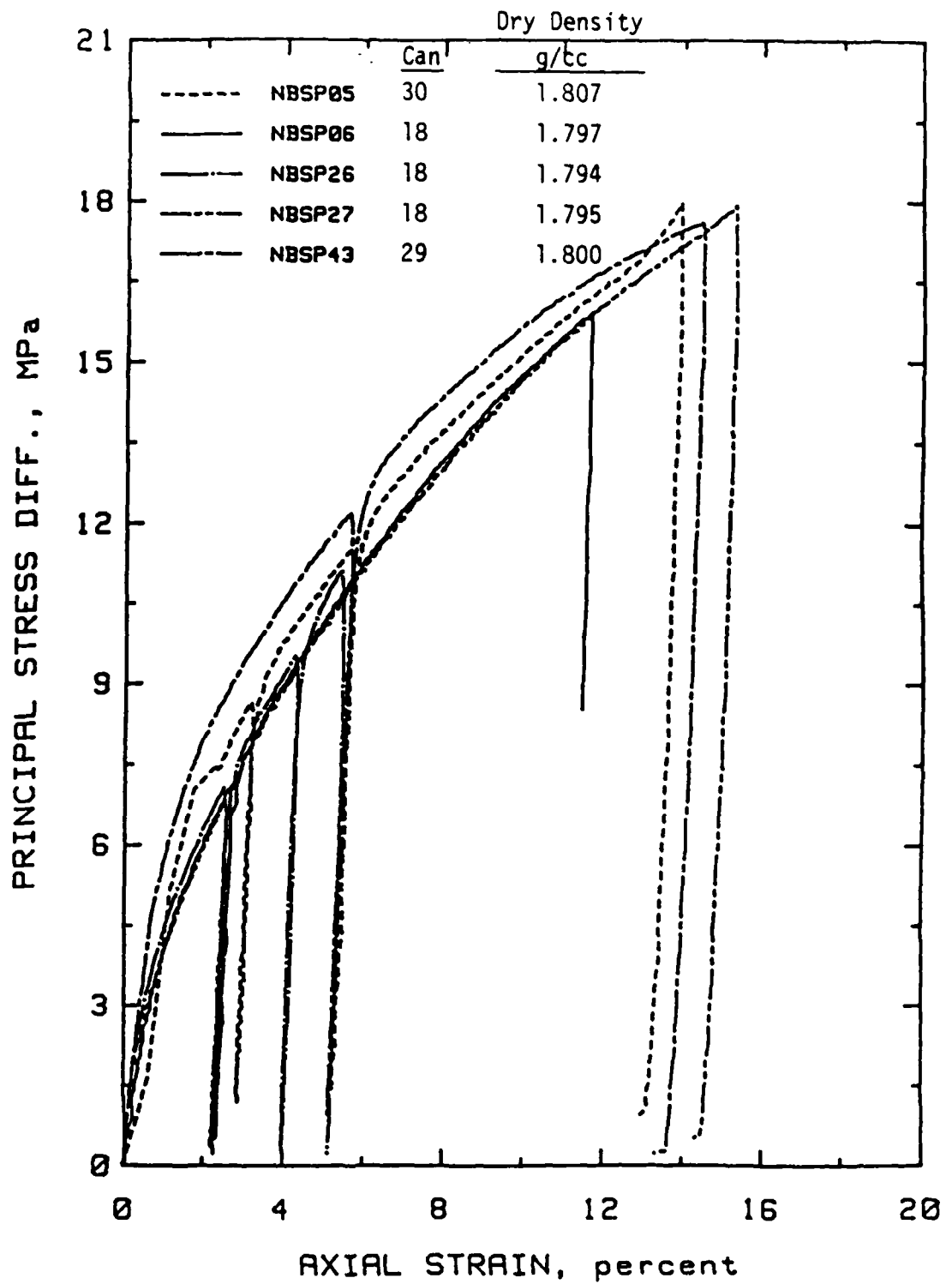


Figure 3.4 TXC test results on Nellis Baseline sand.

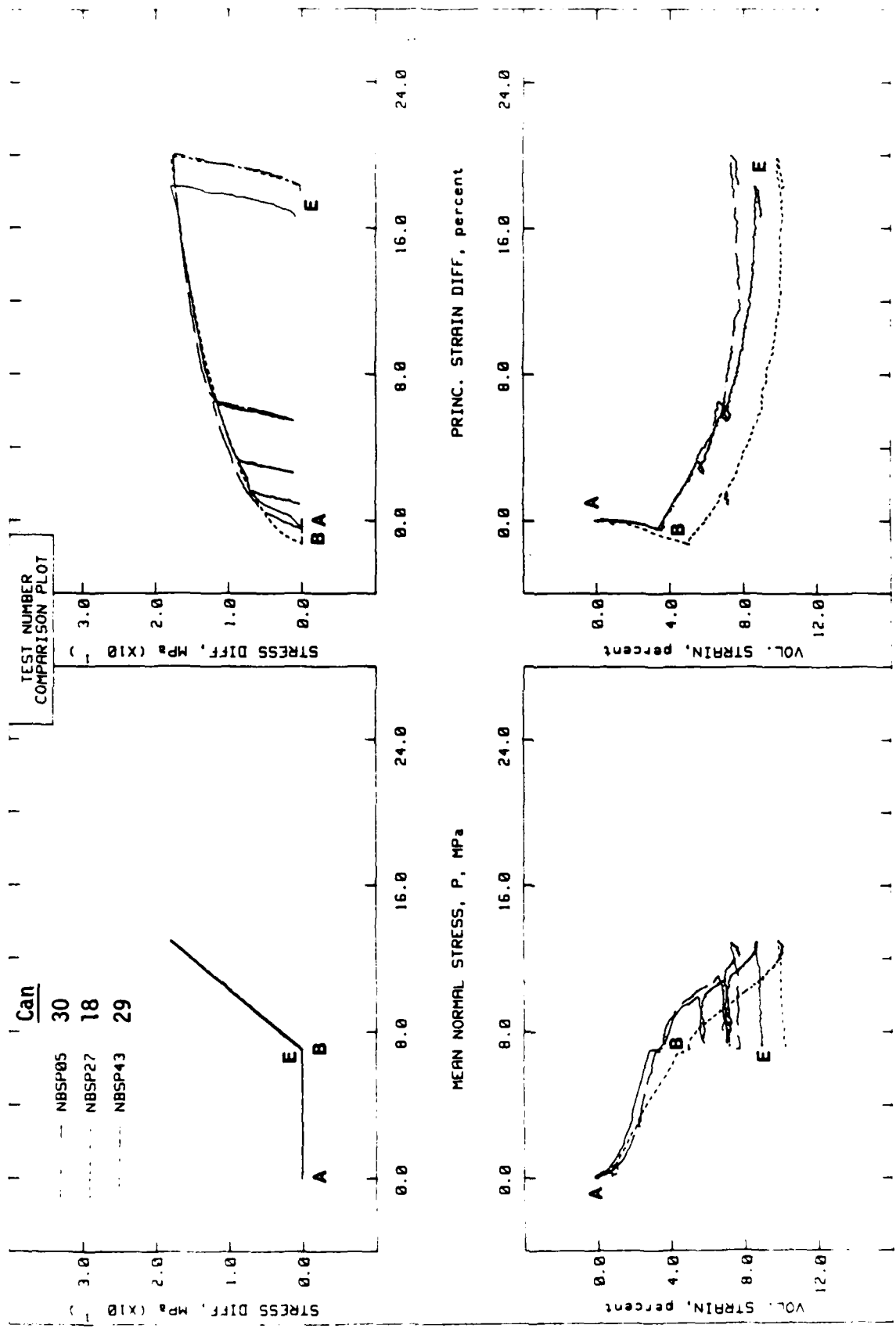


Figure 3.5 Effect of material variations on TXC test results.

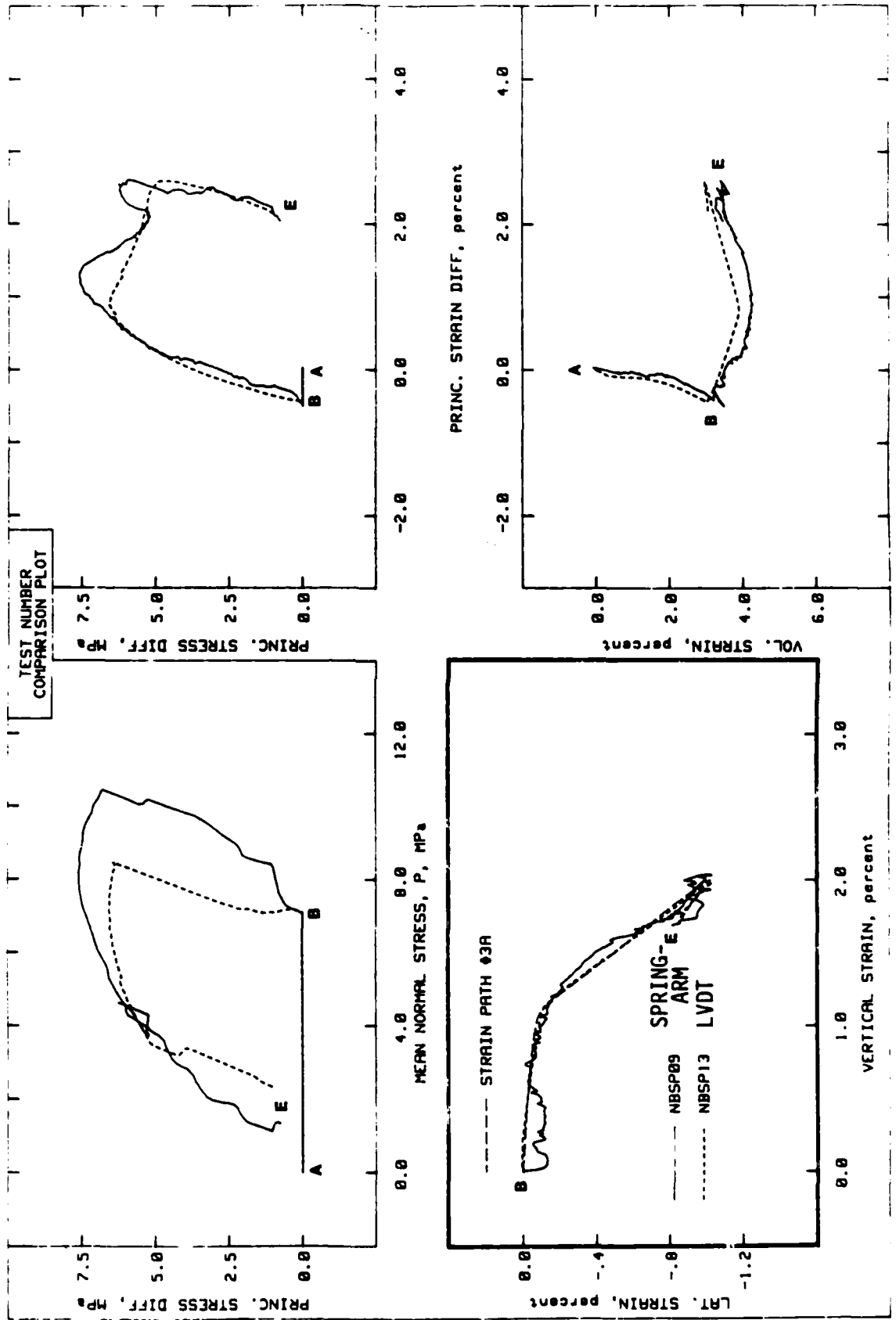


Figure 3.6 Effect of lateral deformation measuring system on strain path test results.

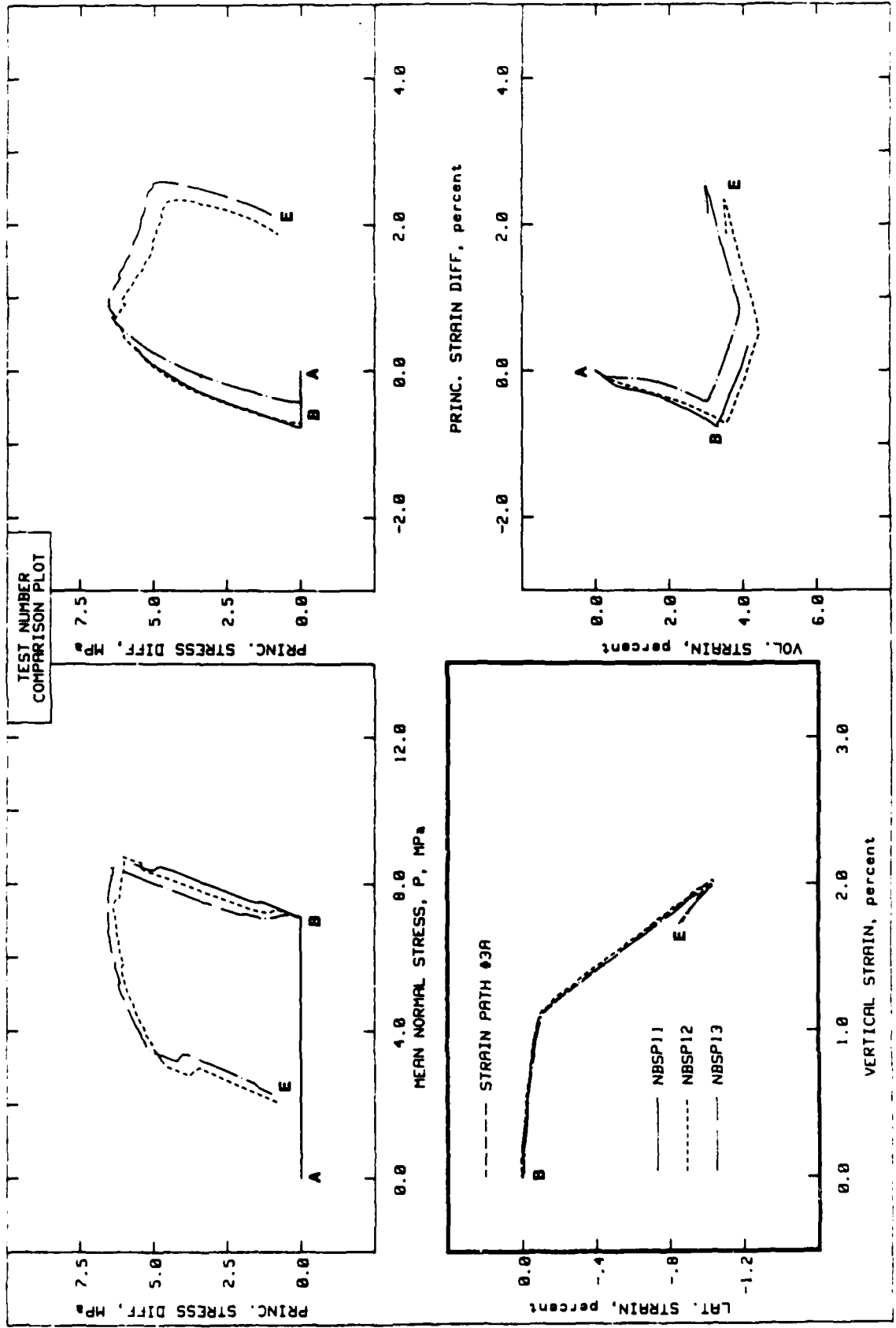


Figure 3.7 Results of tests that followed strain path 3A.

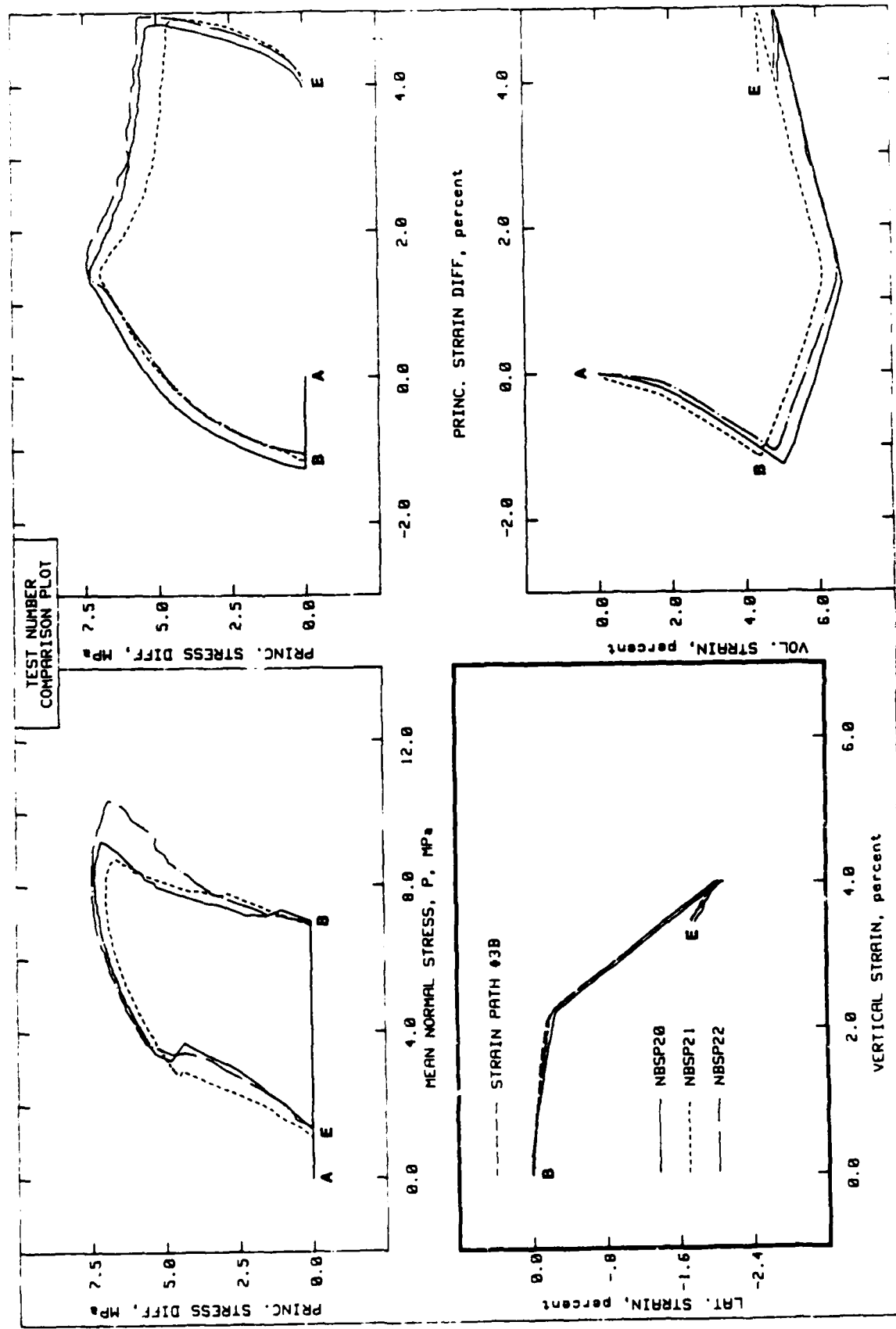


Figure 3.8 Results of tests that followed strain path 3B.

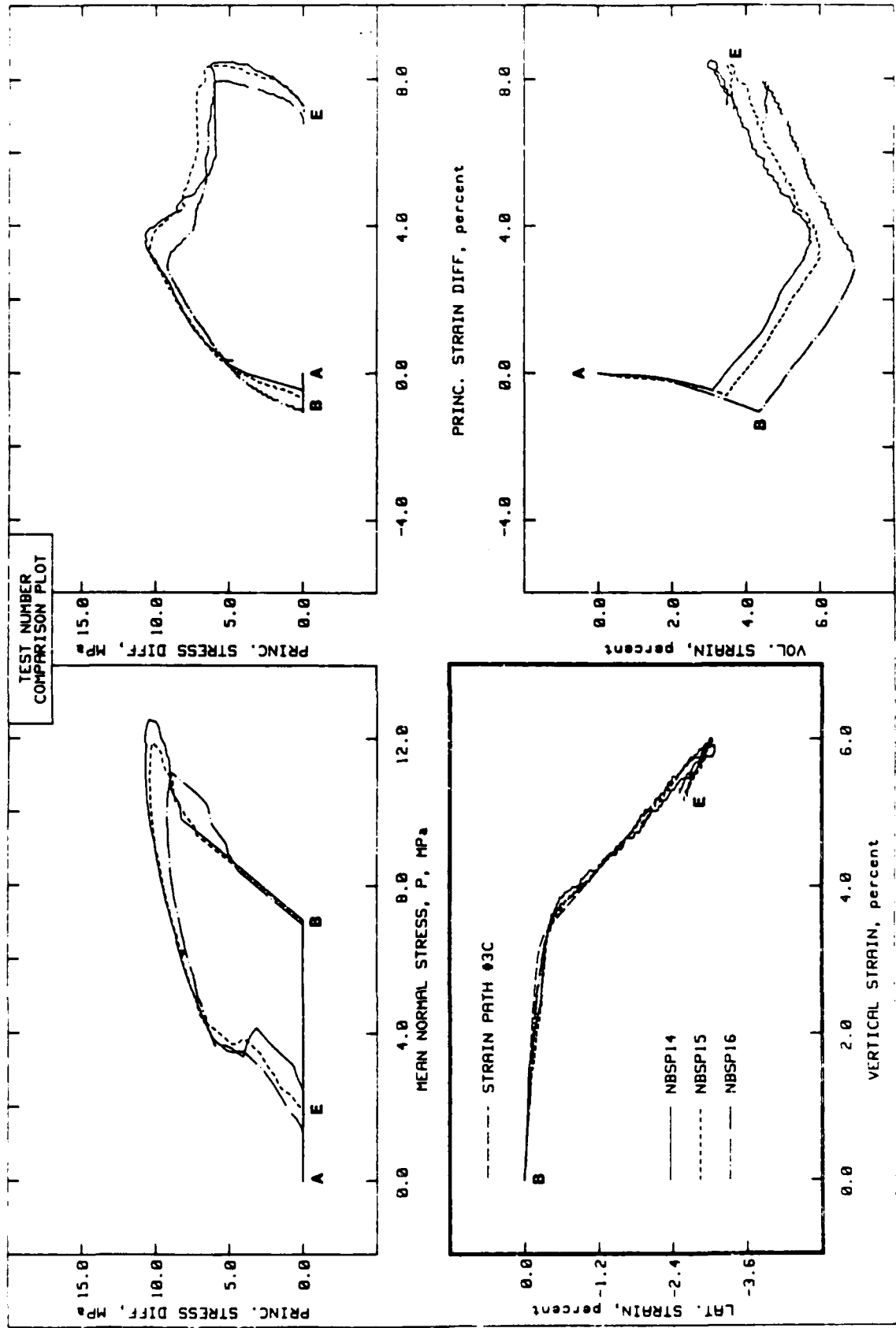


Figure 3.9 Results of tests that followed strain path 3C.

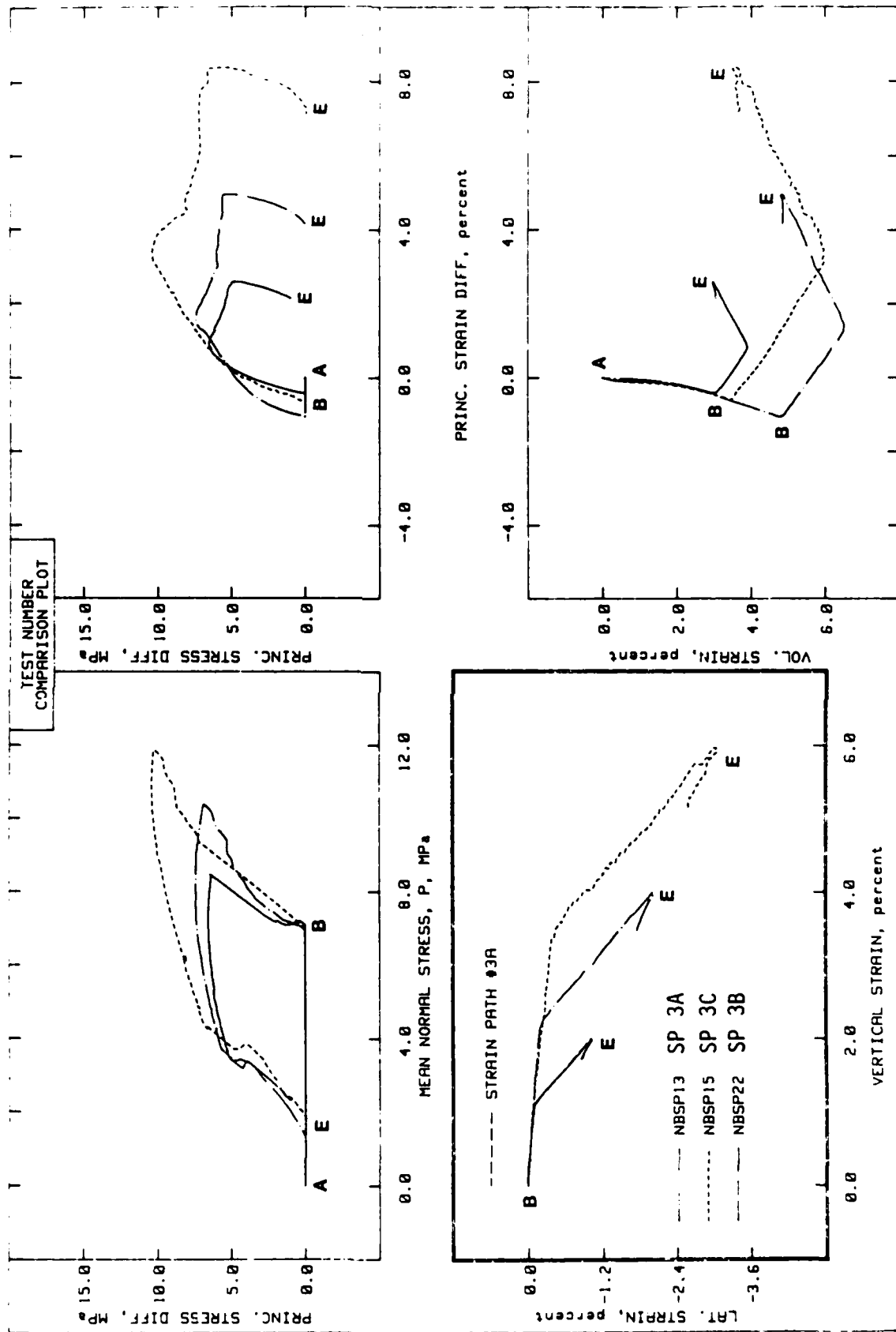


Figure 3.10 Comparison of results of tests that followed strain paths 3A, 3B, and 3C.

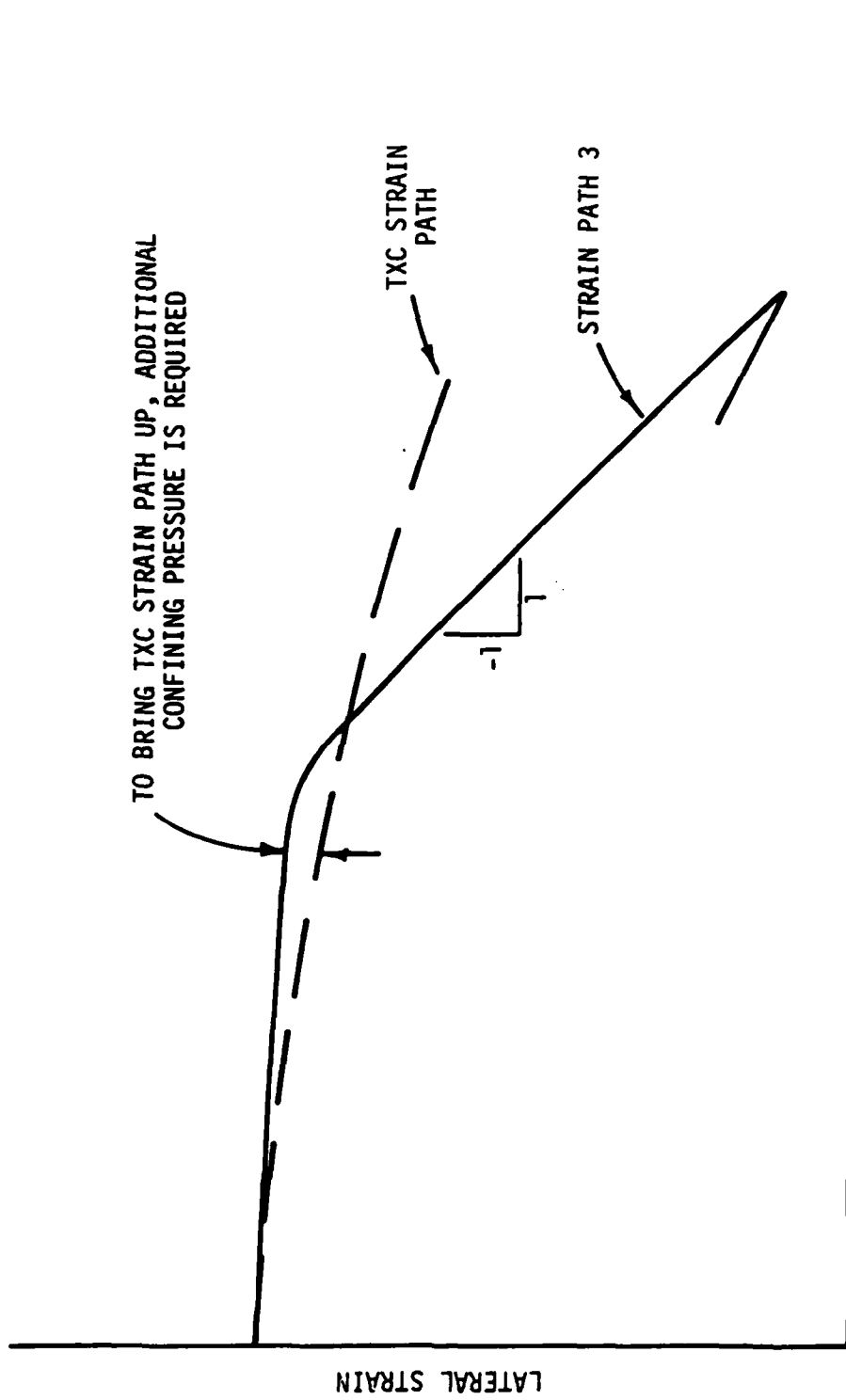


Figure 3.11 Comparison of generalized TXC strain path with generalized strain path 3.

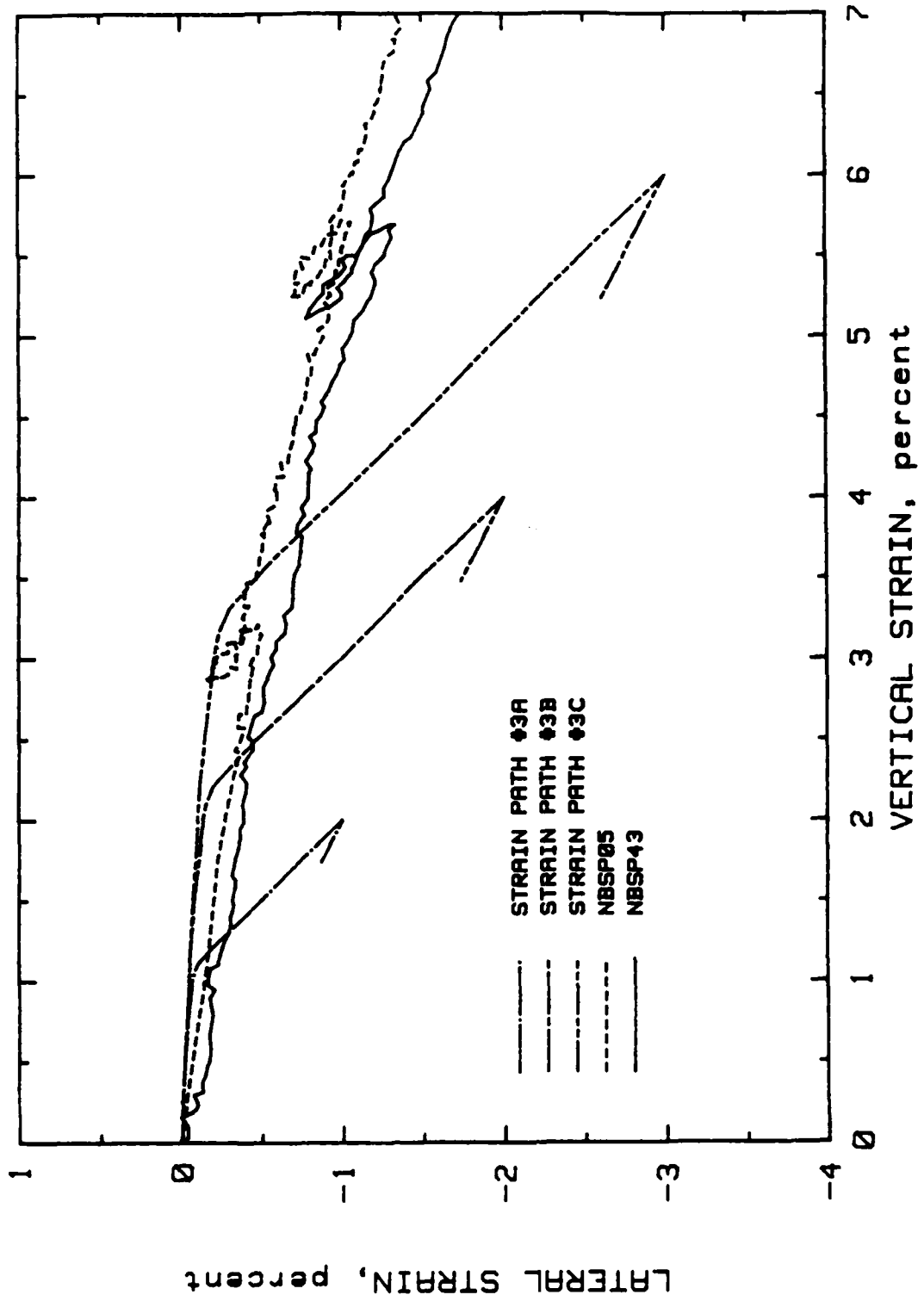


Figure 3.12 Comparison of TXC strain paths with strain paths 3A, 3B, and 3C.

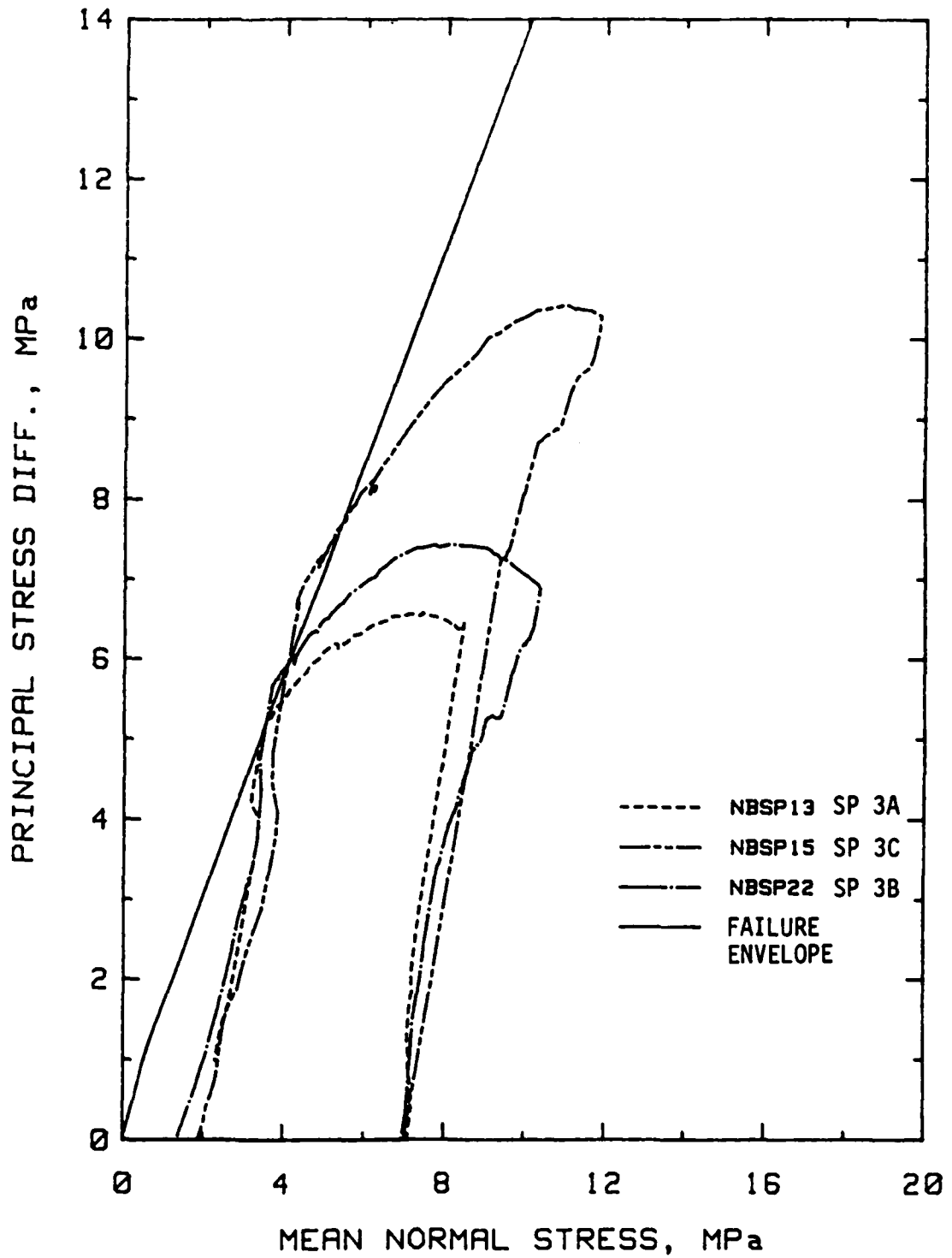


Figure 3.13 Stress path data from SP 3 tests.

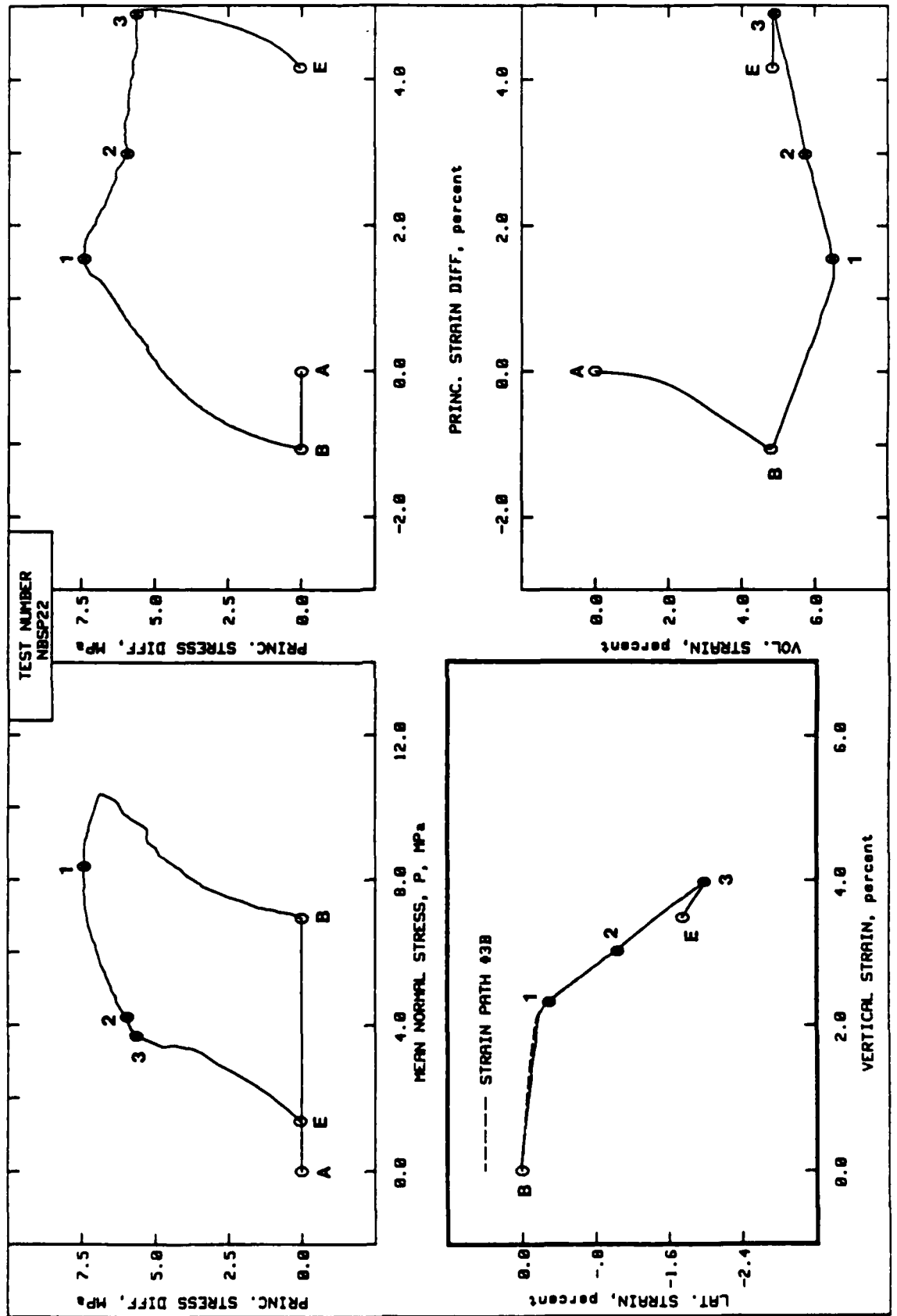


Figure 3.14 Typical plot of SP 3B data showing specimen "yield" or "flow."

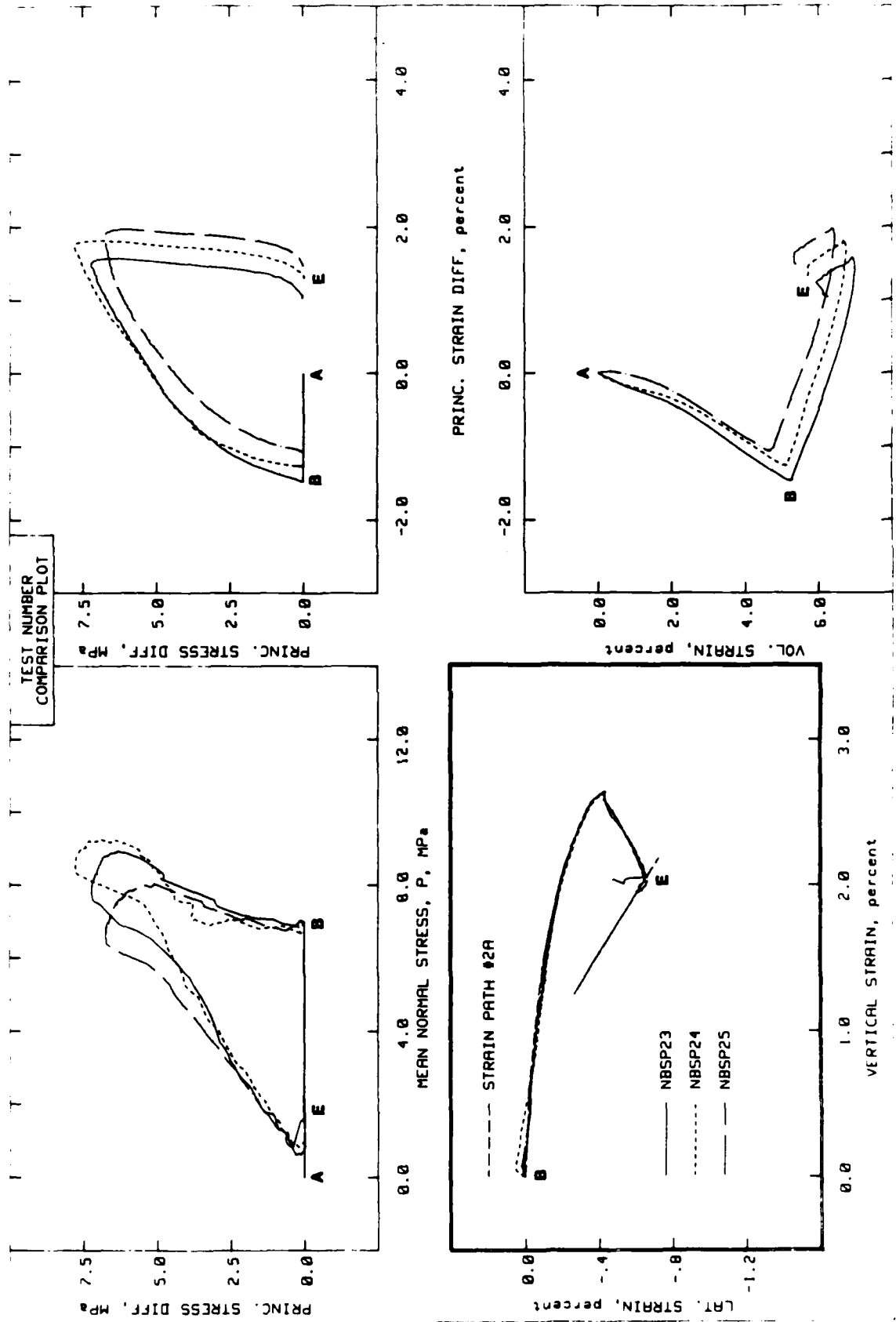


Figure 3.15 Results of tests that followed strain path 2A.

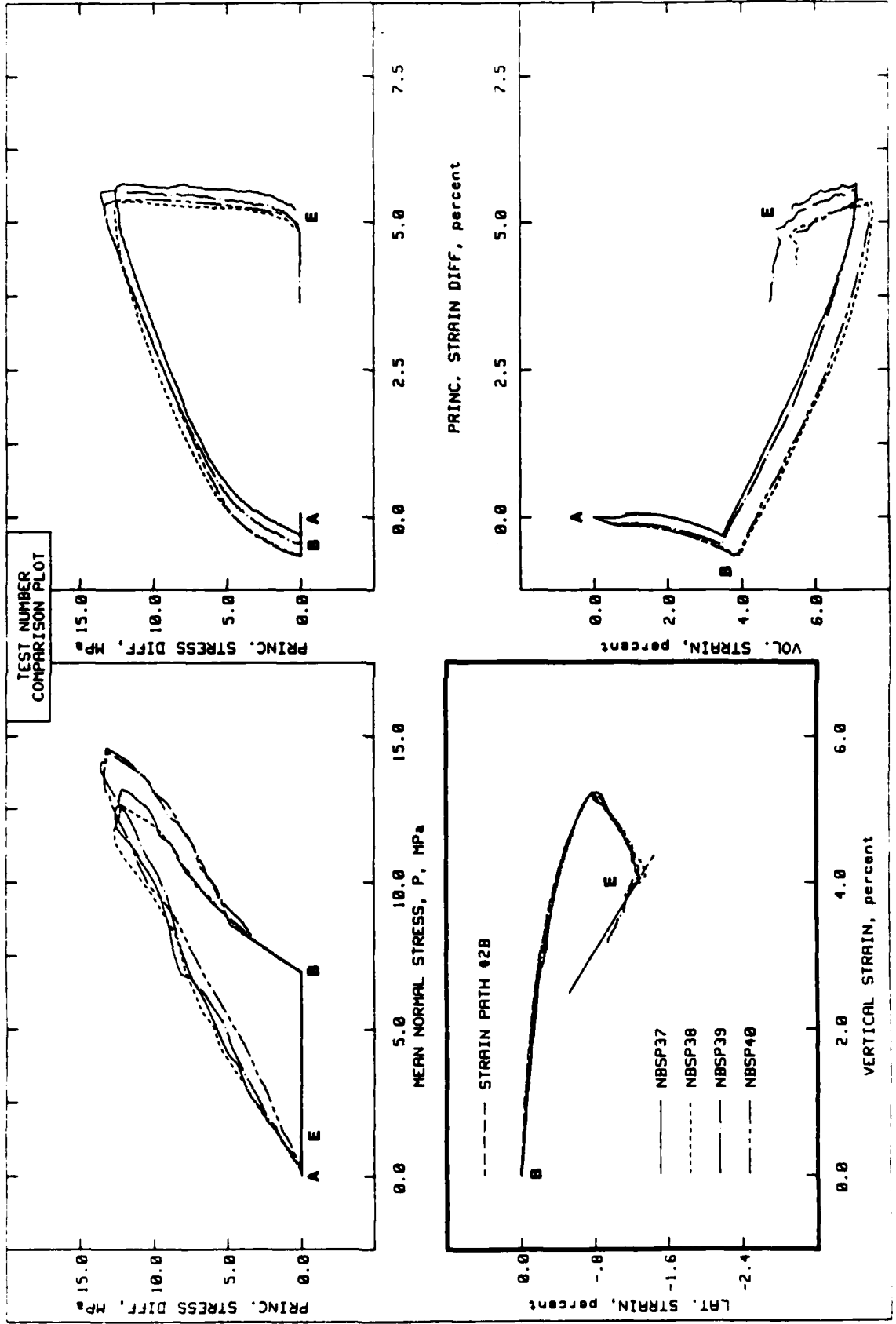


Figure 3.16 Results of tests that followed strain path 2B.

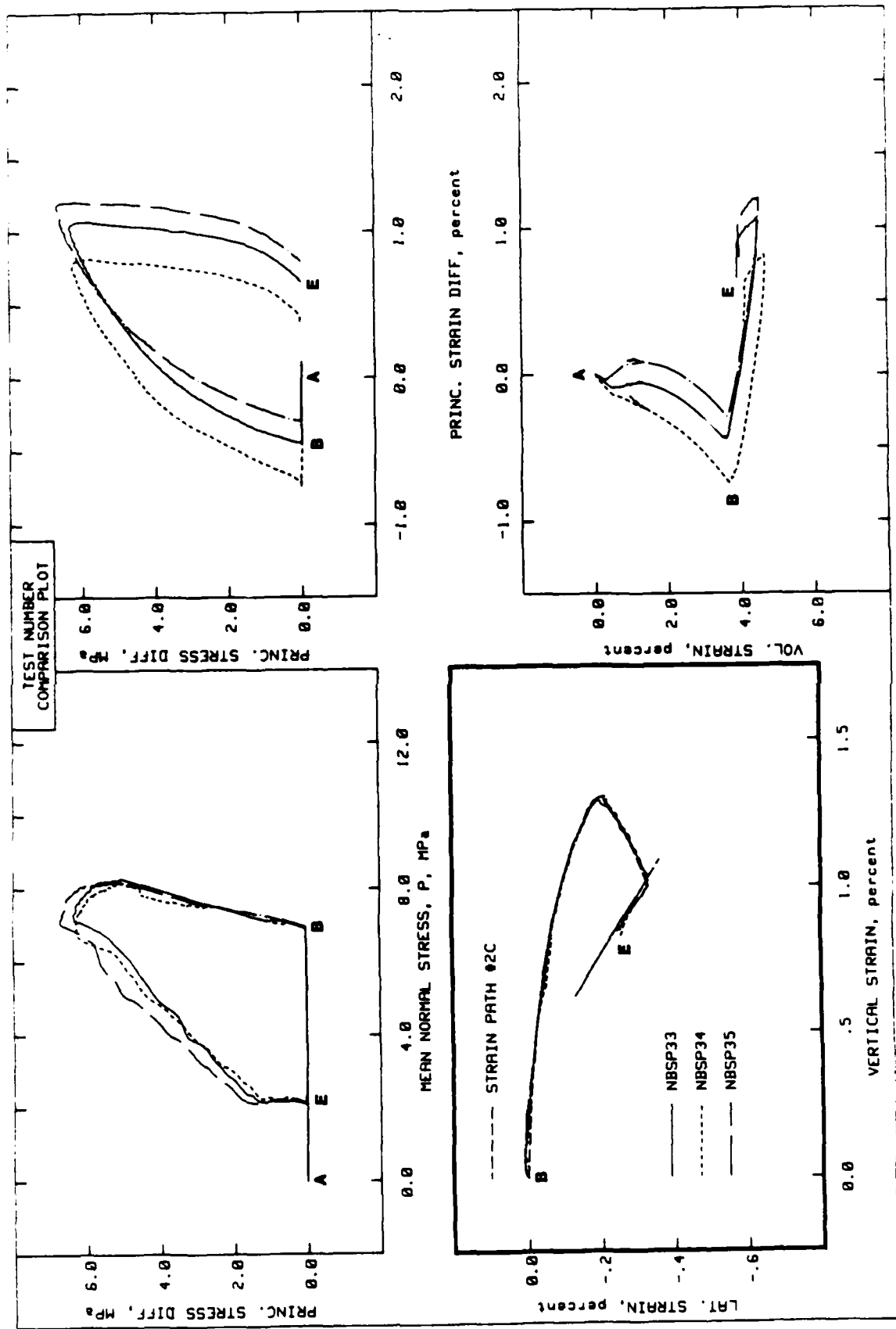


Figure 3.17 Results of tests that followed strain path 2C.

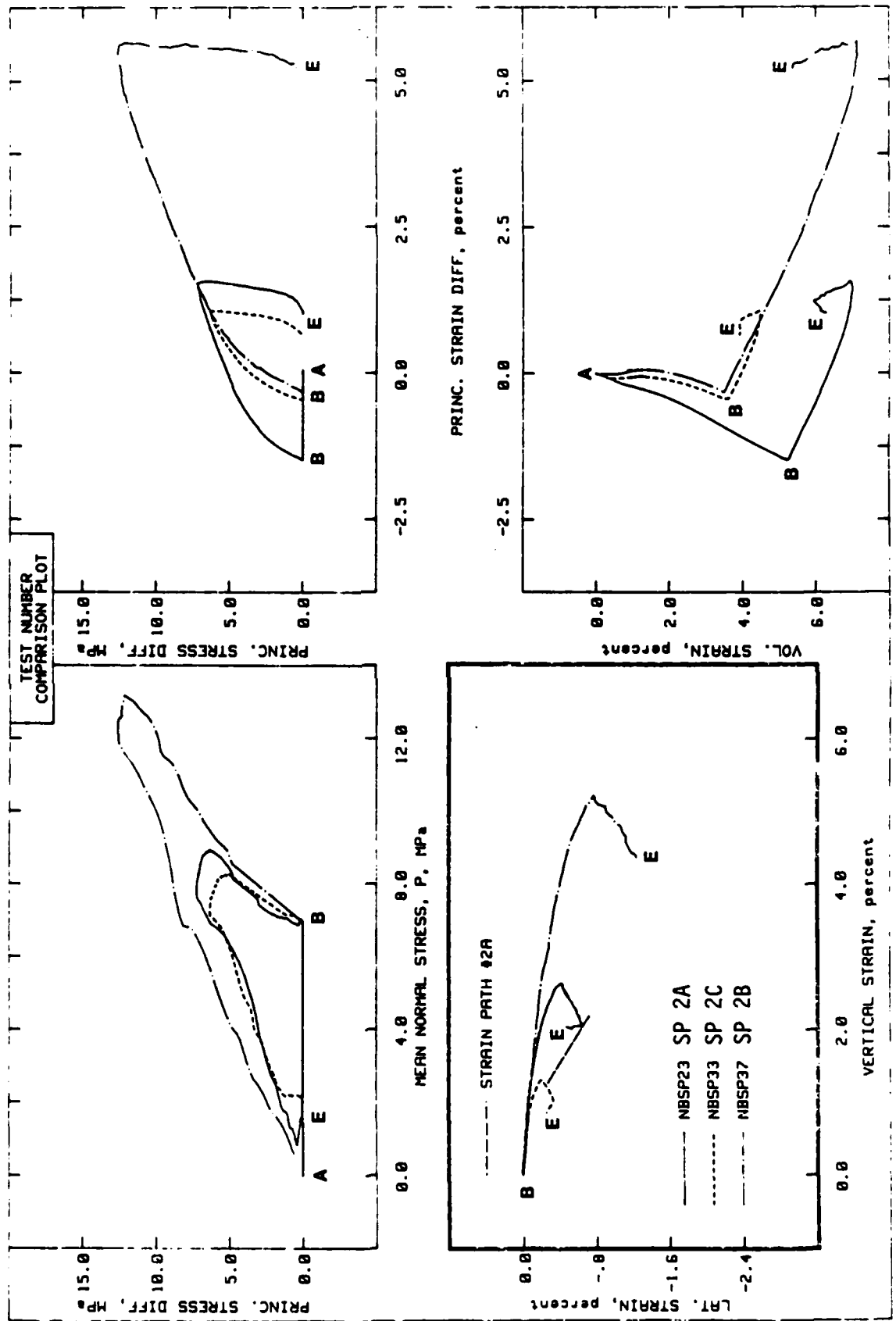


Figure 3.18 Comparison of results of tests that followed strain paths 2A, 2B, and 2C.

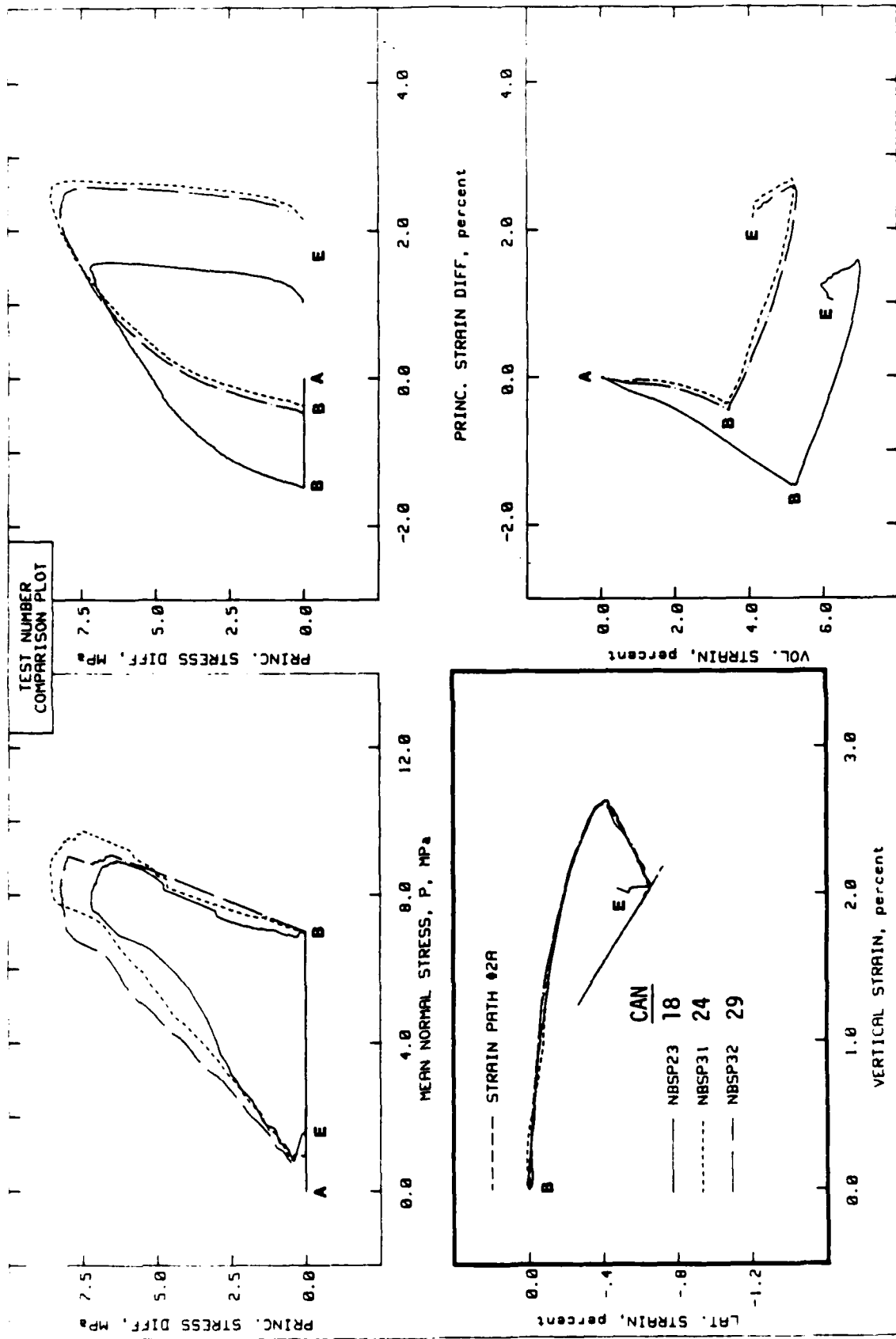


Figure 3.19 Effect of material variations on SP 2A test results.

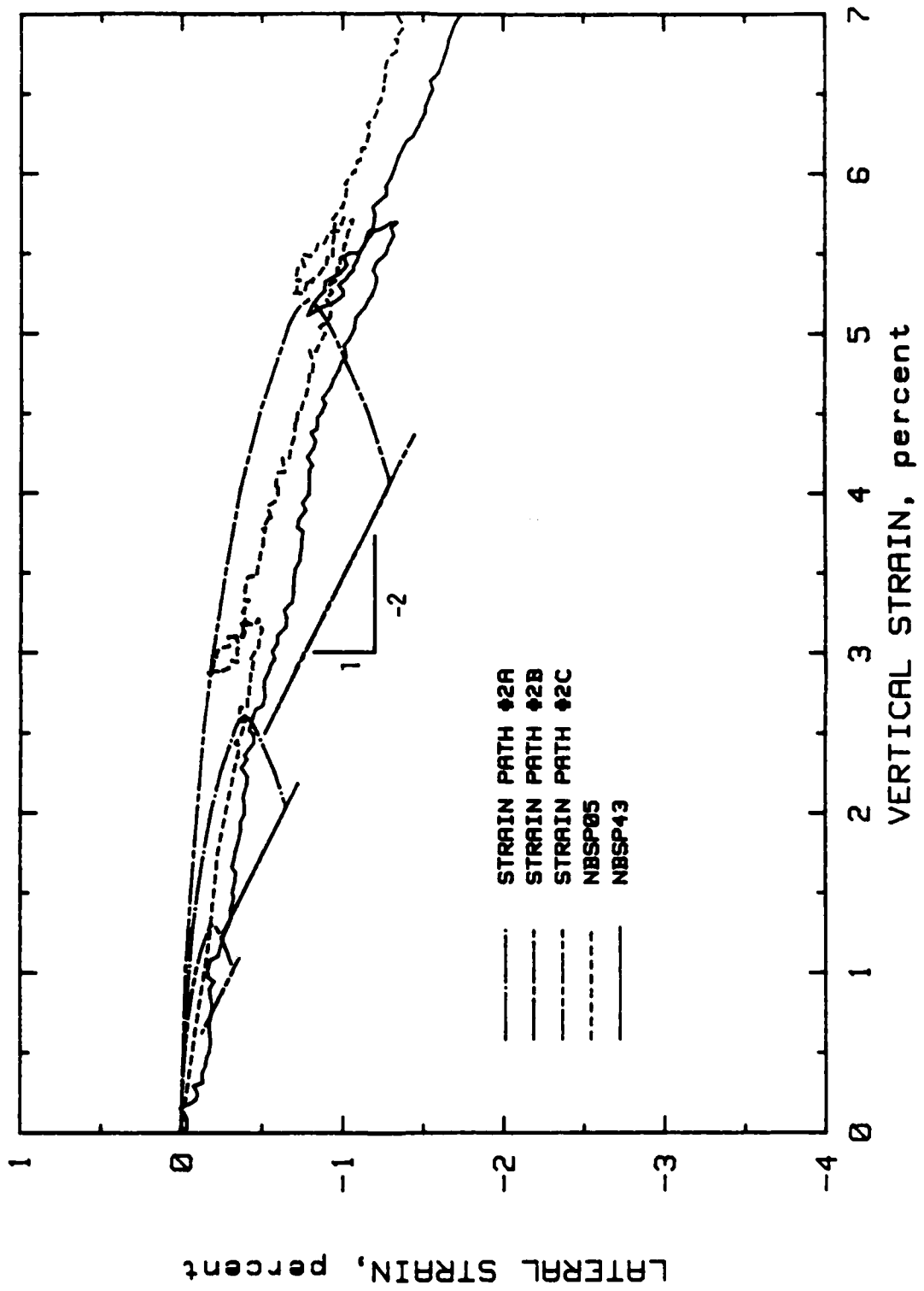


Figure 3.20 Comparison of TXC strain path with strain paths 2A, 2B, and 2C.

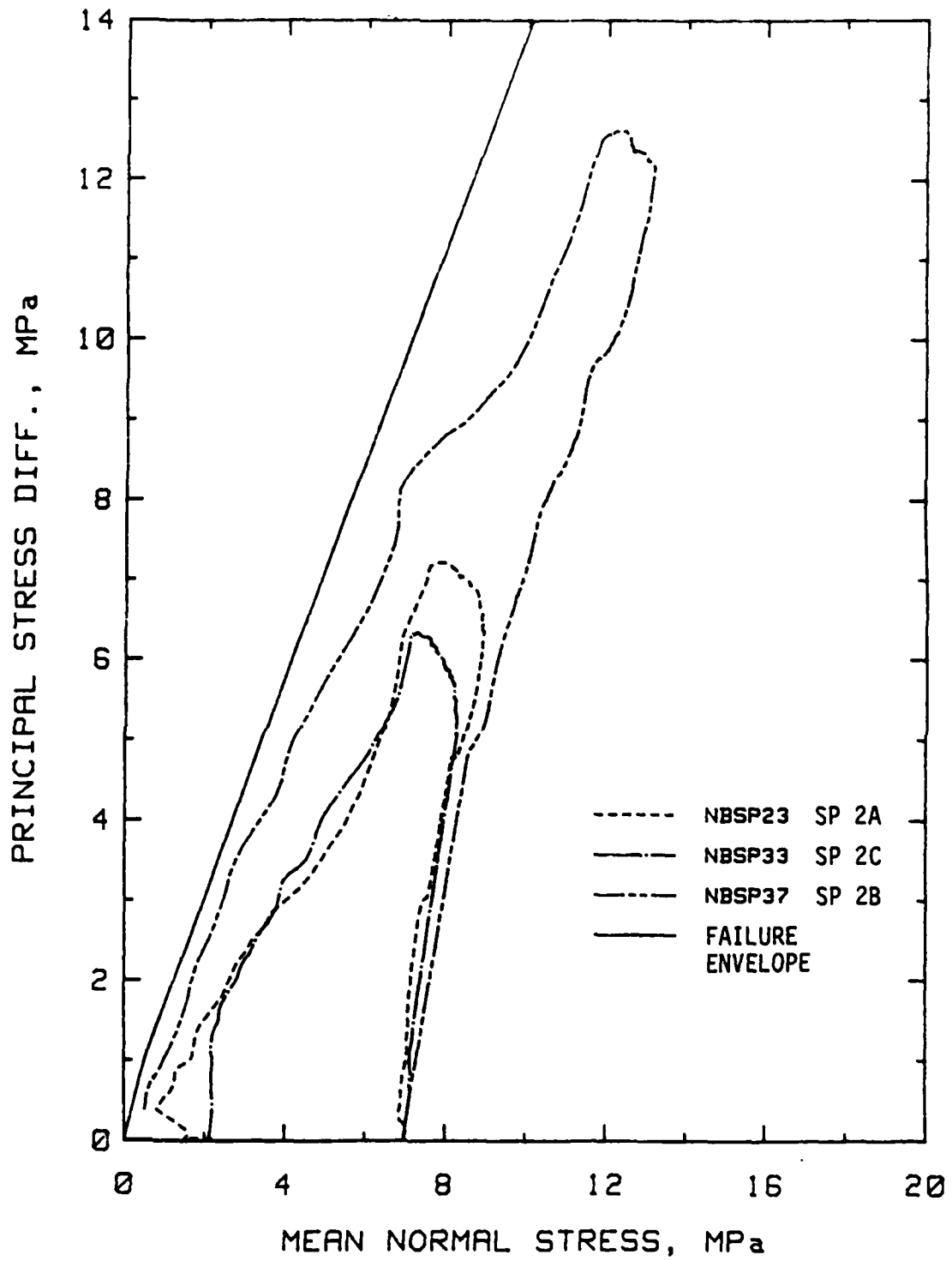


Figure 3.21 Stress path data from SP 2 tests.

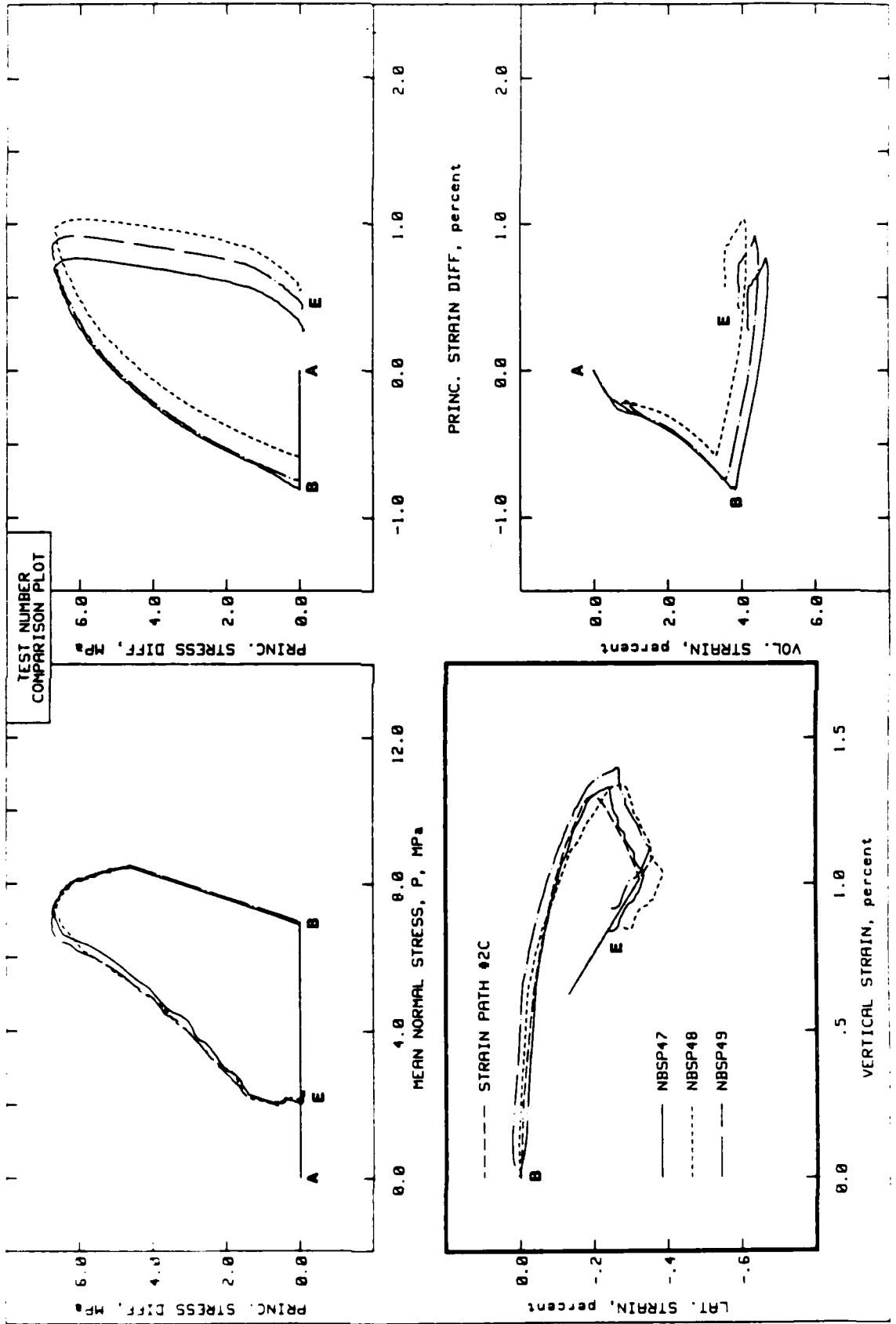


Figure 3.22 Results of reverse strain path tests following stress path 2C.

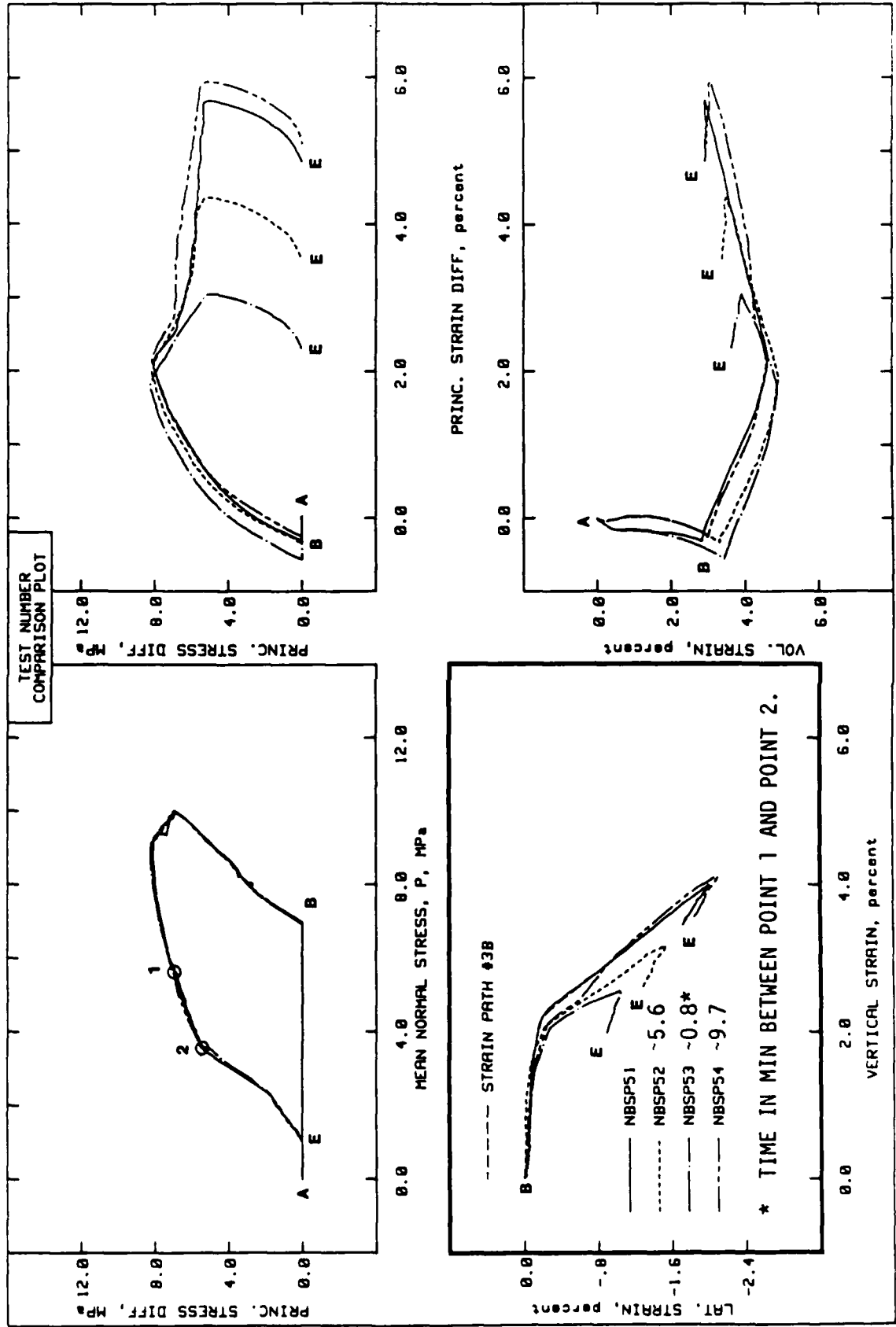


Figure 3.23 Results of reverse strain path tests following stress path derived from strain path 3B.

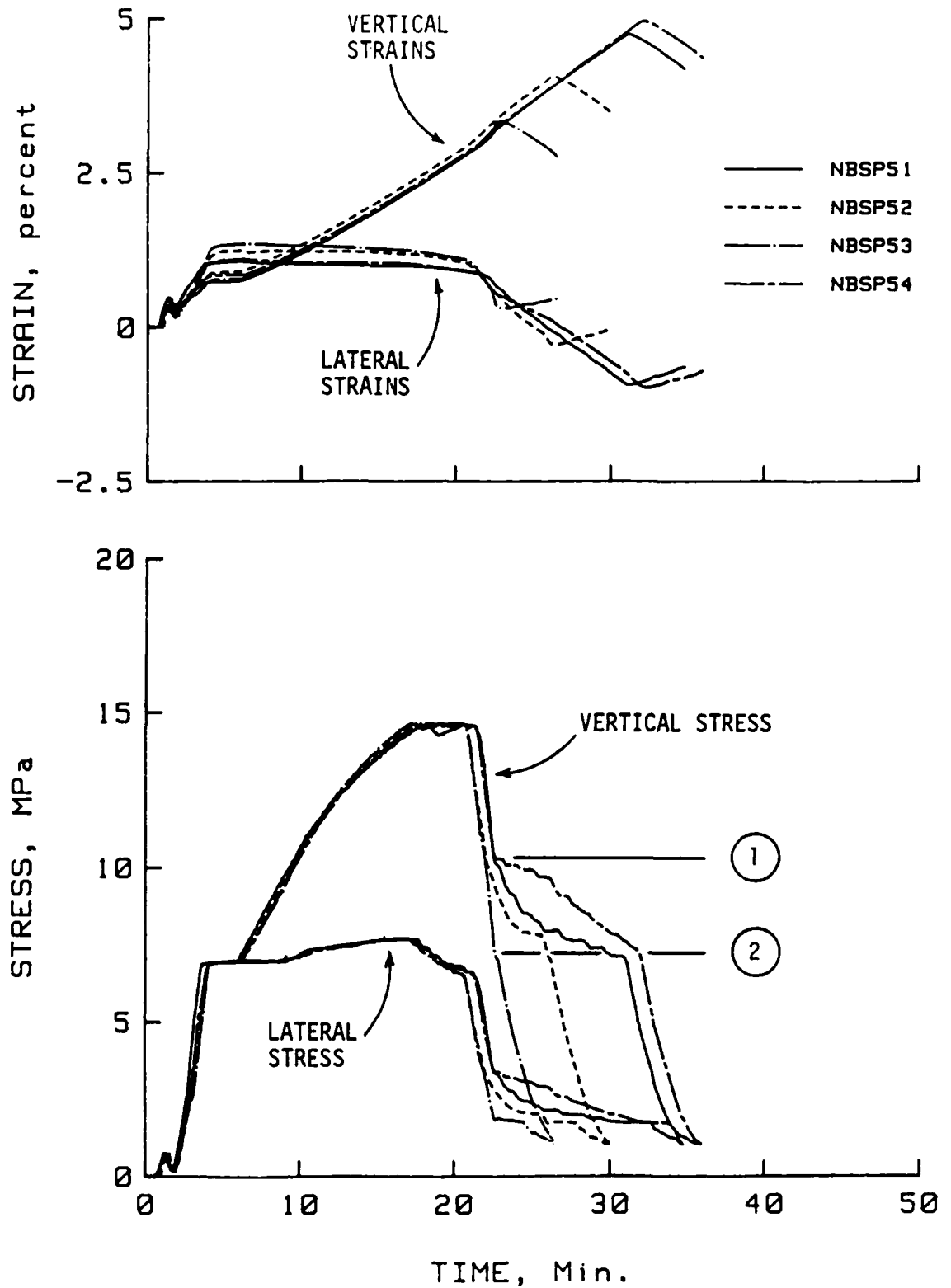


Figure 3.24 Stress-strain-time histories from reverse strain path tests following SP 3B stress path.

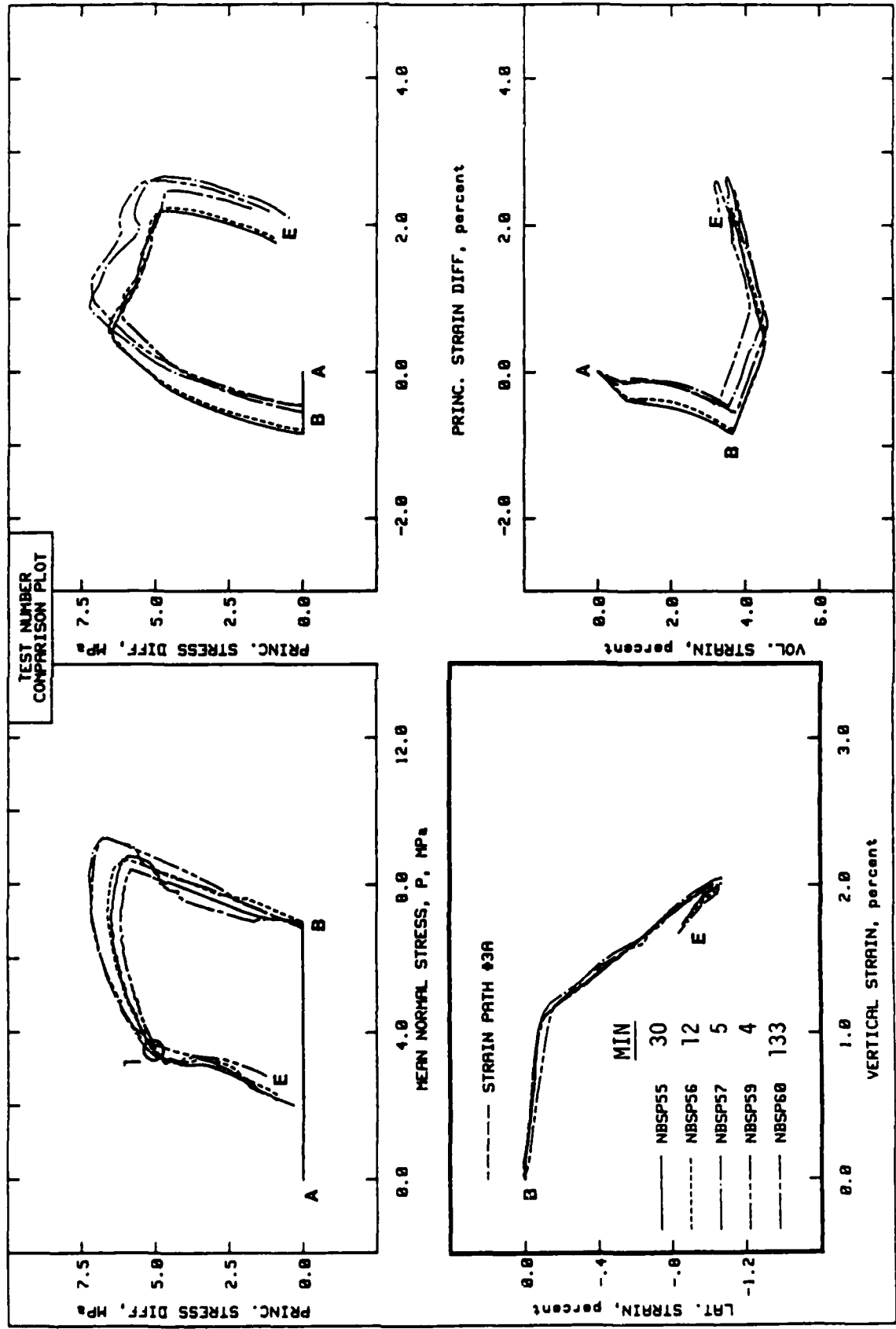


Figure 3.25 Results of strain-rate tests along strain path 3A.

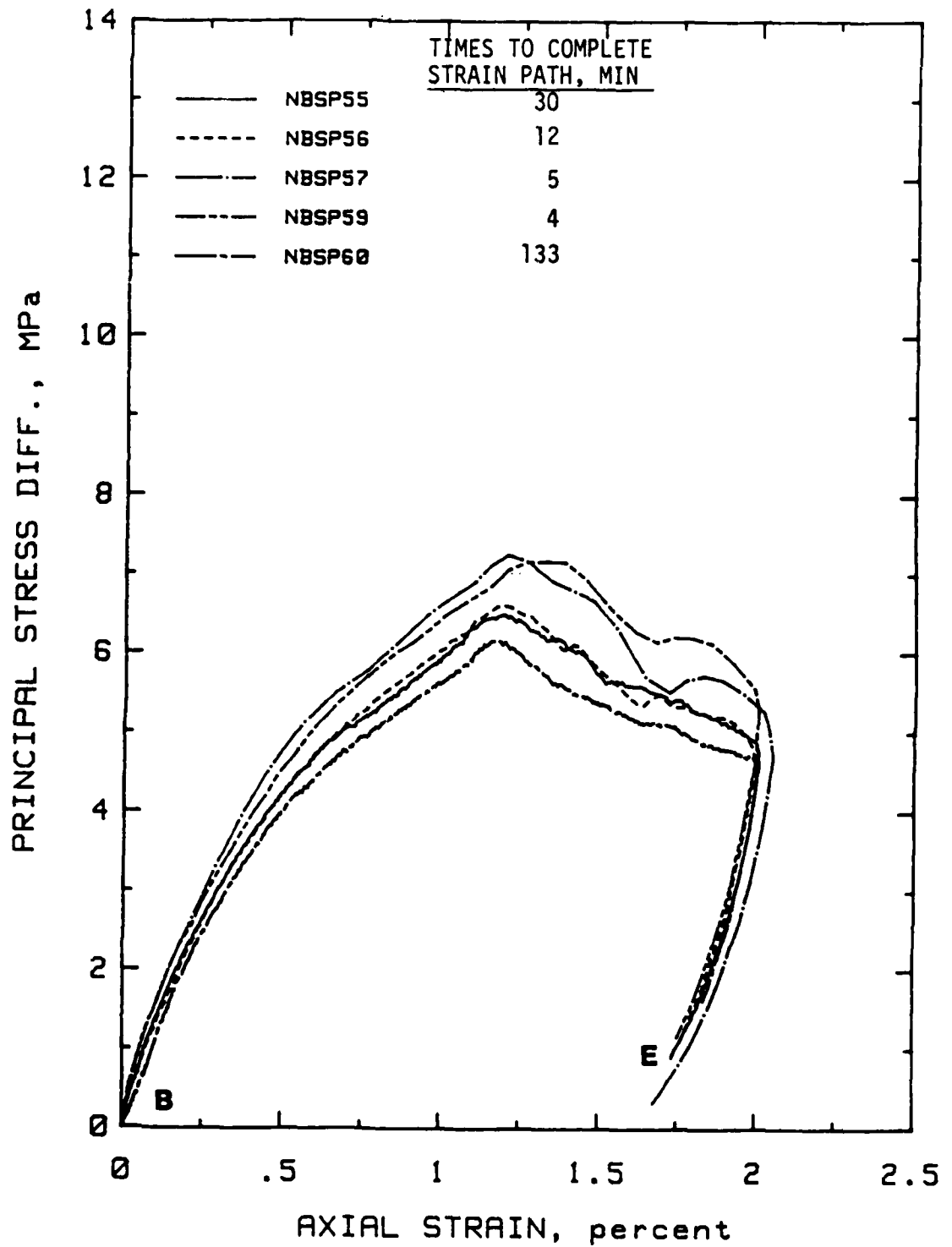


Figure 3.26 Effects of deformation rate on stress-strain curves.

CHAPTER 4

CONCLUSIONS AND RECOMMENDATIONS

This chapter summarizes major observations and conclusions presented in Chapter 3 and contains recommendations for additional strain path testing.

4.1 CONCLUSIONS

The volumetric strain response of NB sand is a function of both density and gradation. Very small differences in gradation caused significant changes in volumetric response. It should be emphasized that these "significant" differences were only 1-2 percent strain; undisturbed test specimens normally exhibit much greater variability. In addition, these response differences were caused by only one batch of material out of five; test specimens constructed from the other four cans of material showed excellent repeatability.

The TXC test results exhibited excellent repeatability for specimens constructed from one material. The volumetric response during these TXC tests was produced by changes in both the applied mean normal stress or pressure and the applied shear stresses. This has an important implication with respect to the strain path tests. Strain path tests are essentially controlled volume tests, i.e., by fixing the vertical and lateral strains, one also fixes the volumetric strains. Thus, if TXC tests on two materials give different volumetric responses, then the stress paths produced by subjecting these same two materials to a common strain path should be different.

TXC test data provided other important information with respect to strain path response. The stress path generated during the initial loading of a strain path test could be estimated by comparing the intended strain path to a typical TXC test strain path. If the TXC strain path plotted below the intended strain path, the confining pressure must be increased for the two paths to coincide. The confining pressure must be decreased if the TXC strain path plotted above the intended strain path.

Results of the Phase I test program demonstrated that by following a given strain path at a given strain rate, a unique stress path will be produced. Excellent repeatability was observed in the strain path test results first, because a given strain path could be followed very closely and second, because consistent high-quality specimens were tested. The reverse tests

conducted during the Phase II test program, however, demonstrated that a unique stress-strain relationship is not always obtained by following a given stress path. For stress paths which plot below the failure envelope, there appears to be a unique and reversible stress-strain relationship. For tests whose stress paths ride the failure envelope, there is no reversible stress-strain relationship. Under these latter conditions, a given stress path can produce several different strain paths due to the time-dependent deformation taking place while riding the failure envelope.

The strain path tests conducted at several different strain rates produced very similar stress paths with only small differences in peak stress level; i.e., less than 20 percent. More significant differences would be expected if tested under millisecond or submillisecond loading rates.

4.2 RECOMMENDATIONS

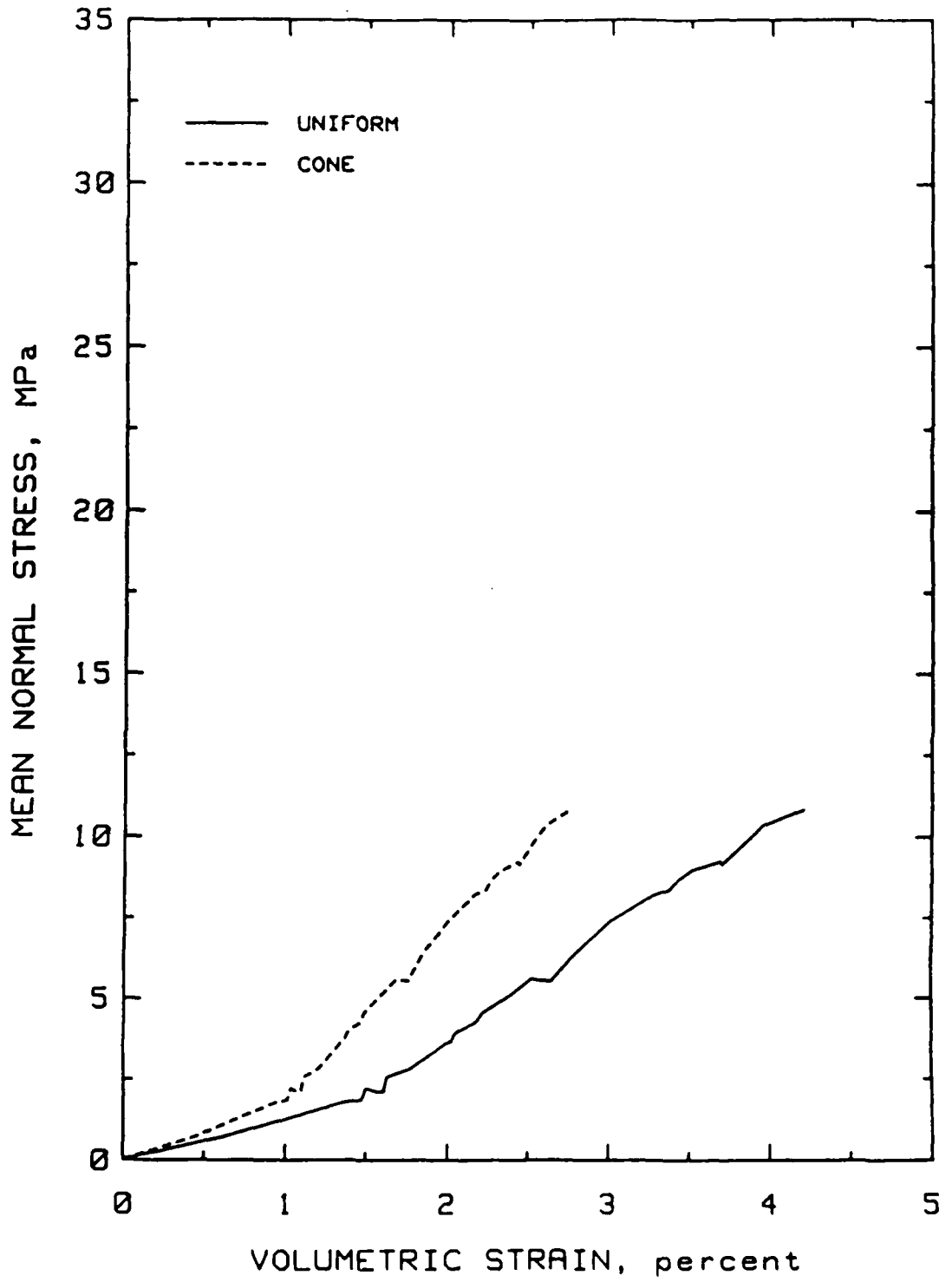
Having demonstrated the ability to conduct strain path tests on cylindrical samples, WES is now ready to conduct tests on other materials. There is an obvious need to obtain test data on undisturbed specimens. The effects of variables such as depth, water content, density, prestress, and strain rate should be investigated. This will require comparative tests on both undisturbed and remolded specimens.

New equipment needs to be developed. At WES, the minimum SP test duration is approximately 4 minutes using the existing manually-controlled system. To achieve higher strain rates, an automated system is required. The ultimate goal would be to achieve millisecond and submillisecond loadings.

REFERENCES

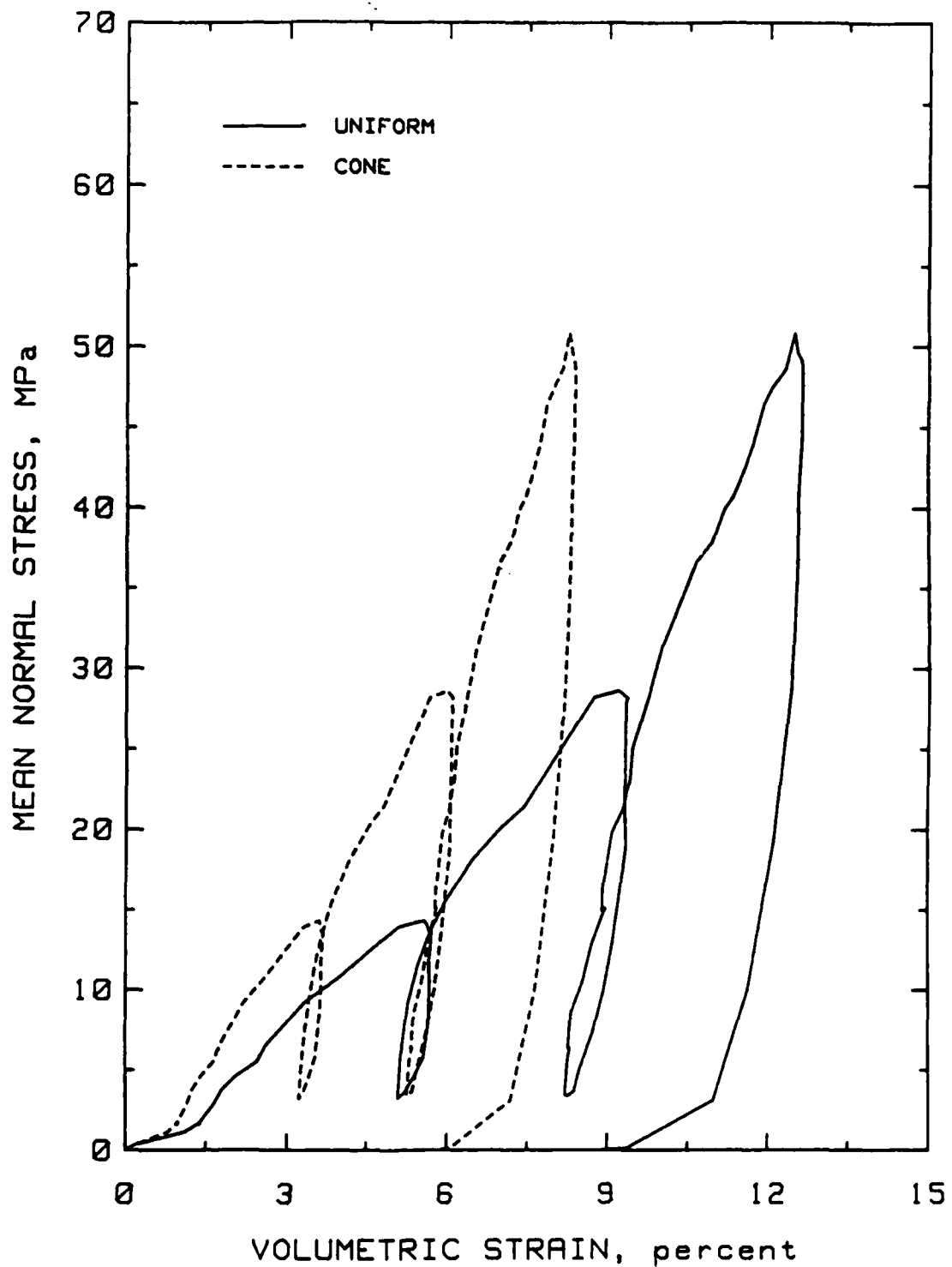
1. J. W. Workman, J. G. Trulio, and E. S. Stokes; "Trajectory Analysis, an Aid in Defining the MX System Ground Motion"; May 1981, AFWL-TR-80-56, Vol 1; Air Force Weapons Laboratory, Kirtland Air Force Base, NM.
2. J. G. Trulio; "Strain Path Analysis and Testing"; May 1982, DNA-IR-82-23-V1; Proceedings of the Strategic Structures Review Conference, 4-6 May 1982, Menlo Park, CA.
3. J. G. Trulio; "Strain Path Modeling for Geo-Materials"; Presentation made at the Workshop on the Theoretical Foundation for Large-Scale Computations of Nonlinear Material Behavior, 24-26 October 1983, Evanston, IL.
4. H. Y. Ko and R. W. Meier; "Cubical Test Data and Strain Path Testing on Nellis Baseline Sand"; January 1983; Department of Civil, Environmental and Architectural Engineering, University of Colorado, Boulder, CO.
5. U. S. Army Engineer Waterways Experiment Station; "The Unified Soil Classification System"; Technical Memorandum No. 3-357, April 1960 (reprinted May 1967, Amended 1 May 1980); CE, Vicksburg, MS.
6. S. A. Akers; "Constitutive Properties for Undisturbed Marine Sediments in Support of the Subseabed Disposal Program, Annual Report No. 4"; March 1983, U. S. Army Engineer Waterways Experiment Station, CE, Vicksburg, MS.
7. Personal communication with Mr. R. W. Meier.
8. Headquarters, Department of the Army, Chief of Engineers; "Laboratory Soils Testing"; Engineering Manual No. EM-1110-2-1906, 30 November 1970; Washington, DC.
9. J. D. Cargile; "Laboratory Test Results for Nellis Baseline Sand"; October 1983; U. S. Army Engineer Waterways Experiment Station, CE, Vicksburg, MS.

NELLIS BASELINE SAND



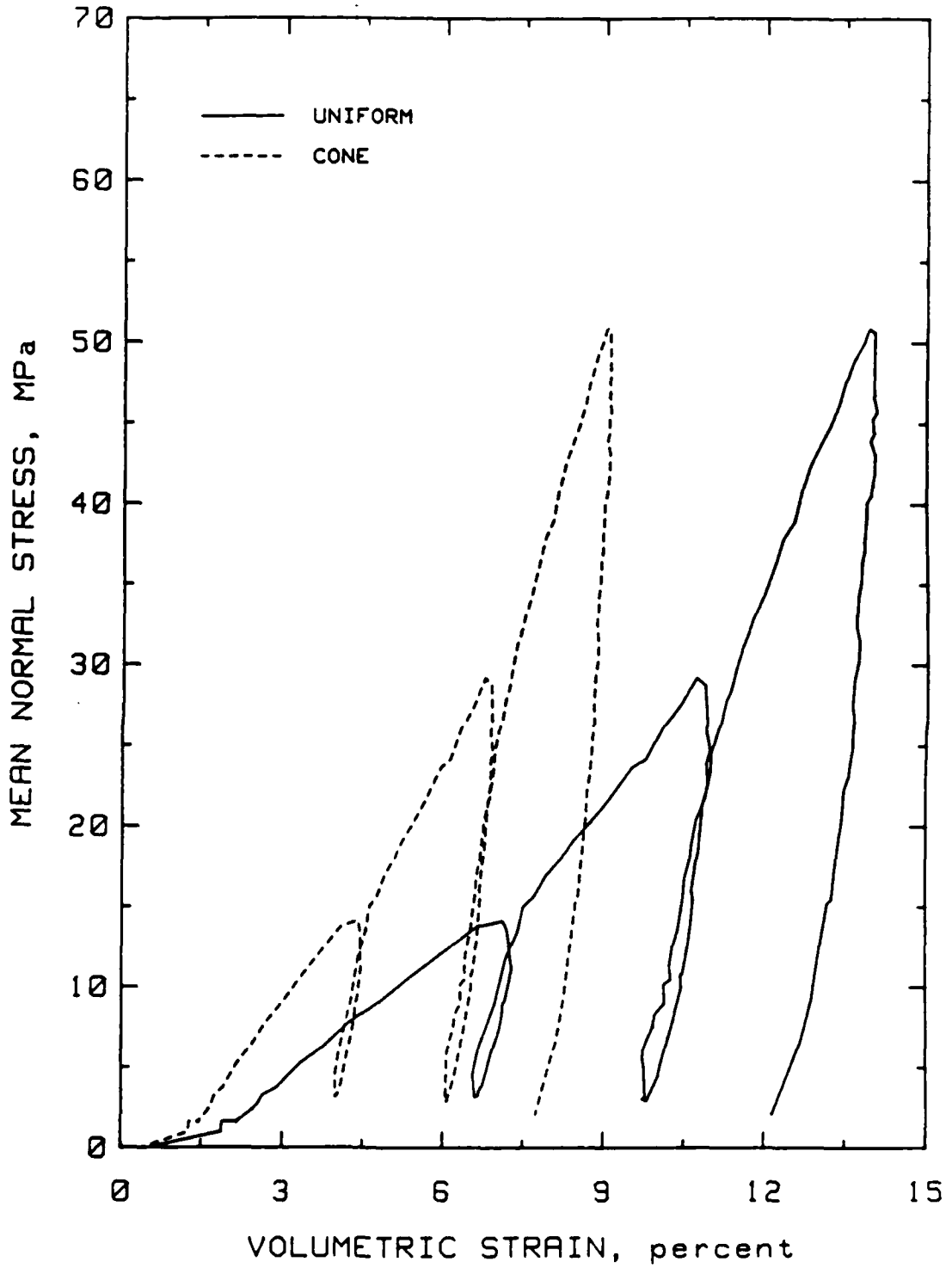
TEST NO: NBSP01
STATIC HYDROSTATIC COMPRESSION TEST
MEAN NORMAL STRESS vs VOLUMETRIC STRAIN

NELLIS BASELINE SAND



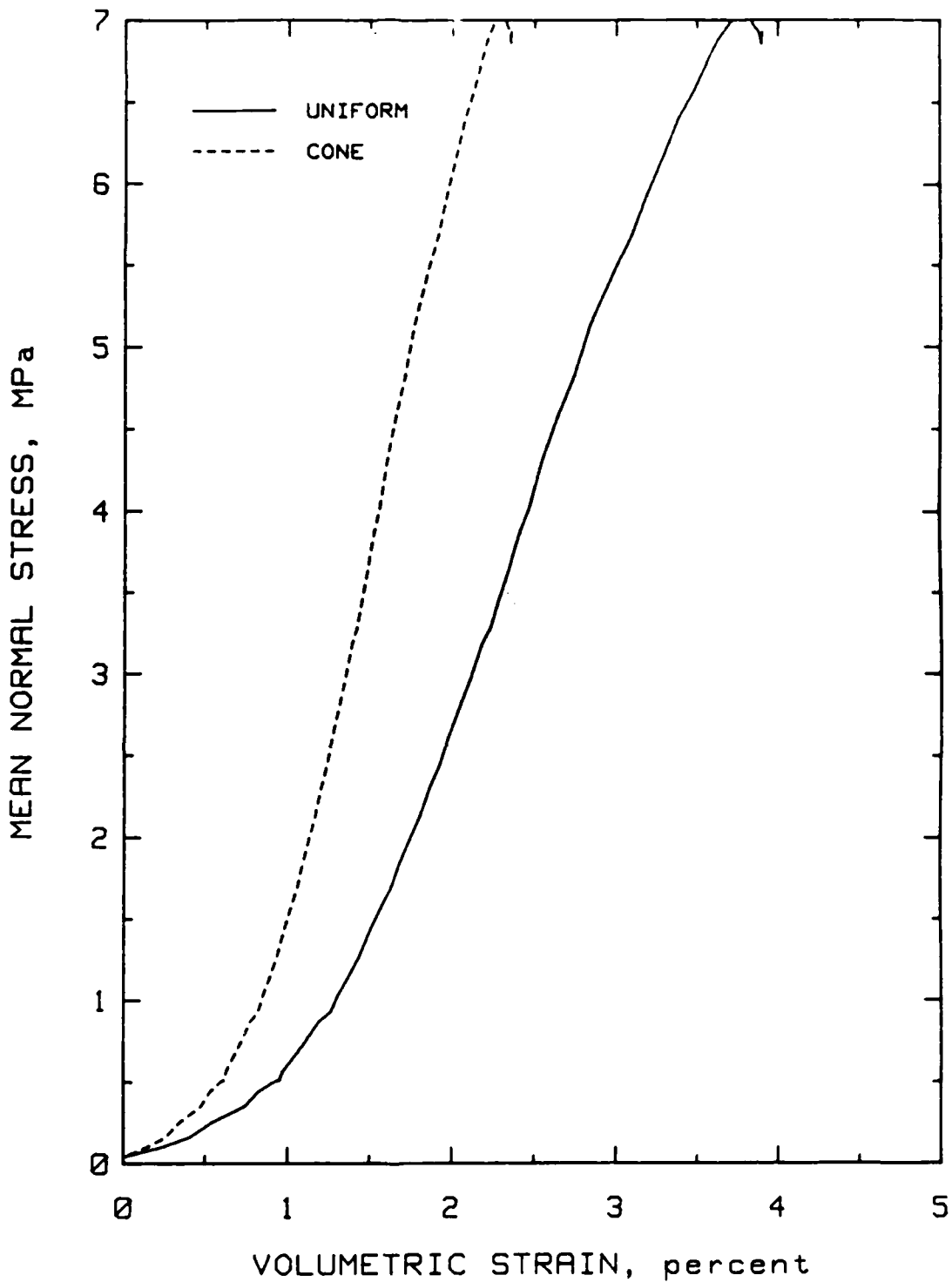
TEST NO: NBSP02
STATIC HYDROSTATIC COMPRESSION TEST
MEAN NORMAL STRESS vs VOLUMETRIC STRAIN

NELLIS BASELINE SAND



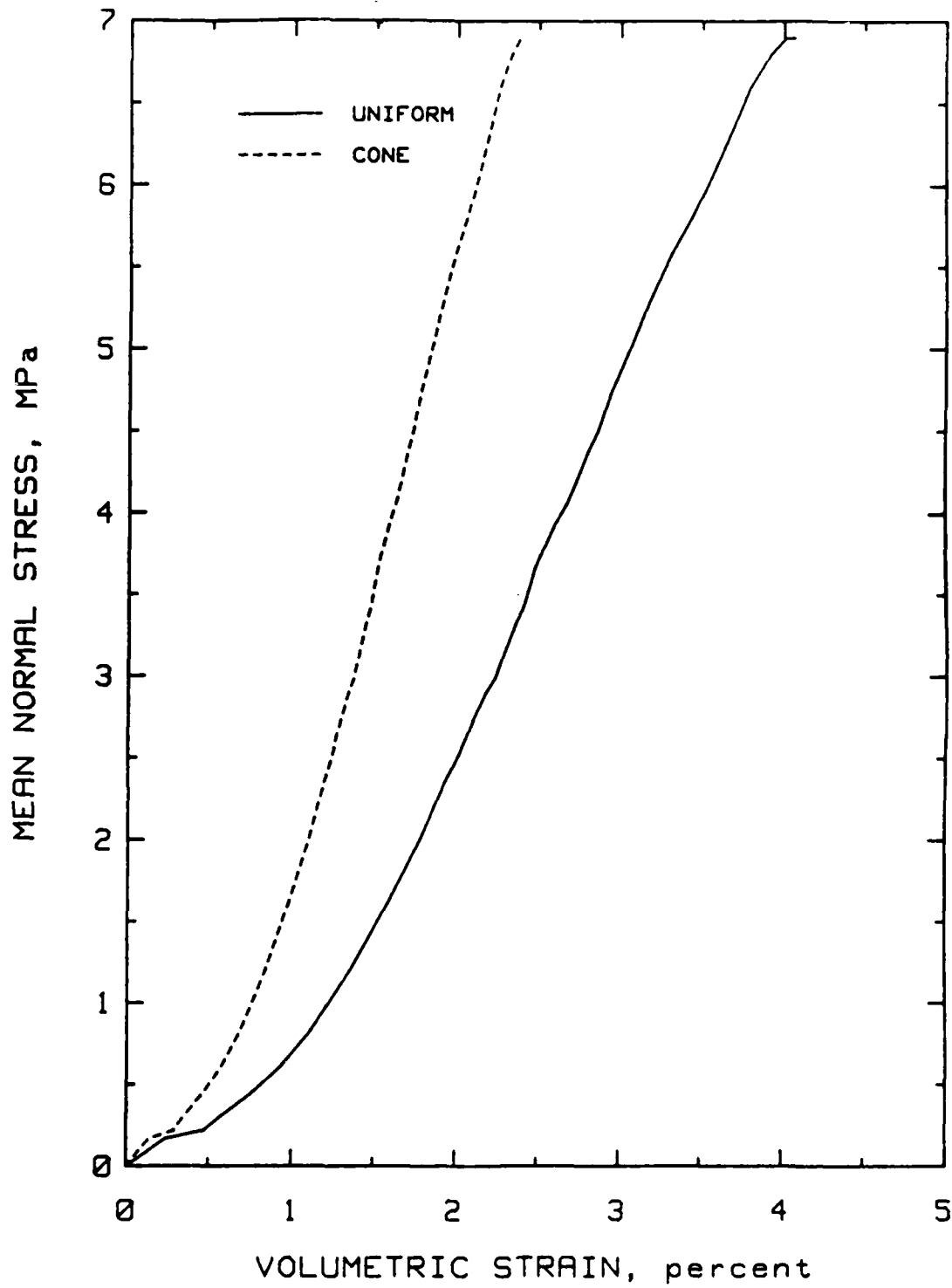
TEST NO: NBSP04
STATIC HYDROSTATIC COMPRESSION TEST
MEAN NORMAL STRESS vs VOLUMETRIC STRAIN

NELLIS BASELINE SAND



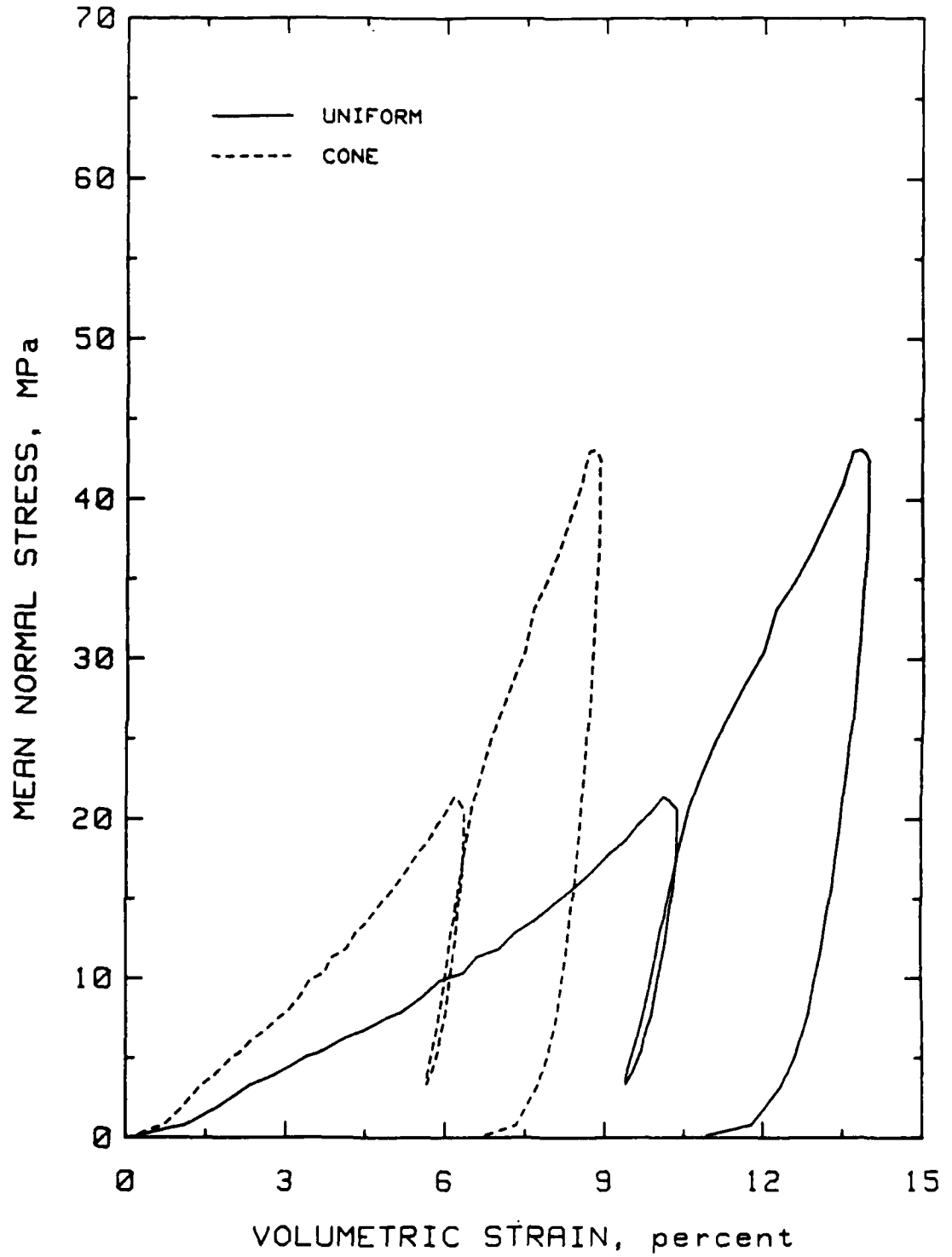
TEST NO: NBSP17
STATIC HYDROSTATIC COMPRESSION TEST
MEAN NORMAL STRESS vs VOLUMETRIC STRAIN

NELLIS BASELINE SAND



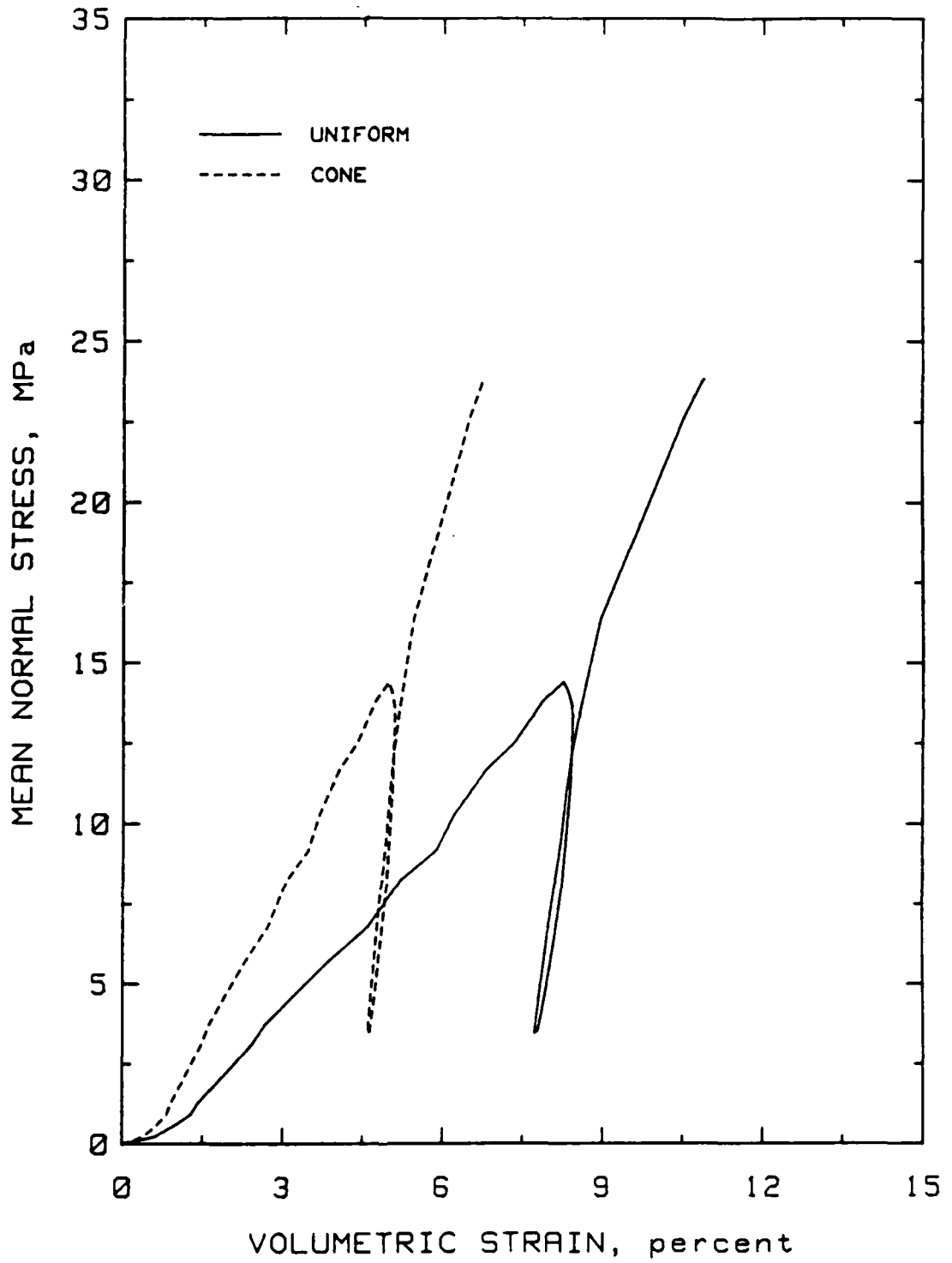
TEST NO: NBSP19
STATIC HYDROSTATIC COMPRESSION TEST
MEAN NORMAL STRESS vs VOLUMETRIC STRAIN

NELLIS BASELINE SAND



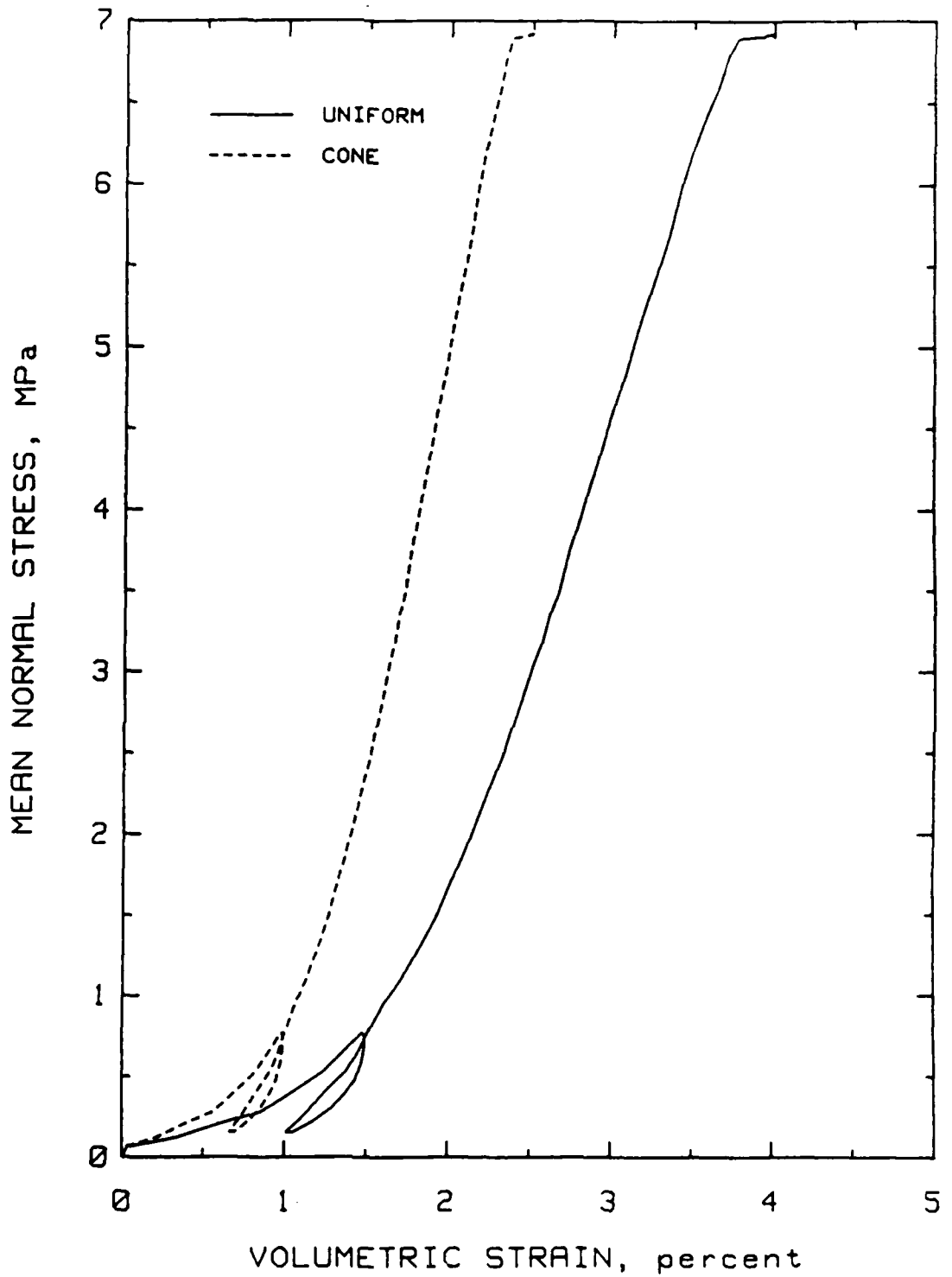
TEST NO: NBSP28
STATIC HYDROSTATIC COMPRESSION TEST
MEAN NORMAL STRESS vs VOLUMETRIC STRAIN

NELLIS BASELINE SAND



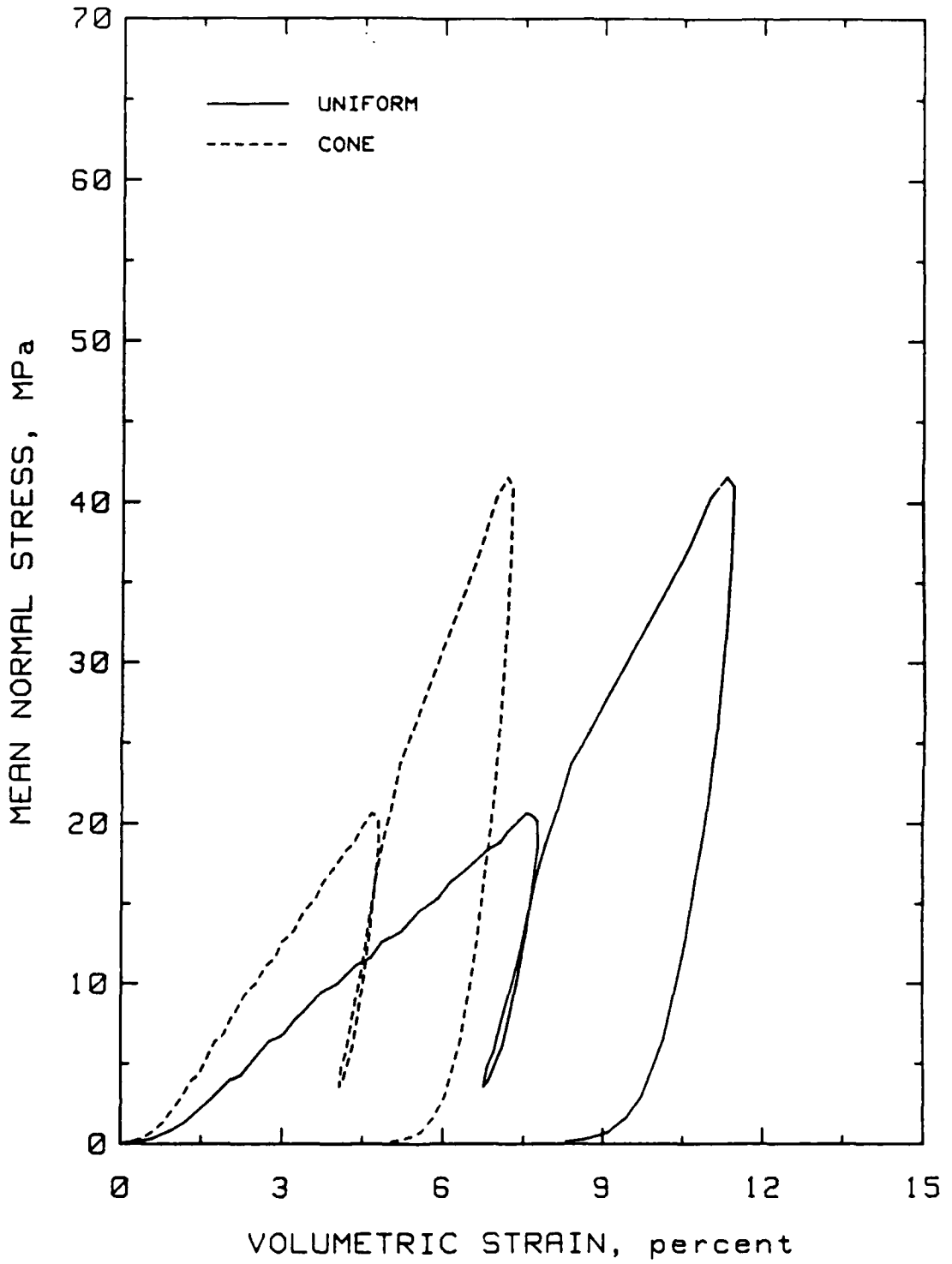
TEST NO: NBSP30
STATIC HYDROSTATIC COMPRESSION TEST
MEAN NORMAL STRESS vs VOLUMETRIC STRAIN

NELLIS BASELINE SAND



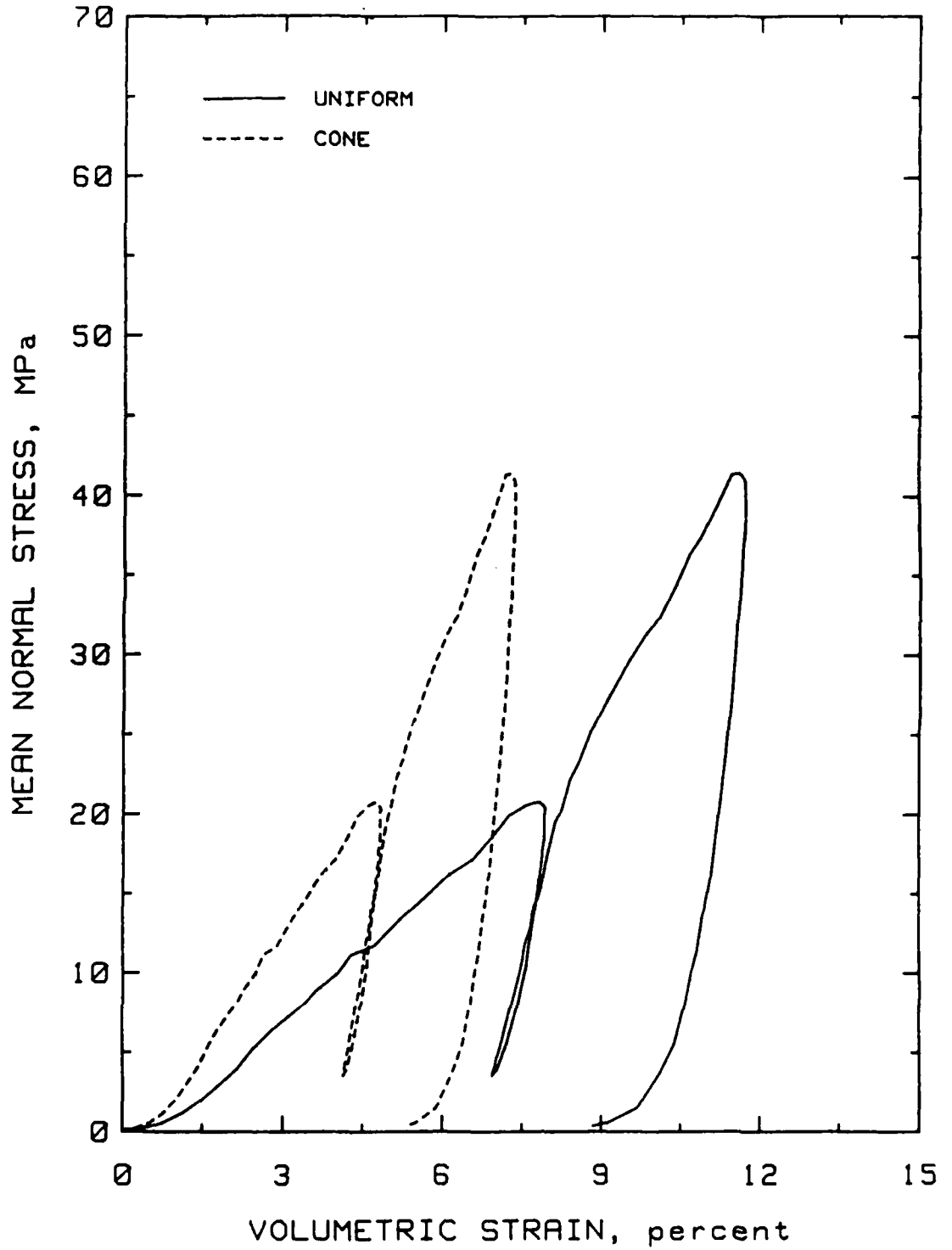
TEST NO: NBSP36
STATIC HYDROSTATIC COMPRESSION TEST
MEAN NORMAL STRESS vs VOLUMETRIC STRAIN

NELLIS BASELINE SAND



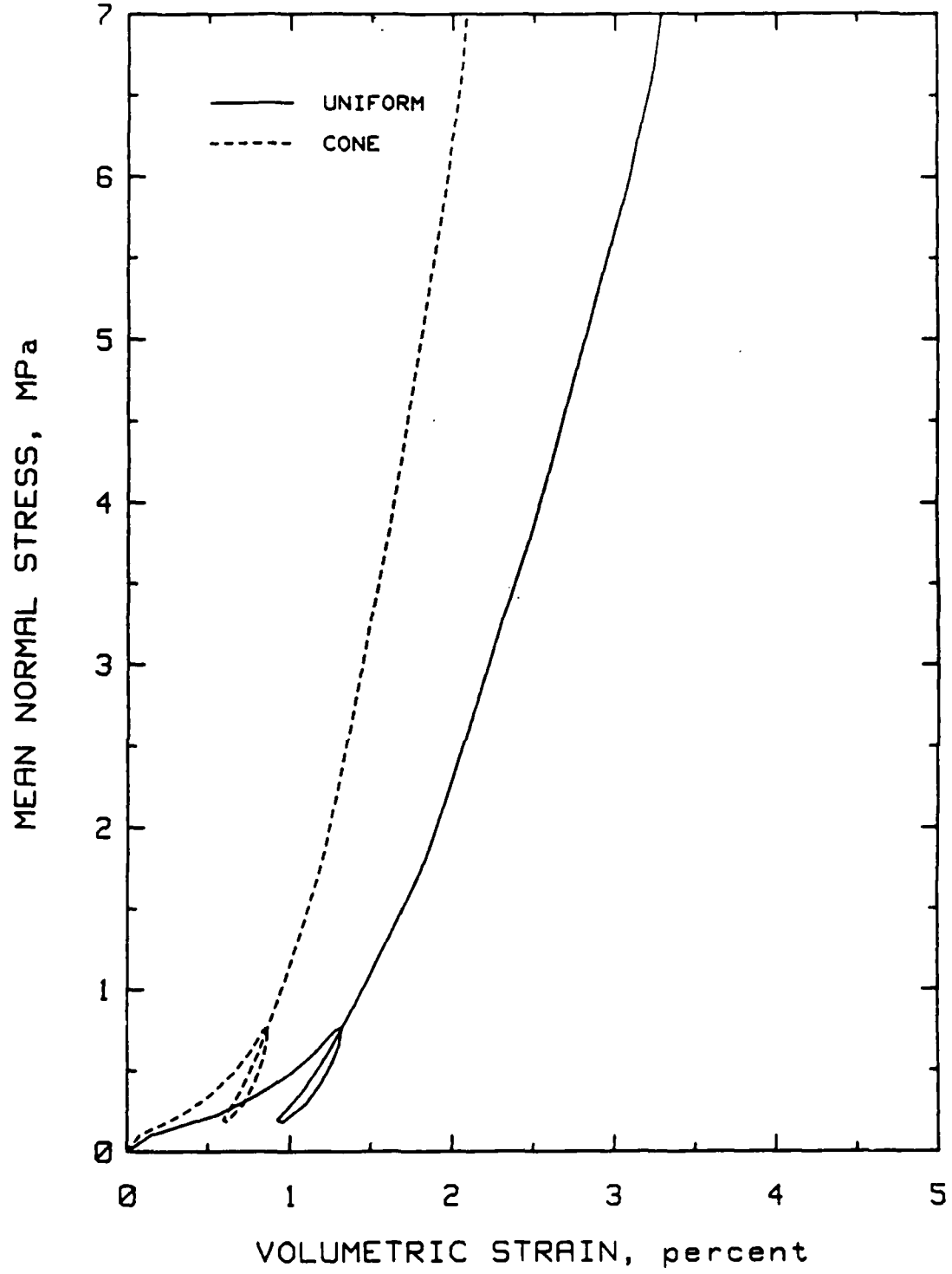
TEST NO: NBSP41
STATIC HYDROSTATIC COMPRESSION TEST
MEAN NORMAL STRESS vs VOLUMETRIC STRAIN

NELLIS BASELINE SAND



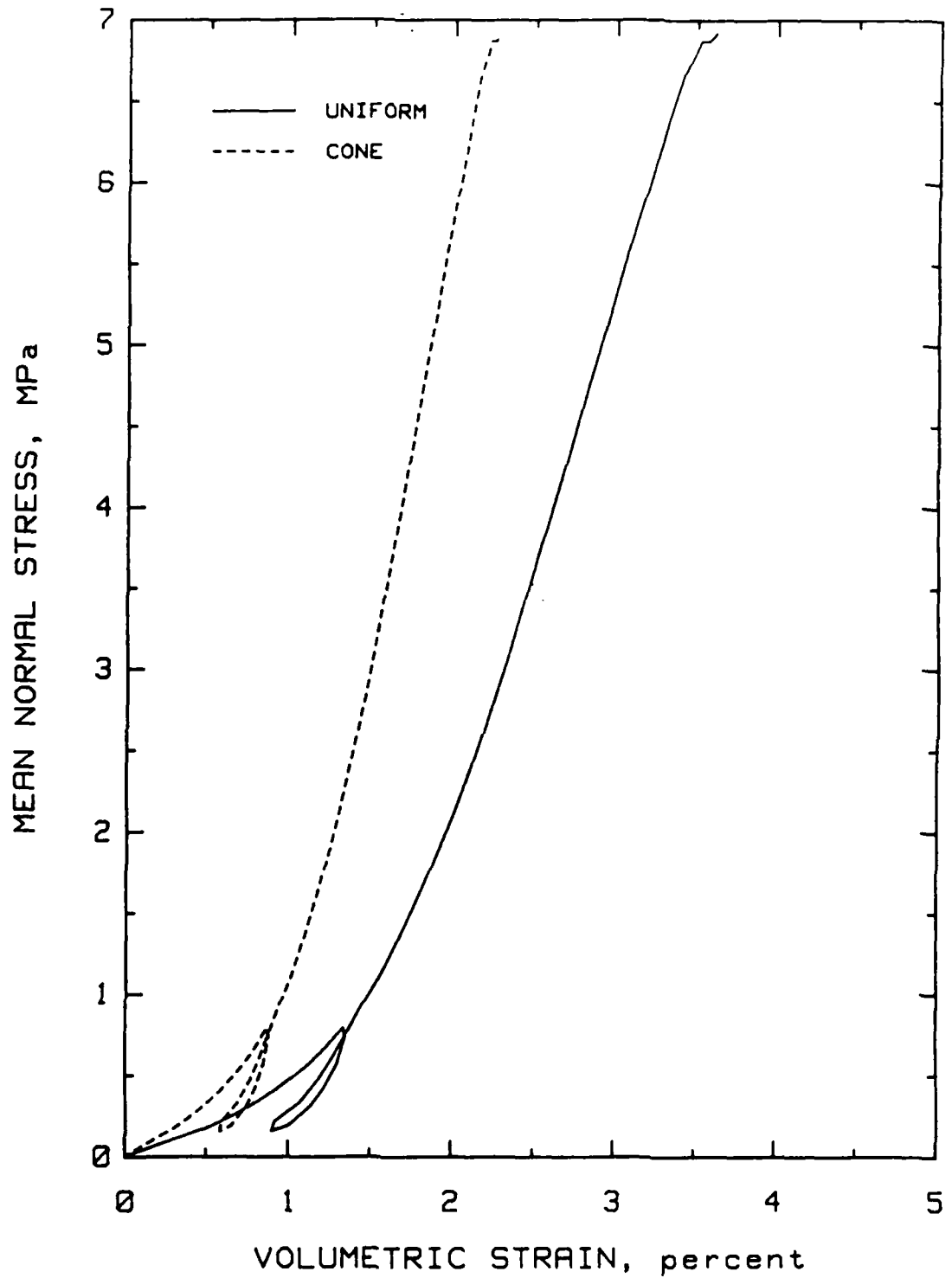
TEST NO: NBSP42
STATIC HYDROSTATIC COMPRESSION TEST
MEAN NORMAL STRESS vs VOLUMETRIC STRAIN

NELLIS BASELINE SAND



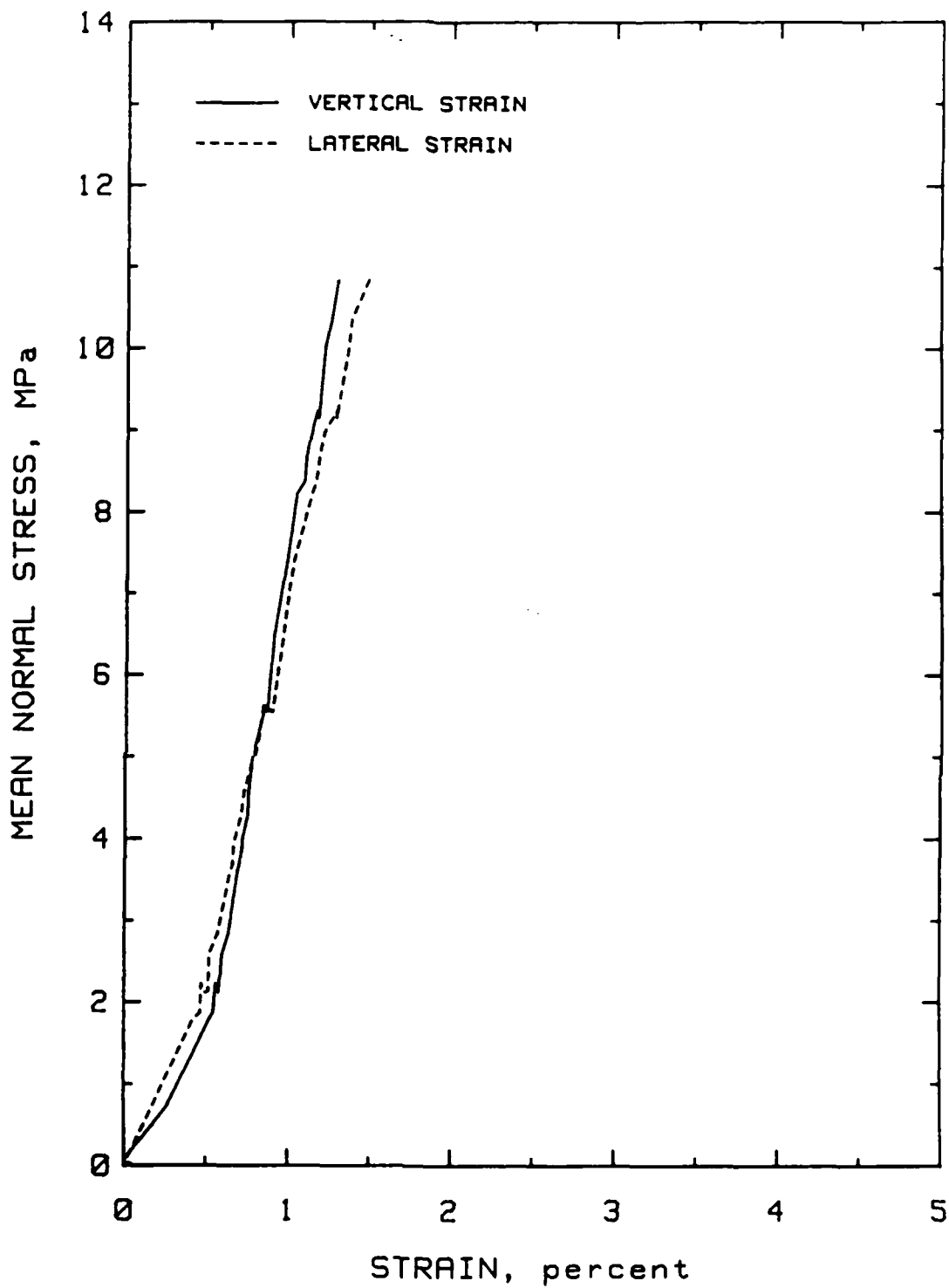
TEST NO: NBSP50
STATIC HYDROSTATIC COMPRESSION TEST
MEAN NORMAL STRESS vs VOLUMETRIC STRAIN

NELLIS BASELINE SAND



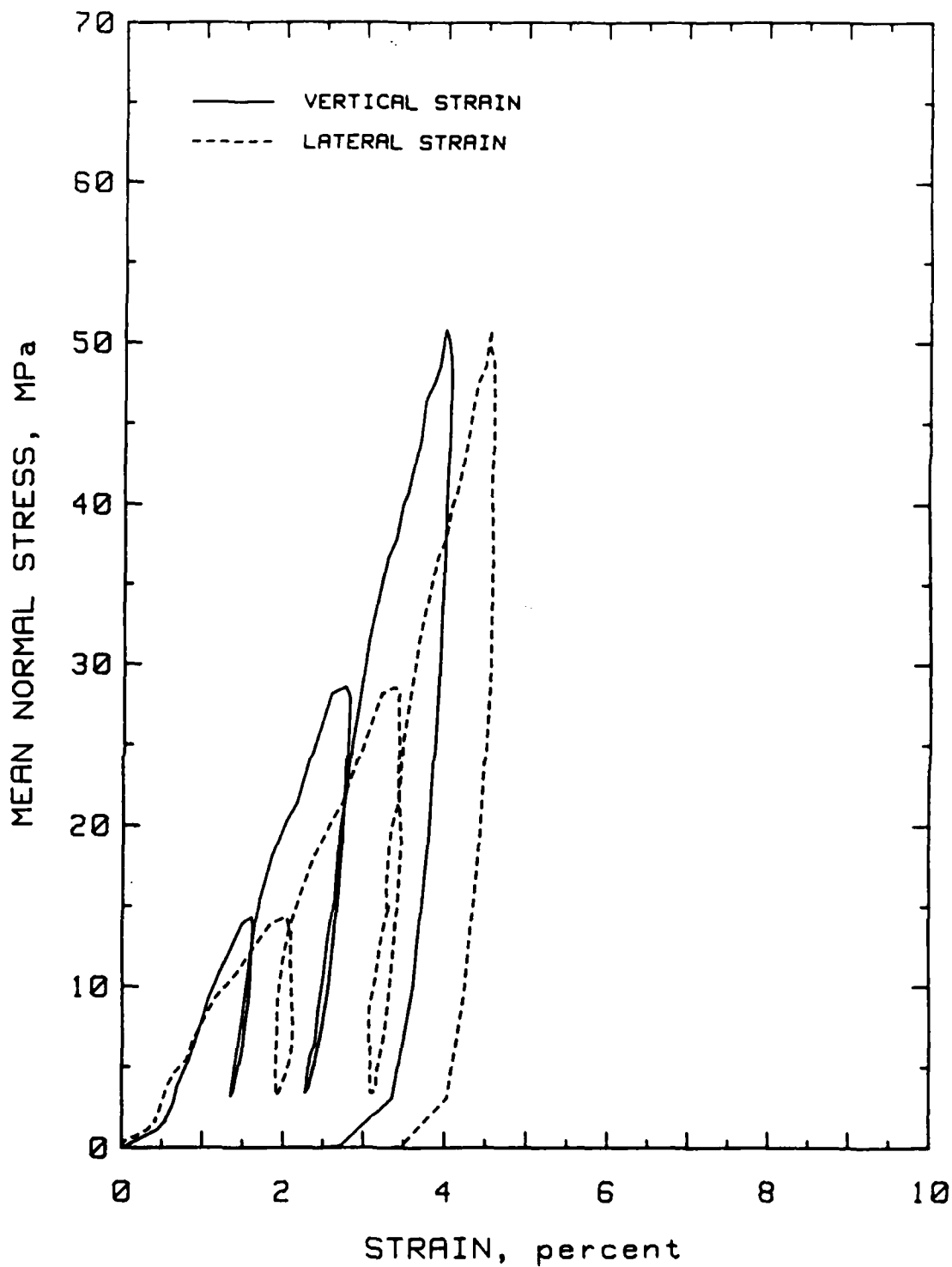
TEST NO: NBSP58
STATIC HYDROSTATIC COMPRESSION TEST
MEAN NORMAL STRESS vs VOLUMETRIC STRAIN

NELLIS BASELINE SAND



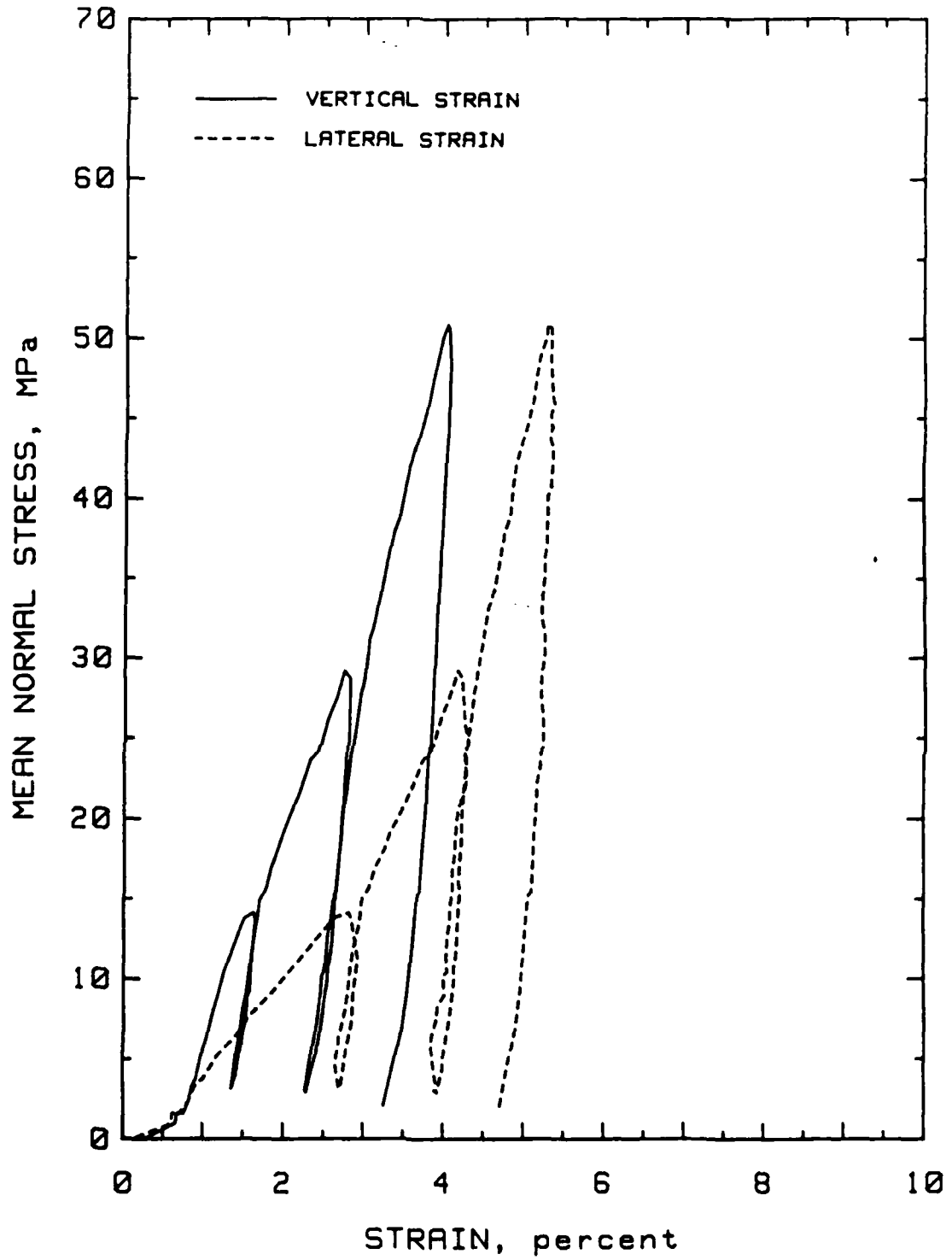
TEST NO: NBSP01
STATIC HYDROSTATIC COMPRESSION TEST
MEAN NORMAL STRESS vs STRAIN

NELLIS BASELINE SAND



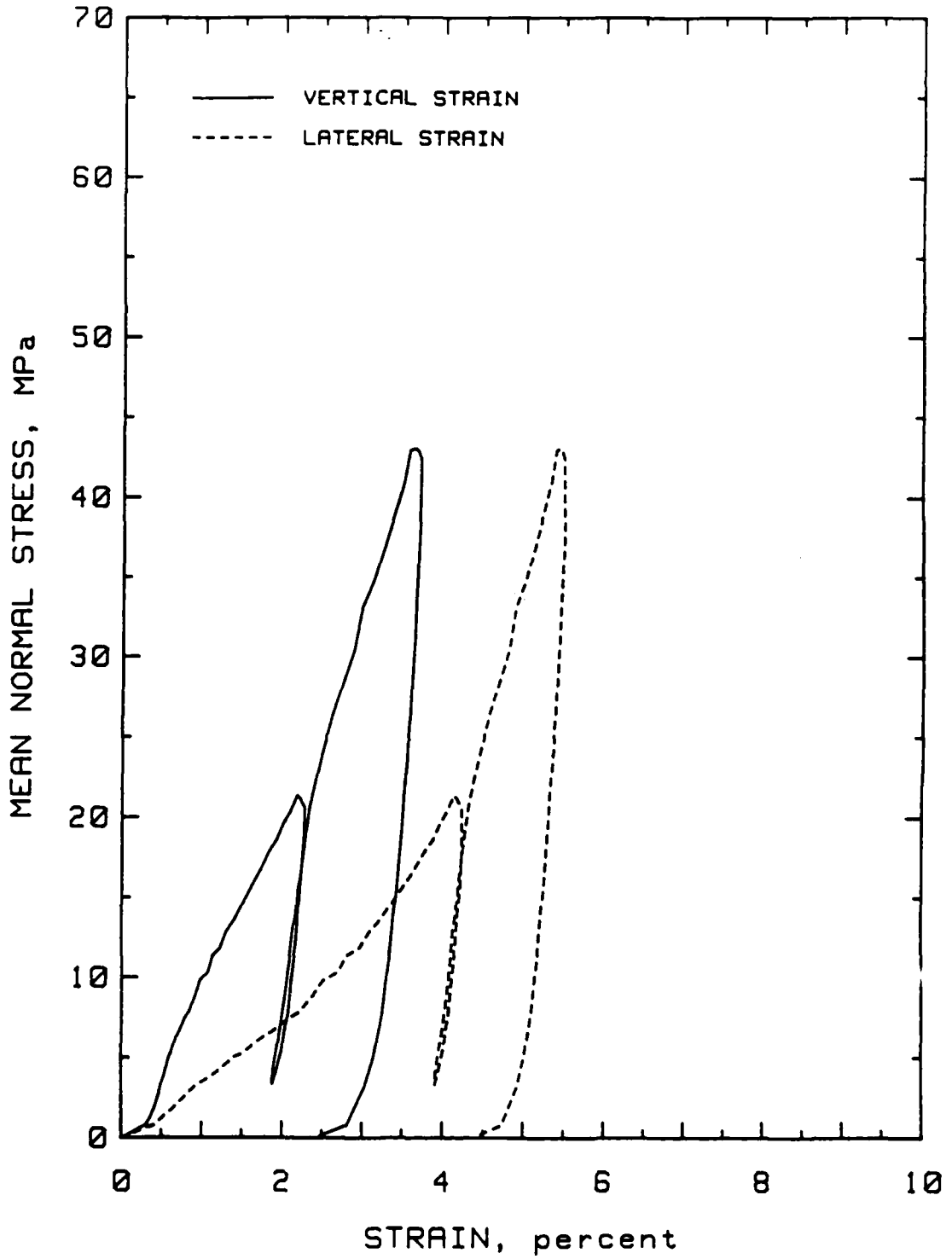
TEST NO: NBSP02
STATIC HYDROSTATIC COMPRESSION TEST
MEAN NORMAL STRESS vs STRAIN

NELLIS BASELINE SAND



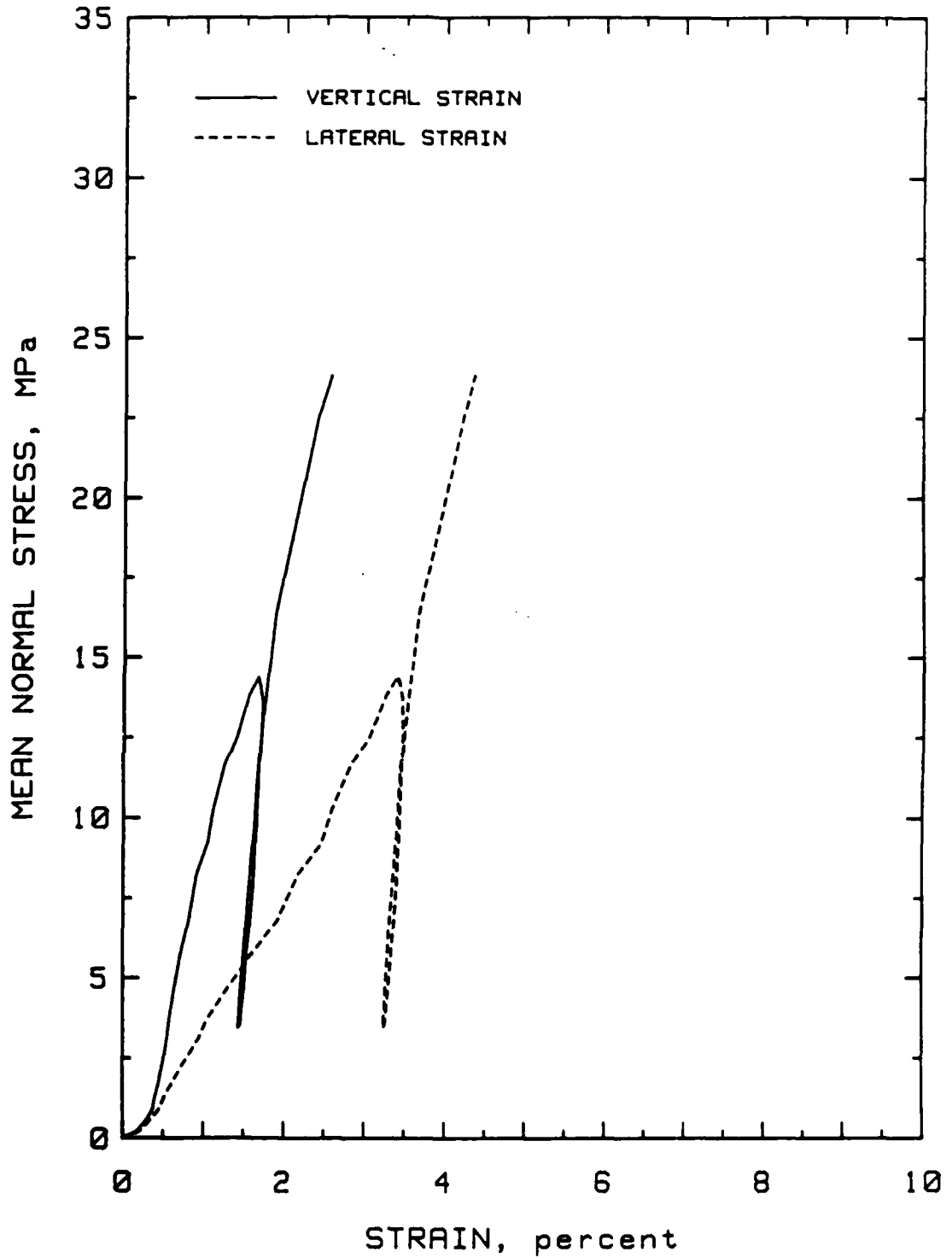
TEST NO: NBSP04
STATIC HYDROSTATIC COMPRESSION TEST
MEAN NORMAL STRESS vs STRAIN

NELLIS BASELINE SAND



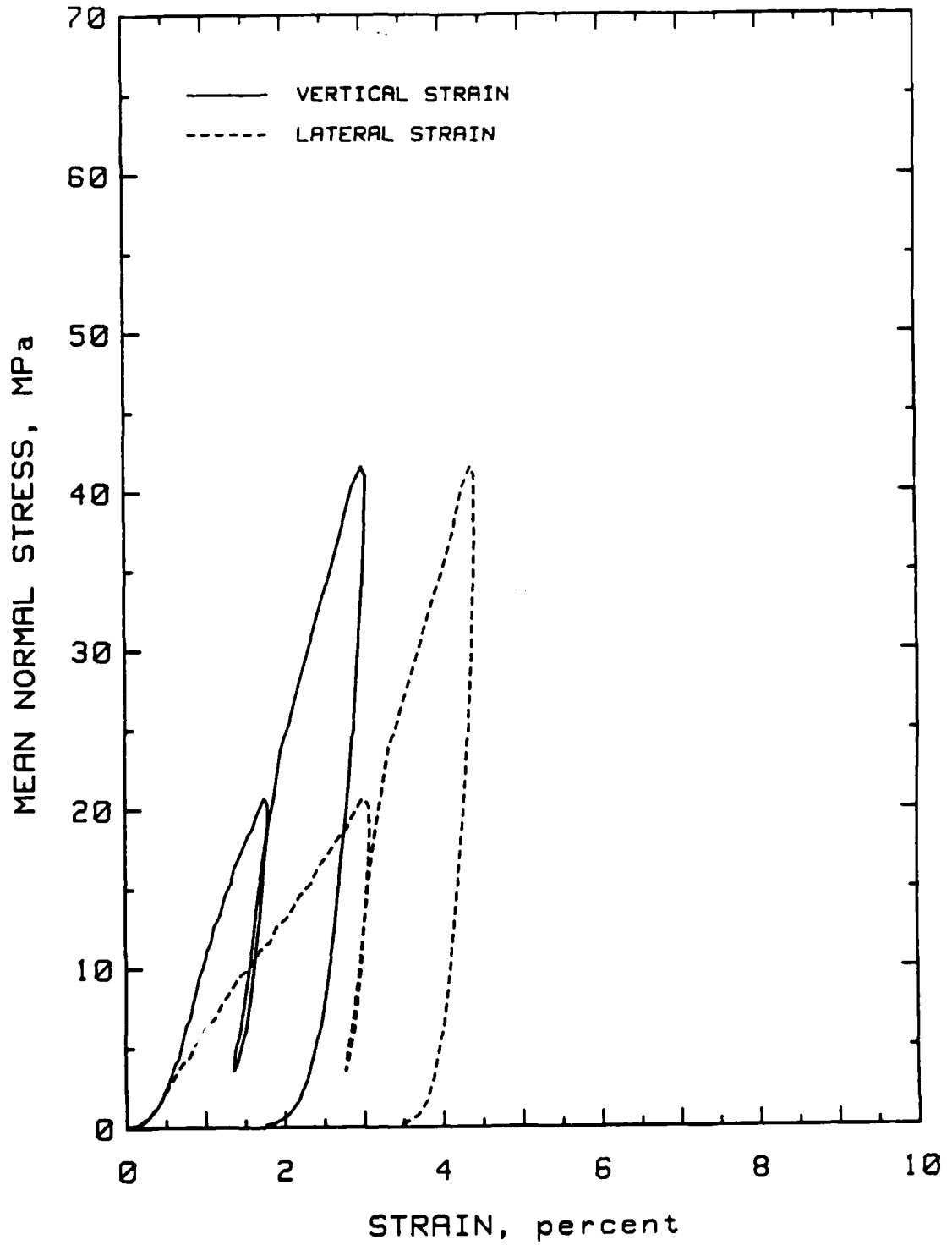
TEST NO: NBSP28
STATIC HYDROSTATIC COMPRESSION TEST
MEAN NORMAL STRESS vs STRAIN

NELLIS BASELINE SAND



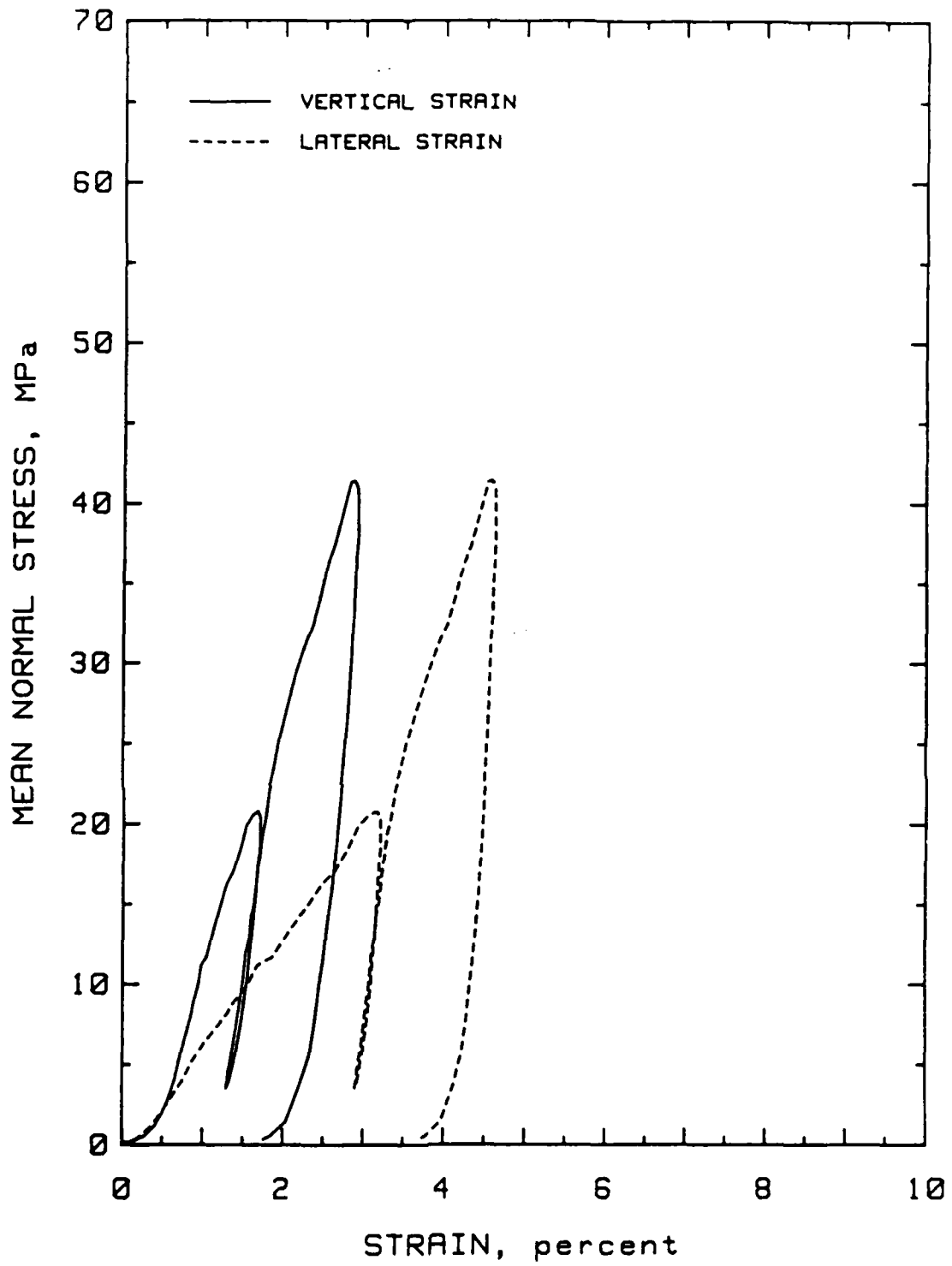
TEST NO: NBSP30
STATIC HYDROSTATIC COMPRESSION TEST
MEAN NORMAL STRESS vs STRAIN

NELLIS BASELINE SAND



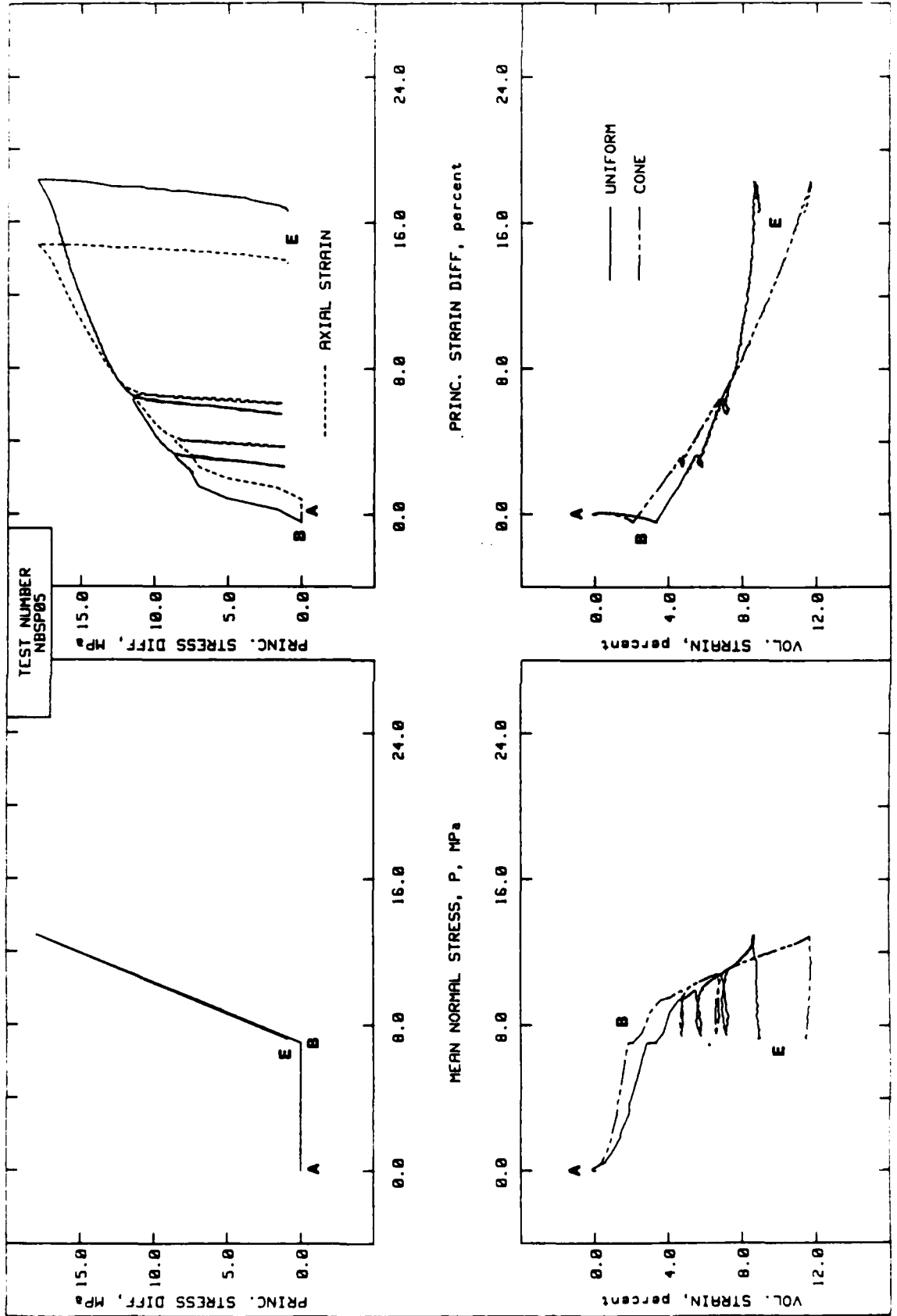
TEST NO: NBSP41
STATIC HYDROSTATIC COMPRESSION TEST
MEAN NORMAL STRESS vs STRAIN

NELLIS BASELINE SAND

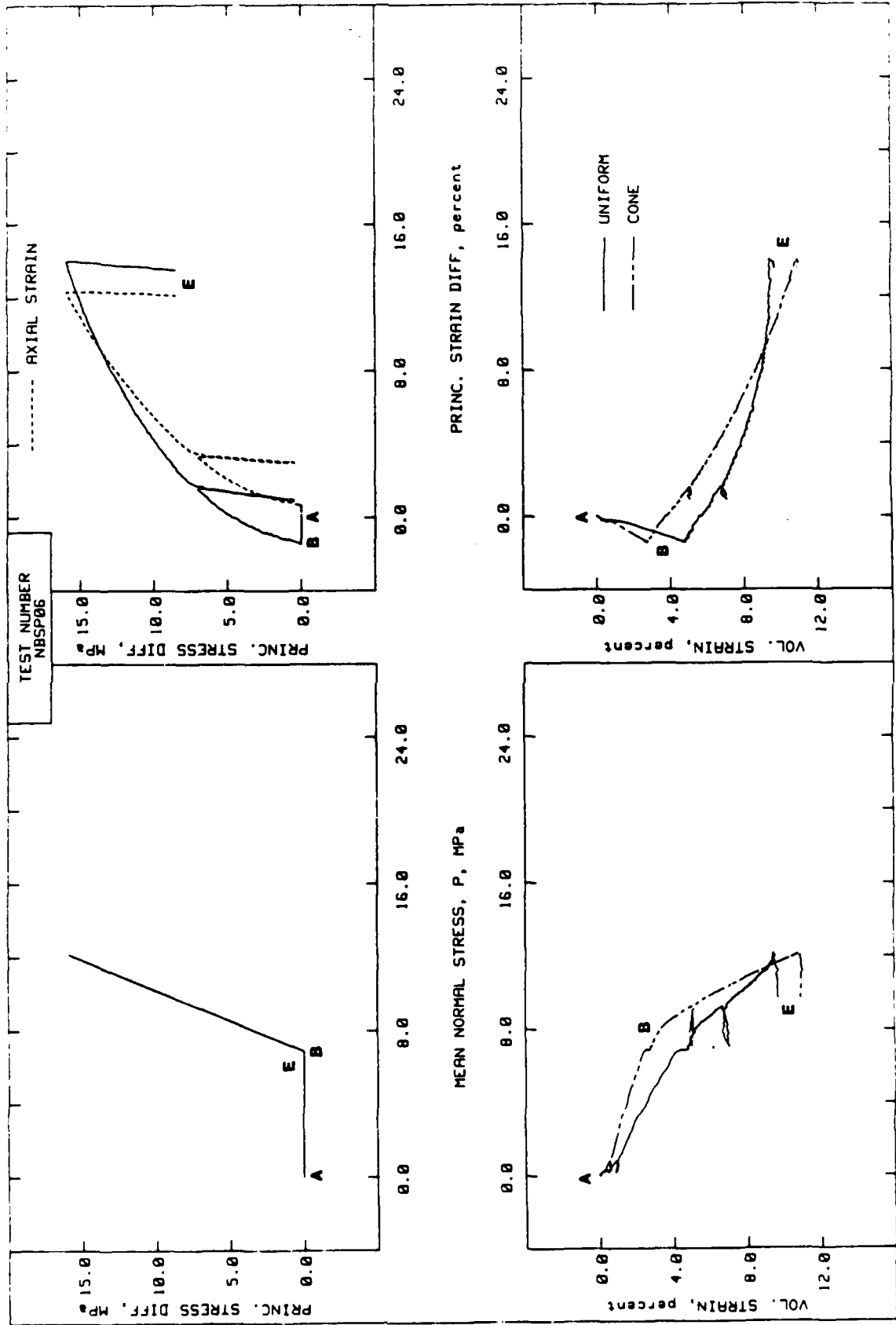


TEST NO: NBSP42
STATIC HYDROSTATIC COMPRESSION TEST
MEAN NORMAL STRESS vs STRAIN

NELLIS BASELINE SAND



NELLIS BASELINE SAND



NELLIS BASELINE SAND

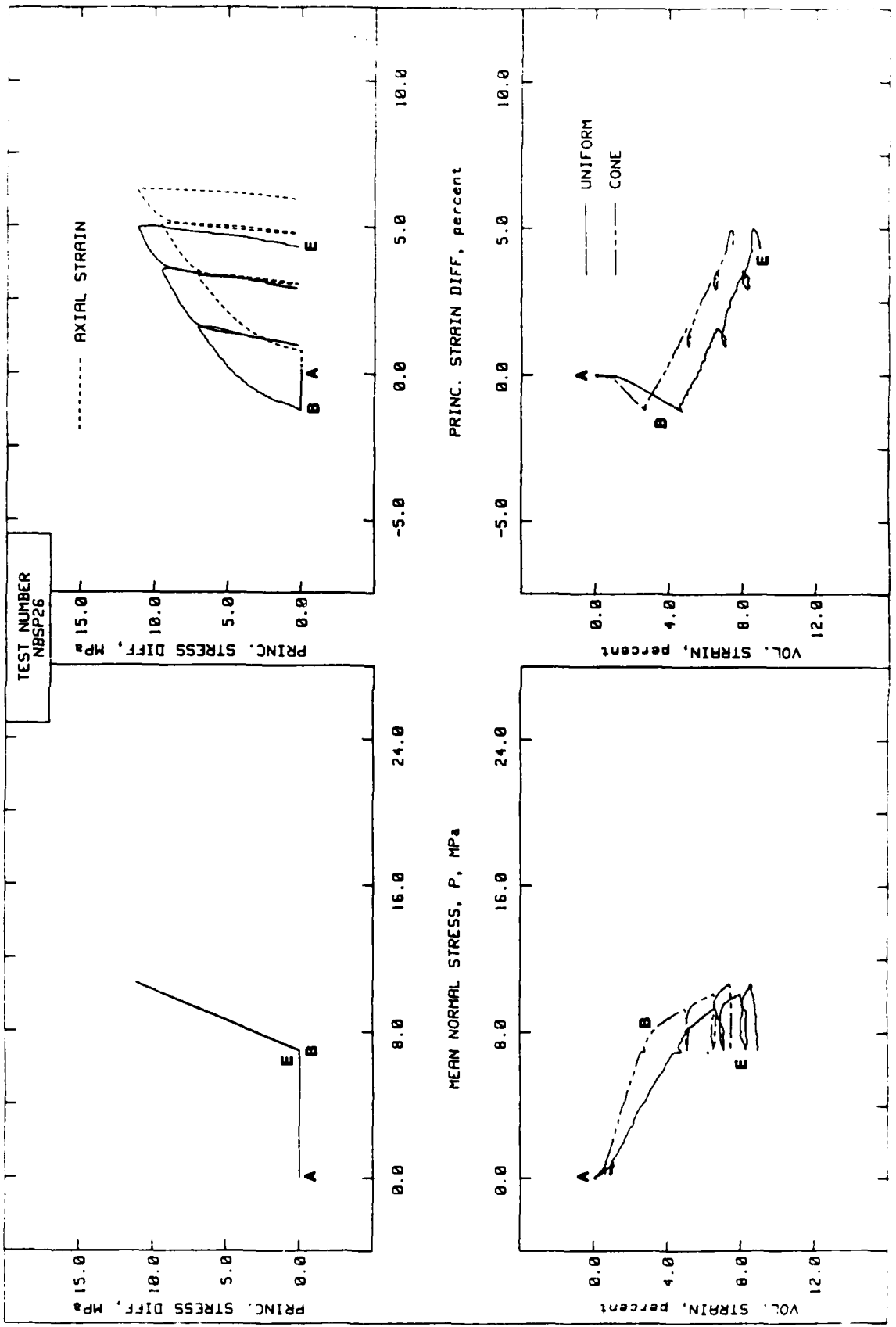
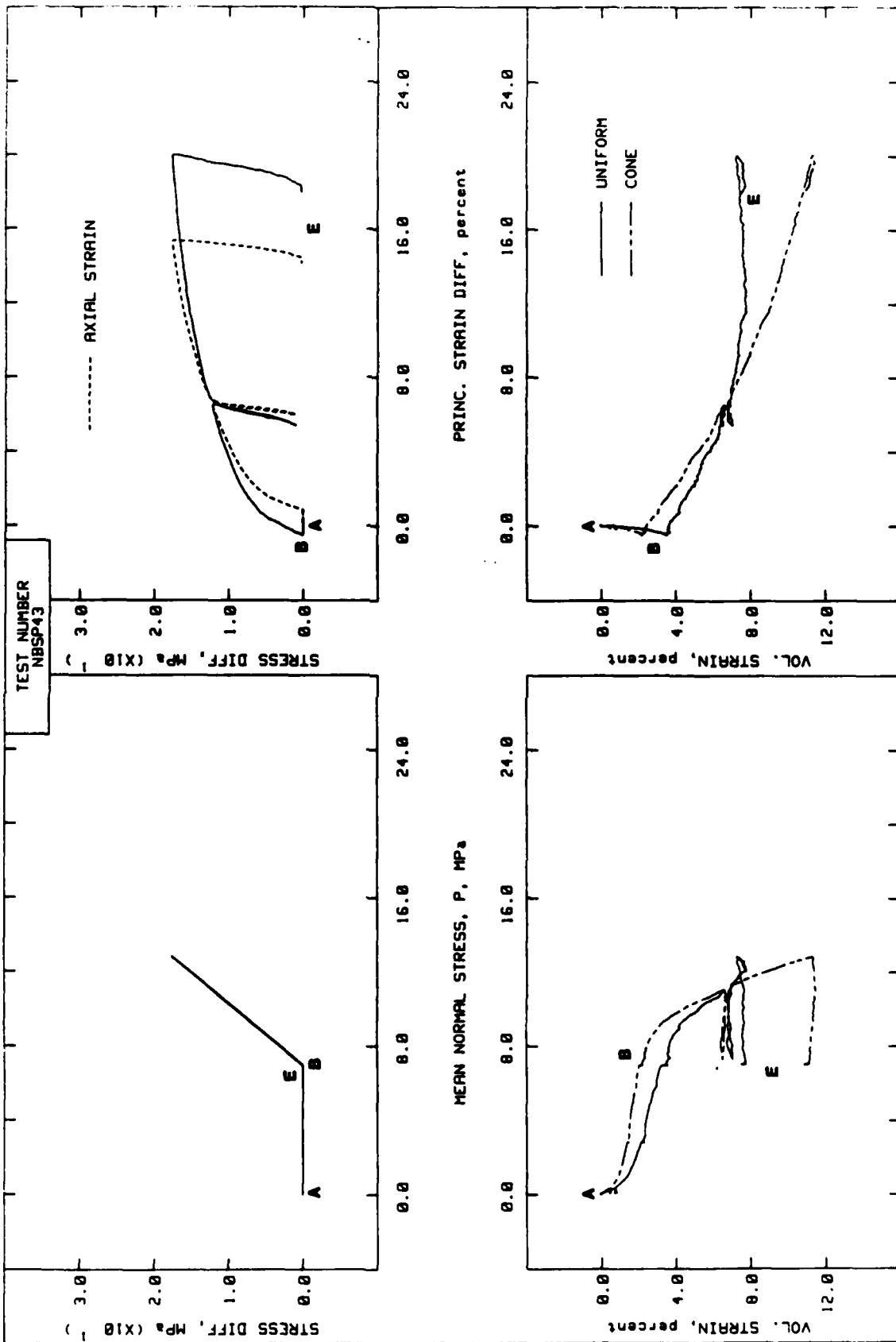
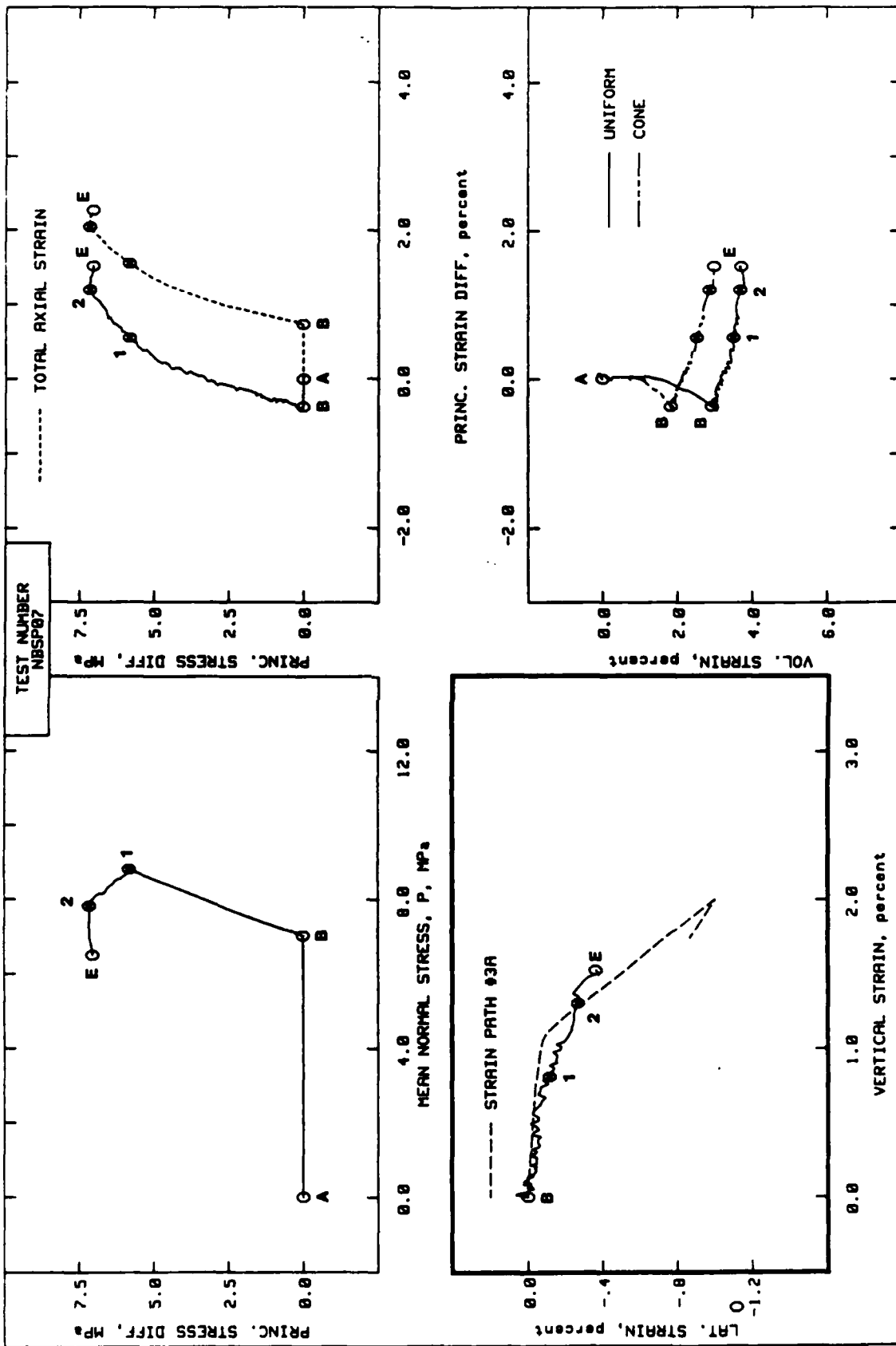


PLATE 22

NELLIS BASELINE SAND



NELLIS BASELINE SAND



NELLIS BASELINE SAND

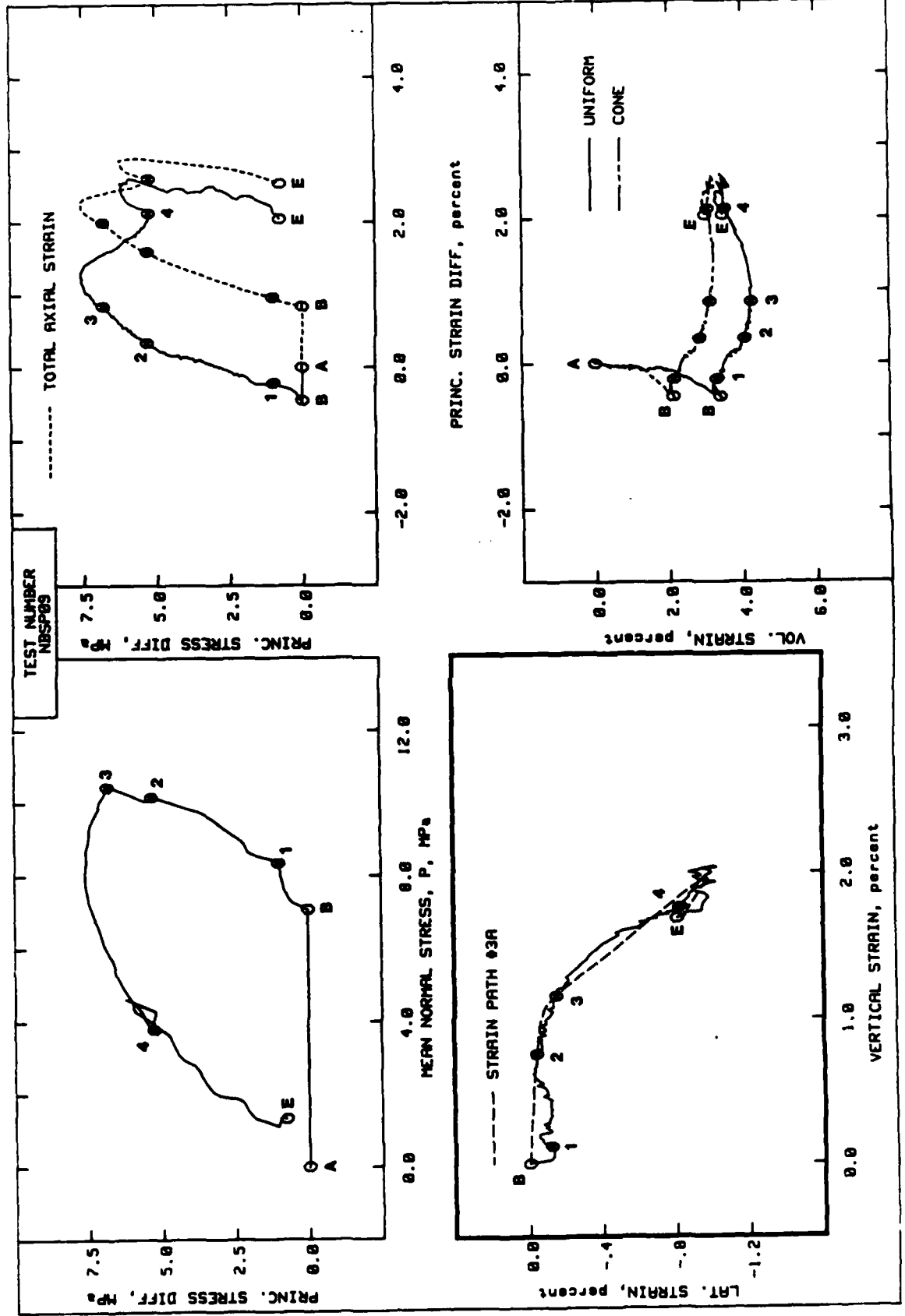
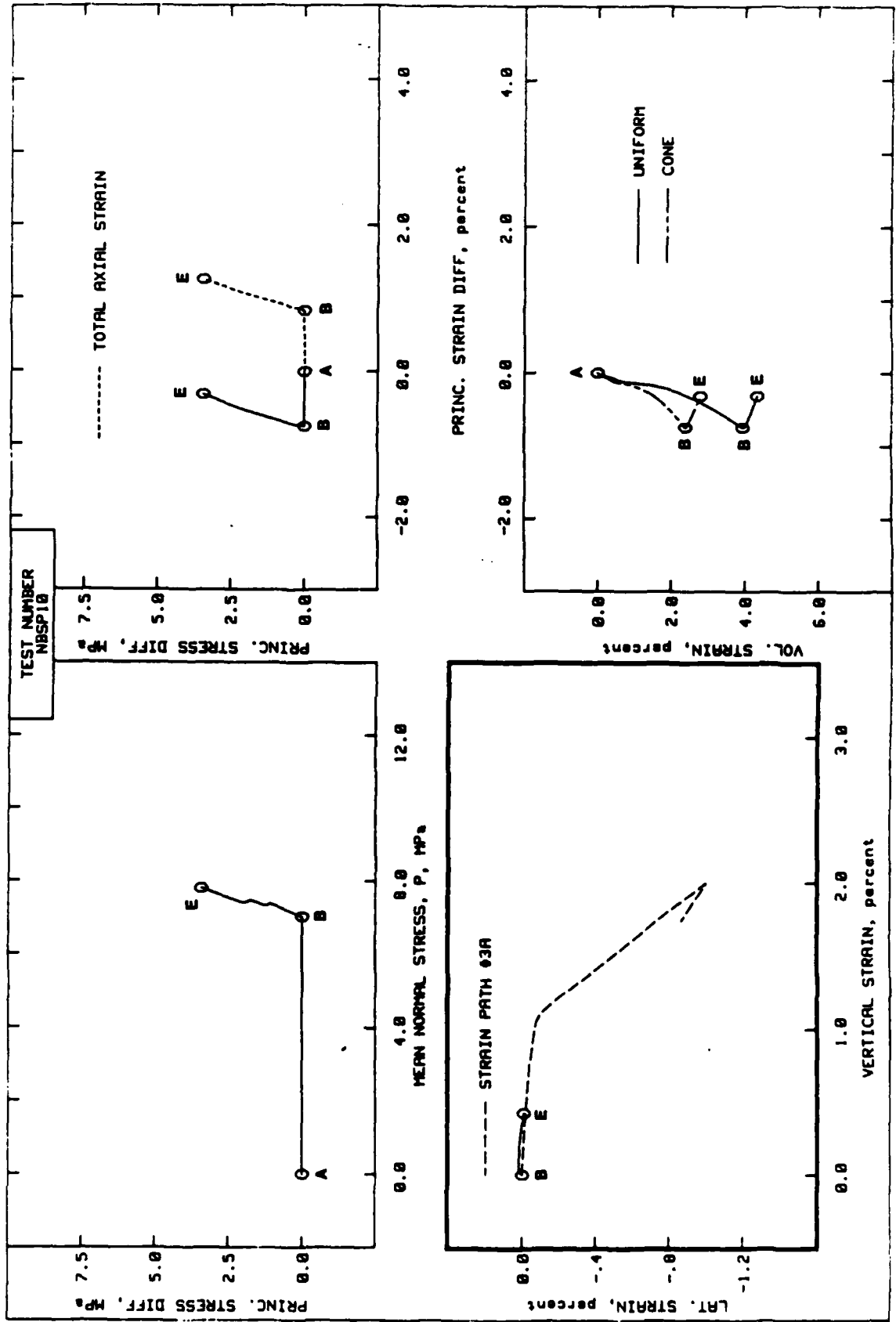
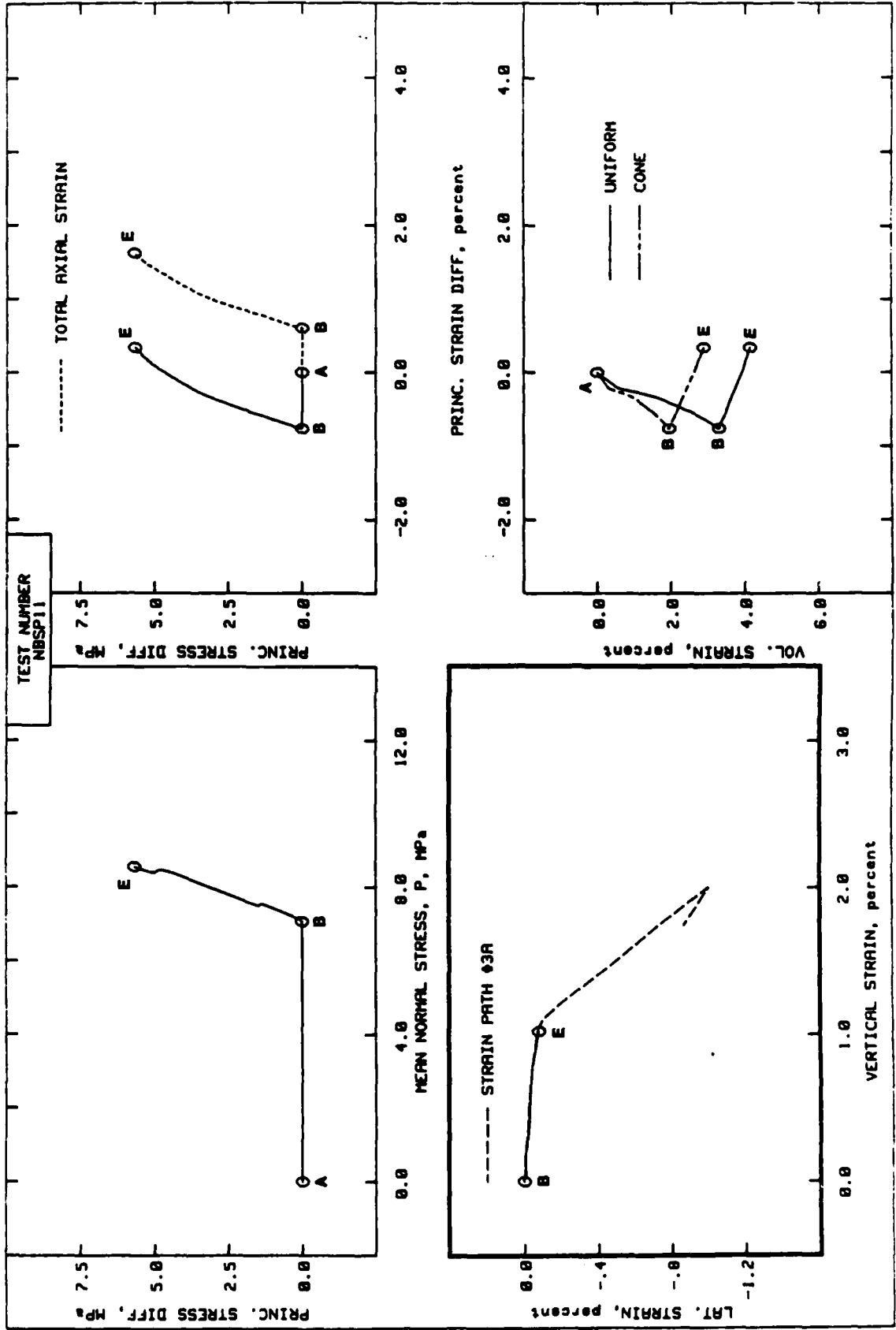


PLATE 26

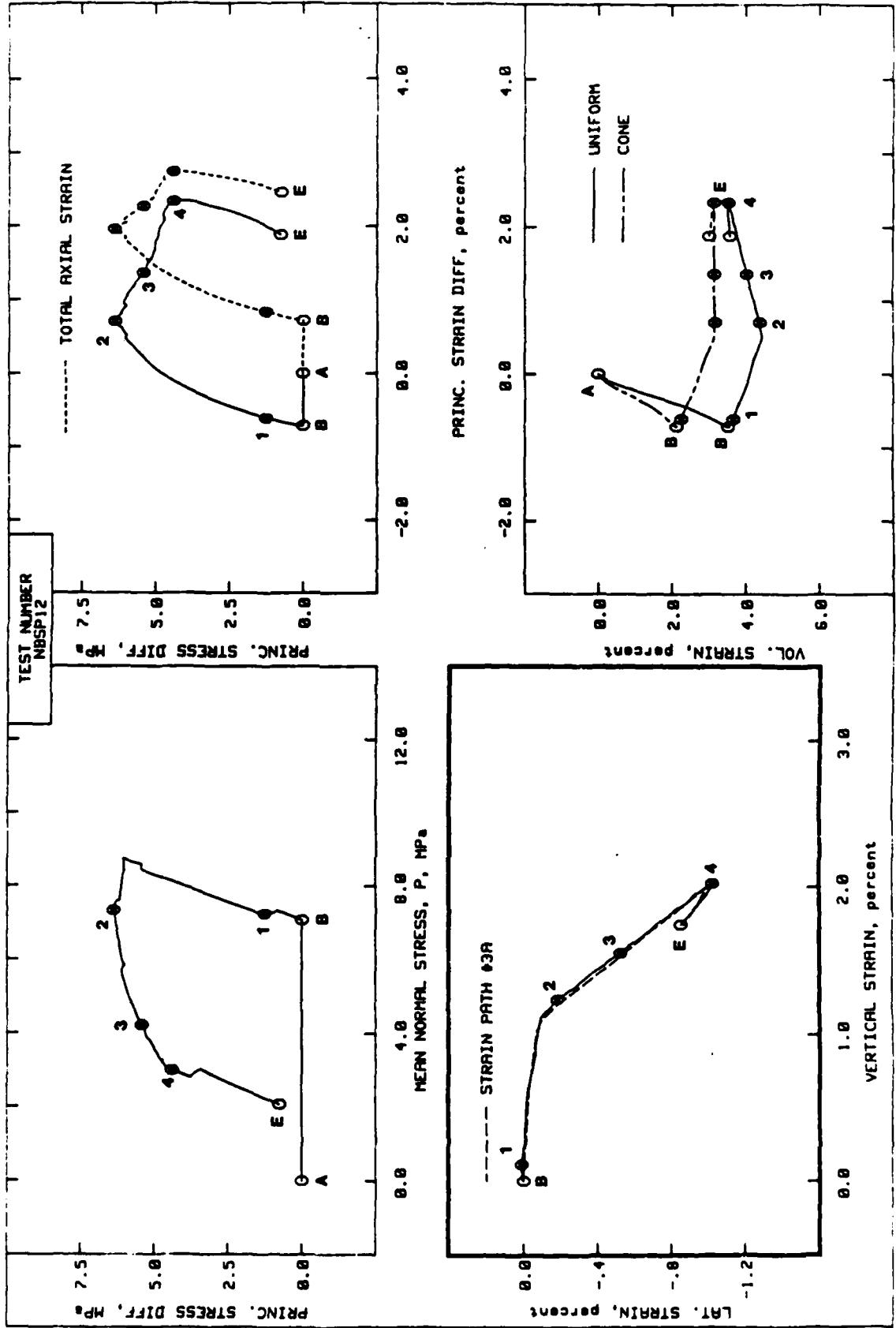
NELLIS BASELINE SAND



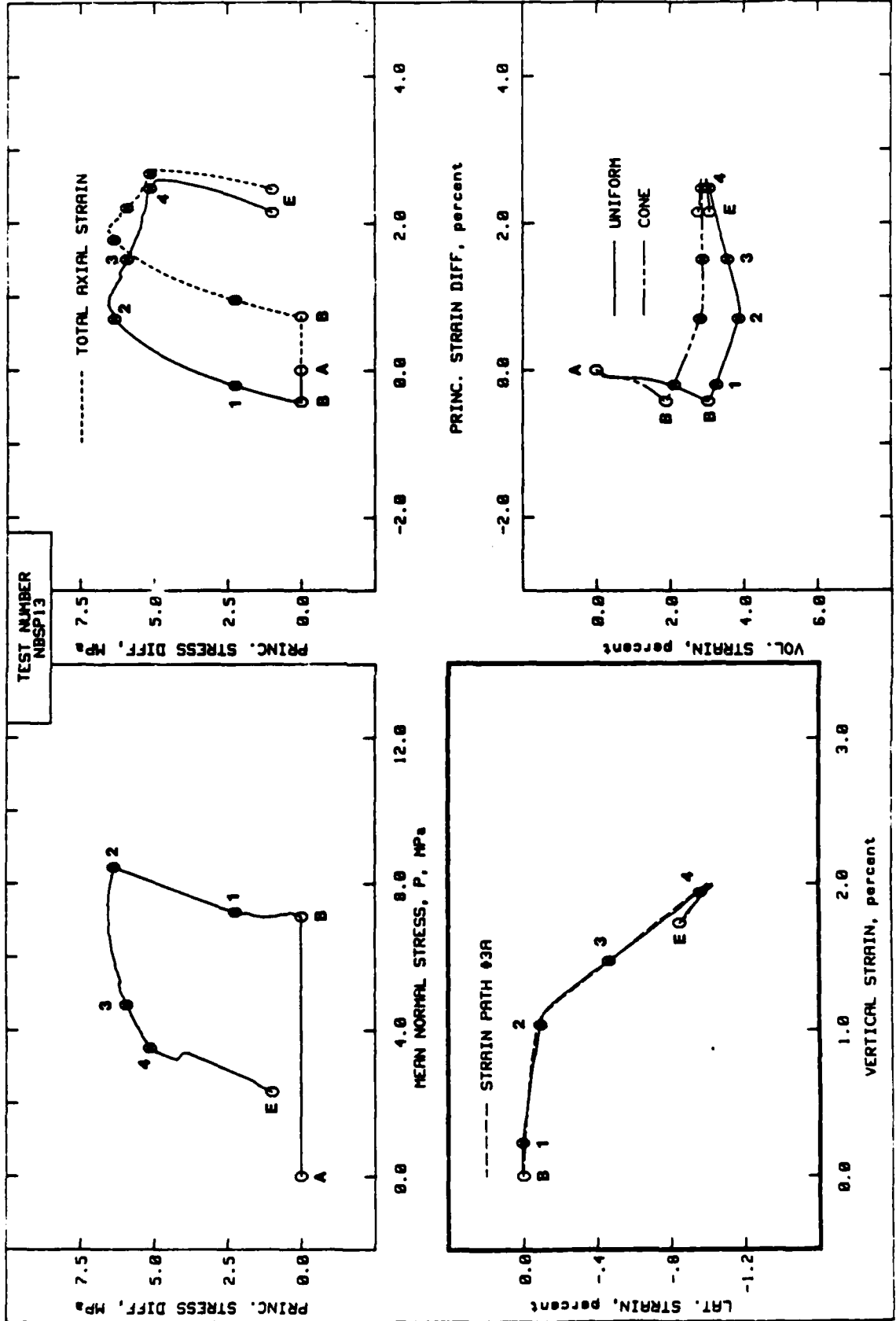
NELLIS BASELINE SAND



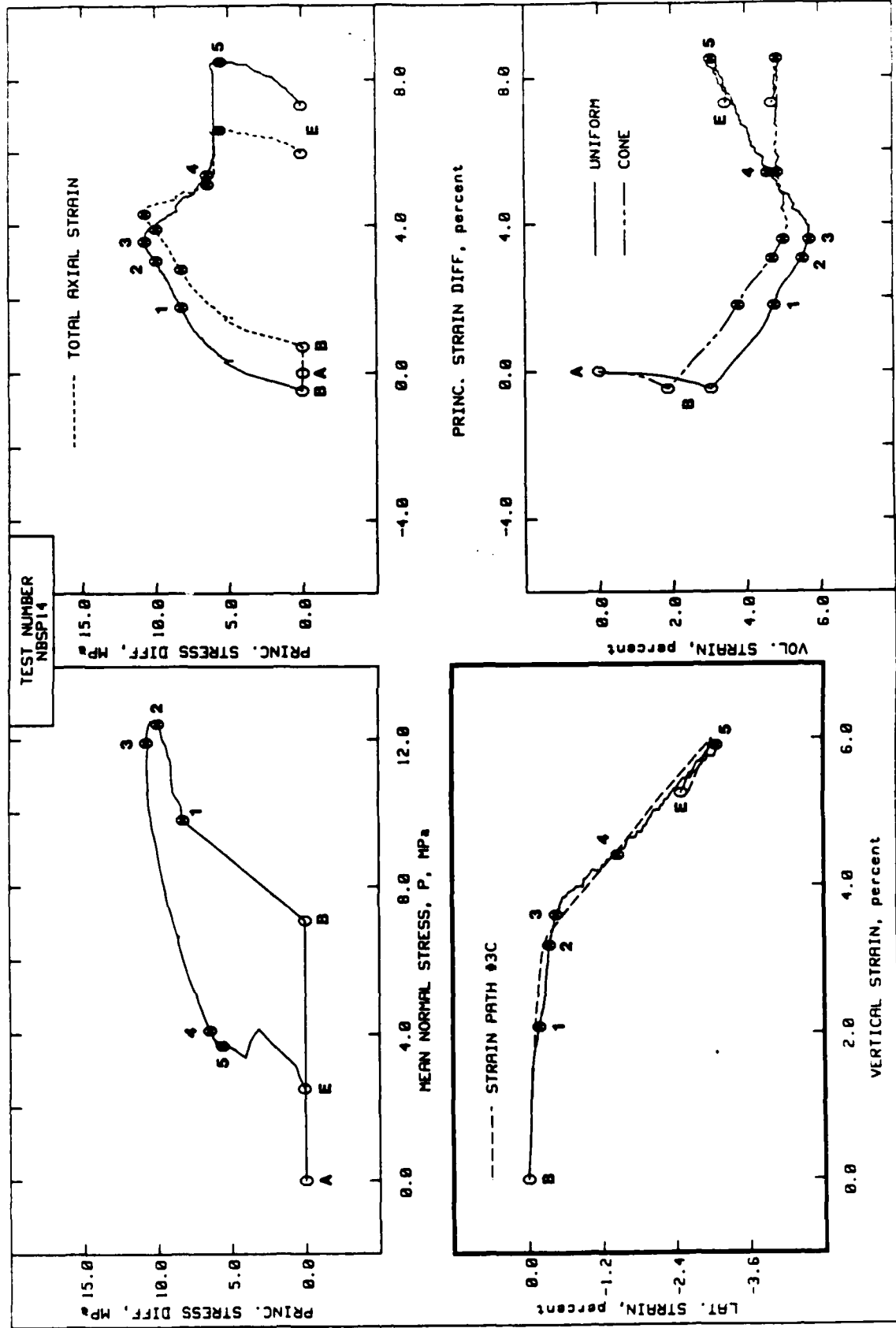
NELLIS BASELINE SAND



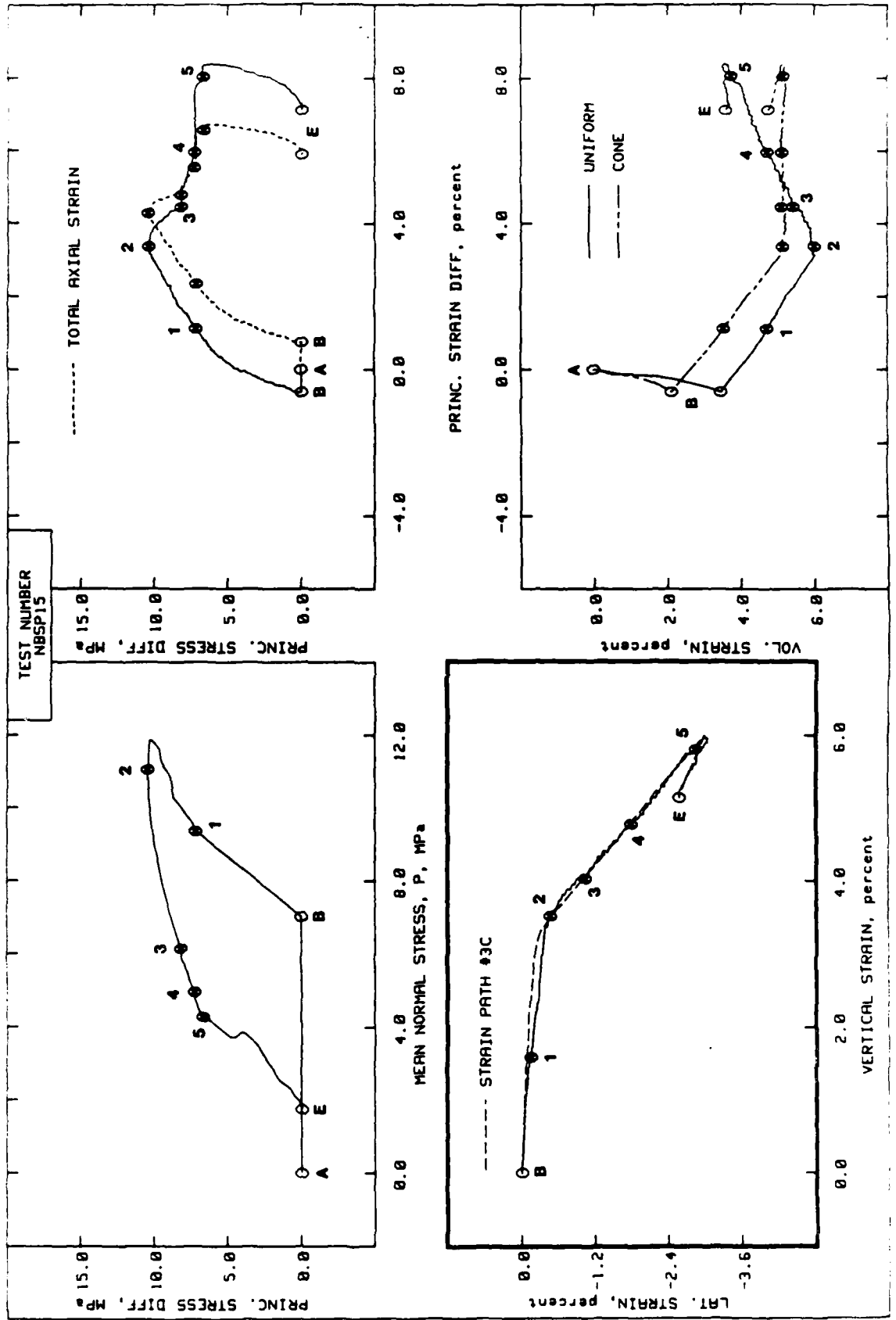
NELLIS BASELINE SAND



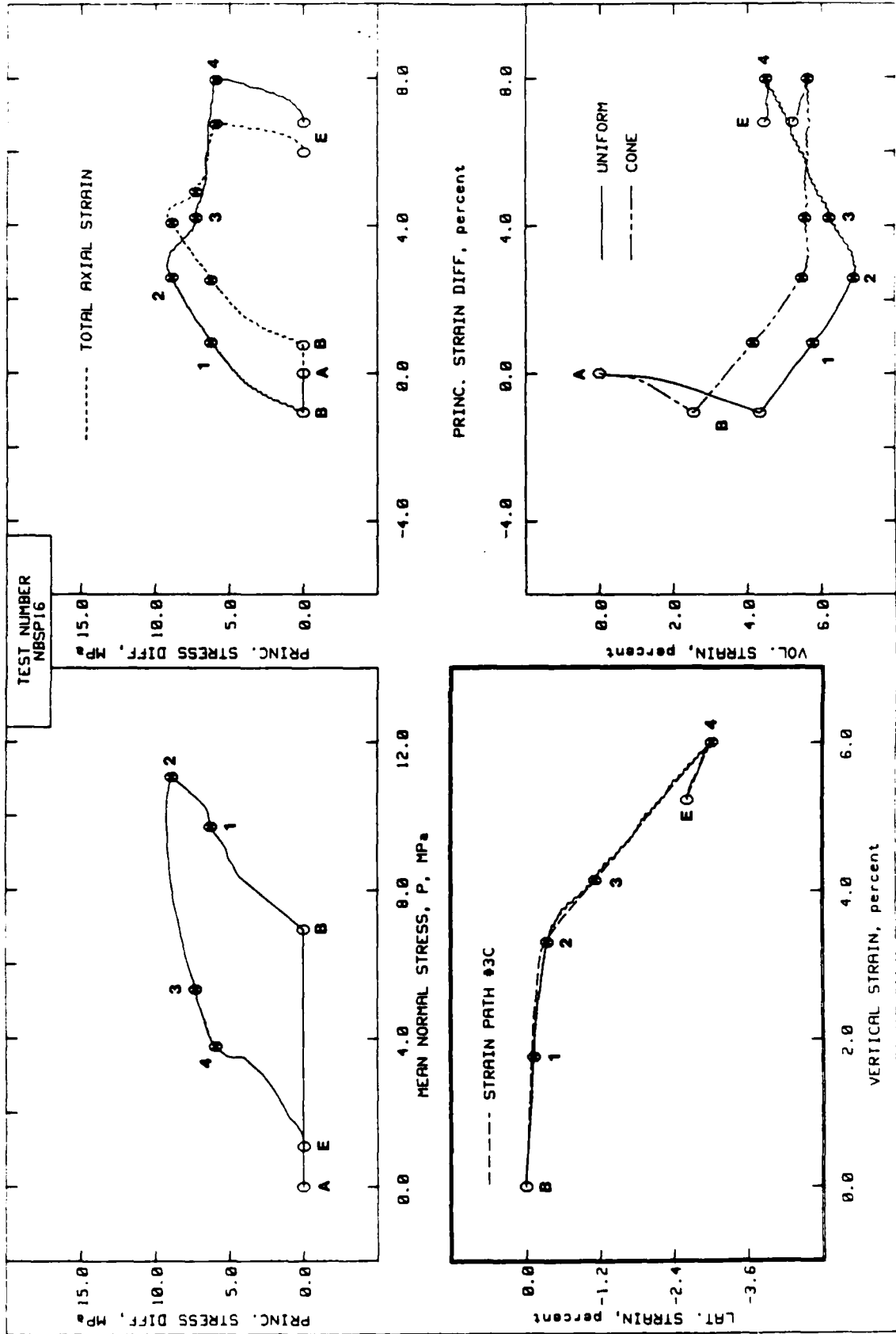
NELLIS BASELINE SAND



NELLIS BASELINE SAND



NELLIS BASELINE SAND



NELLIS BASELINE SAND

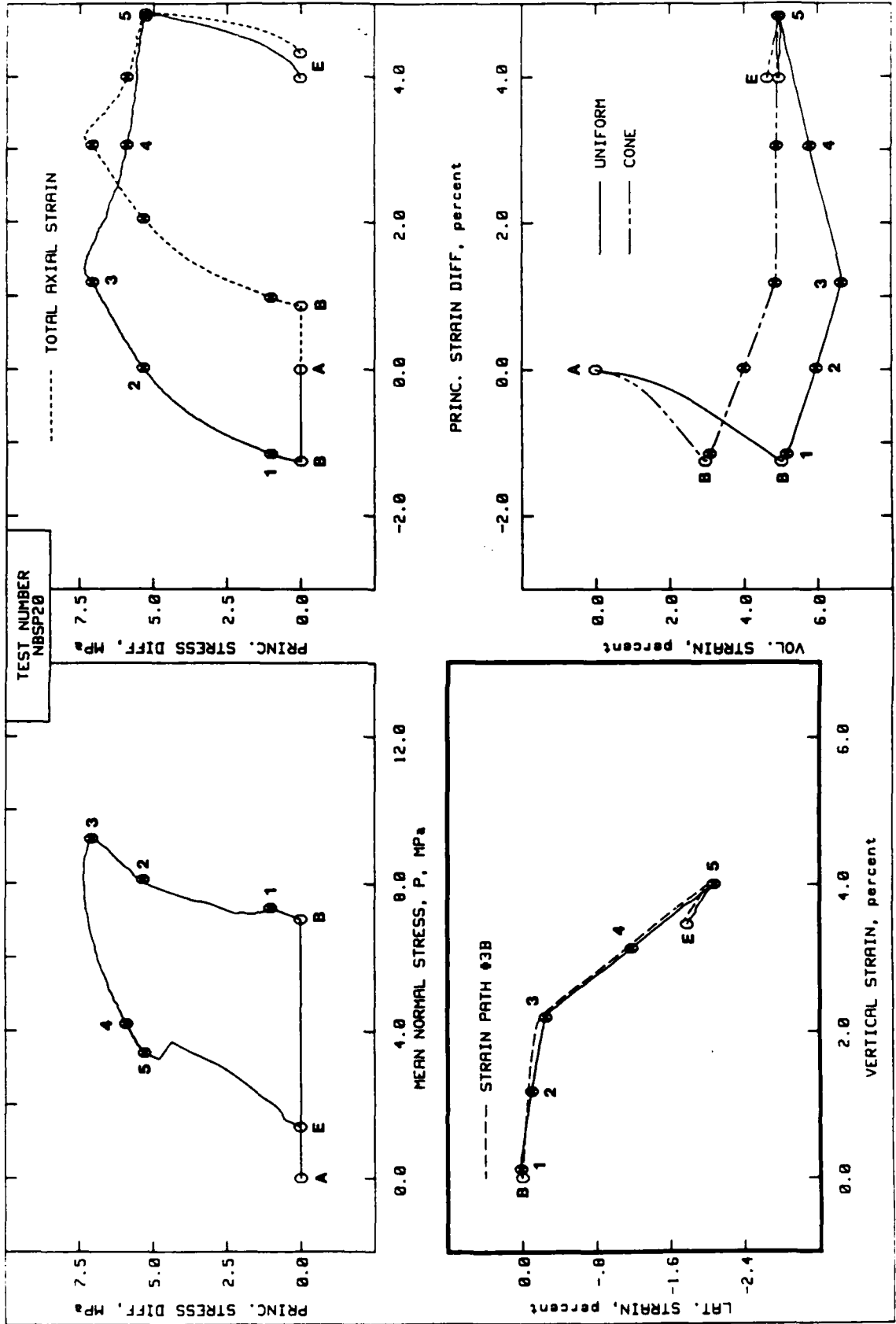
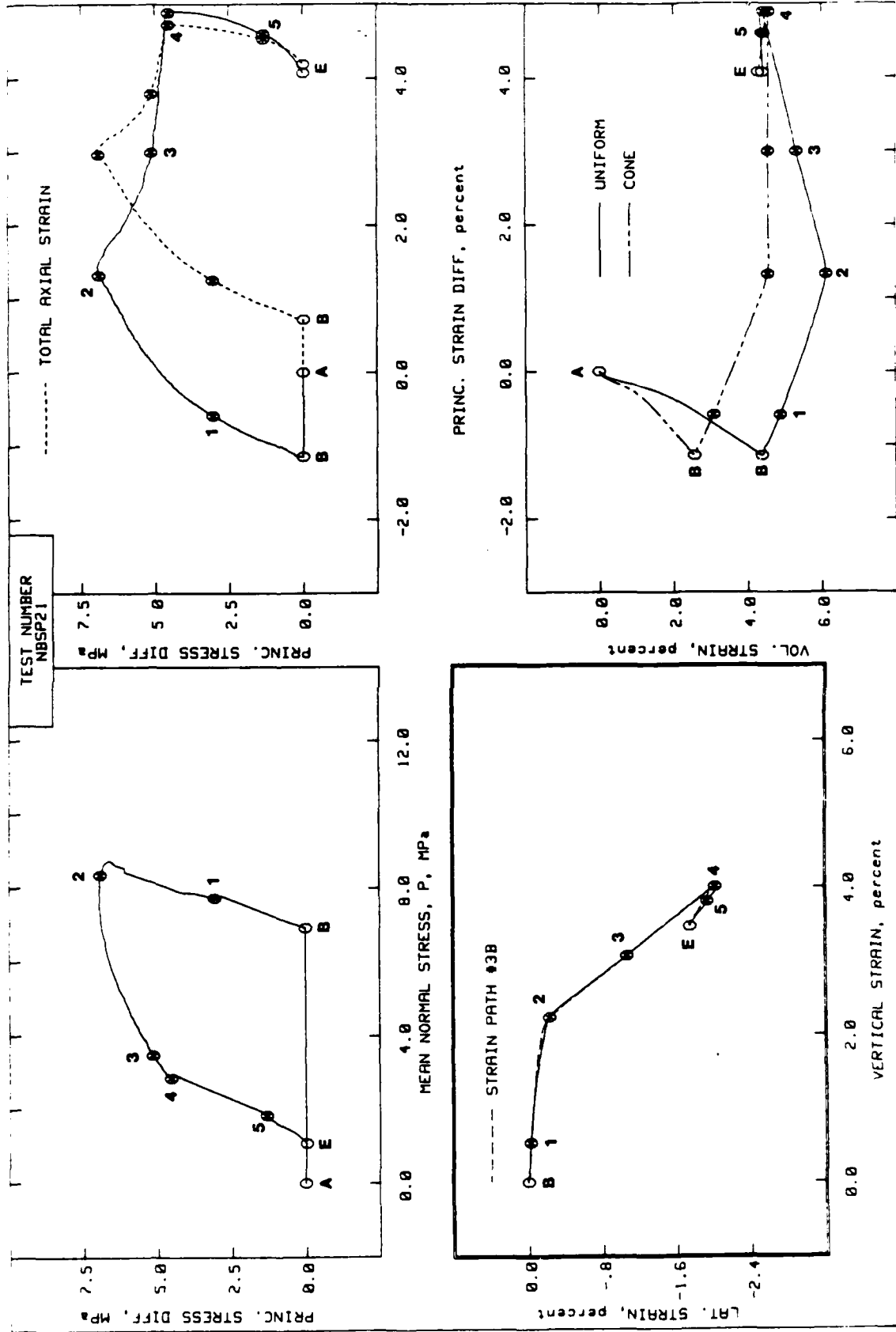
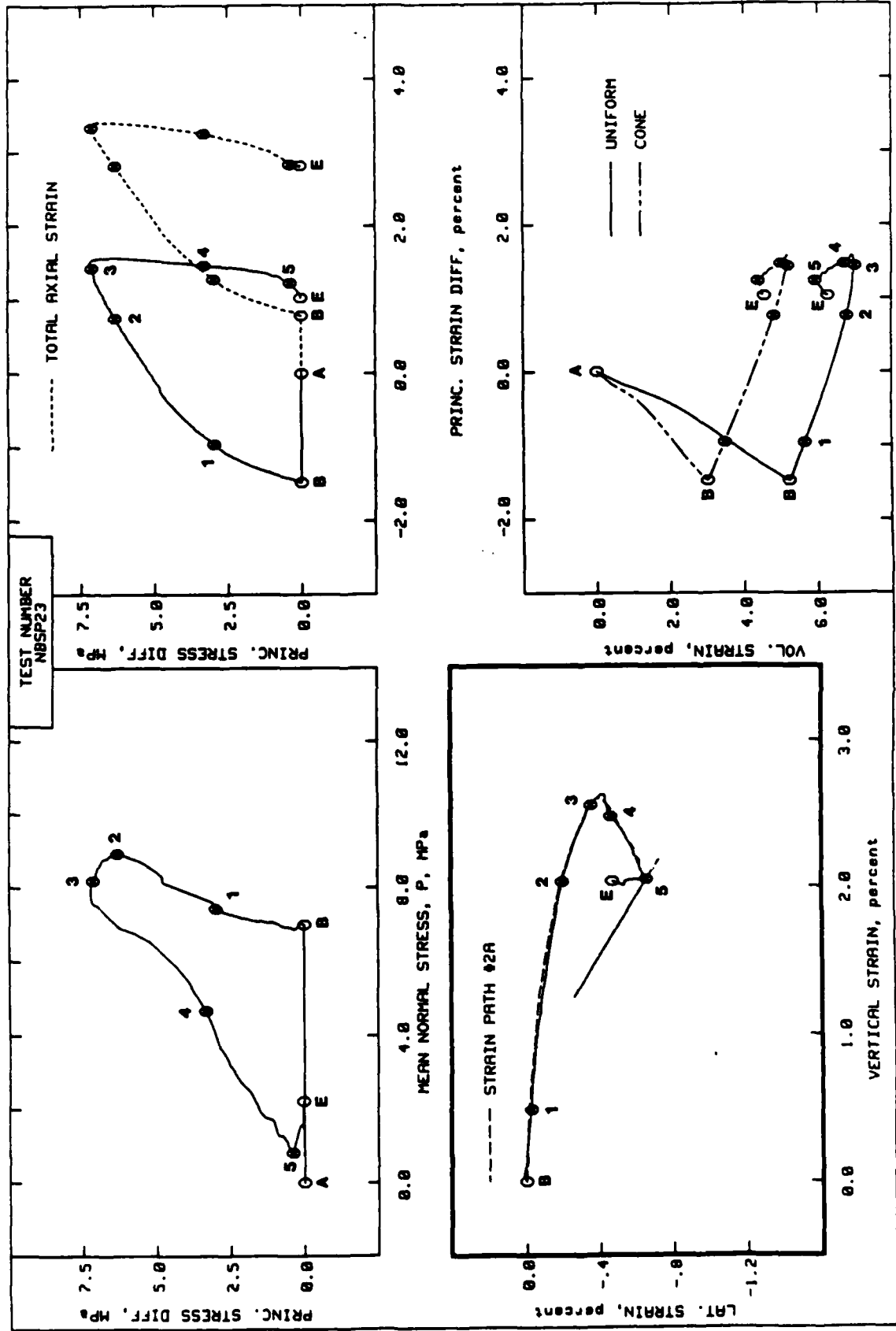


PLATE 34

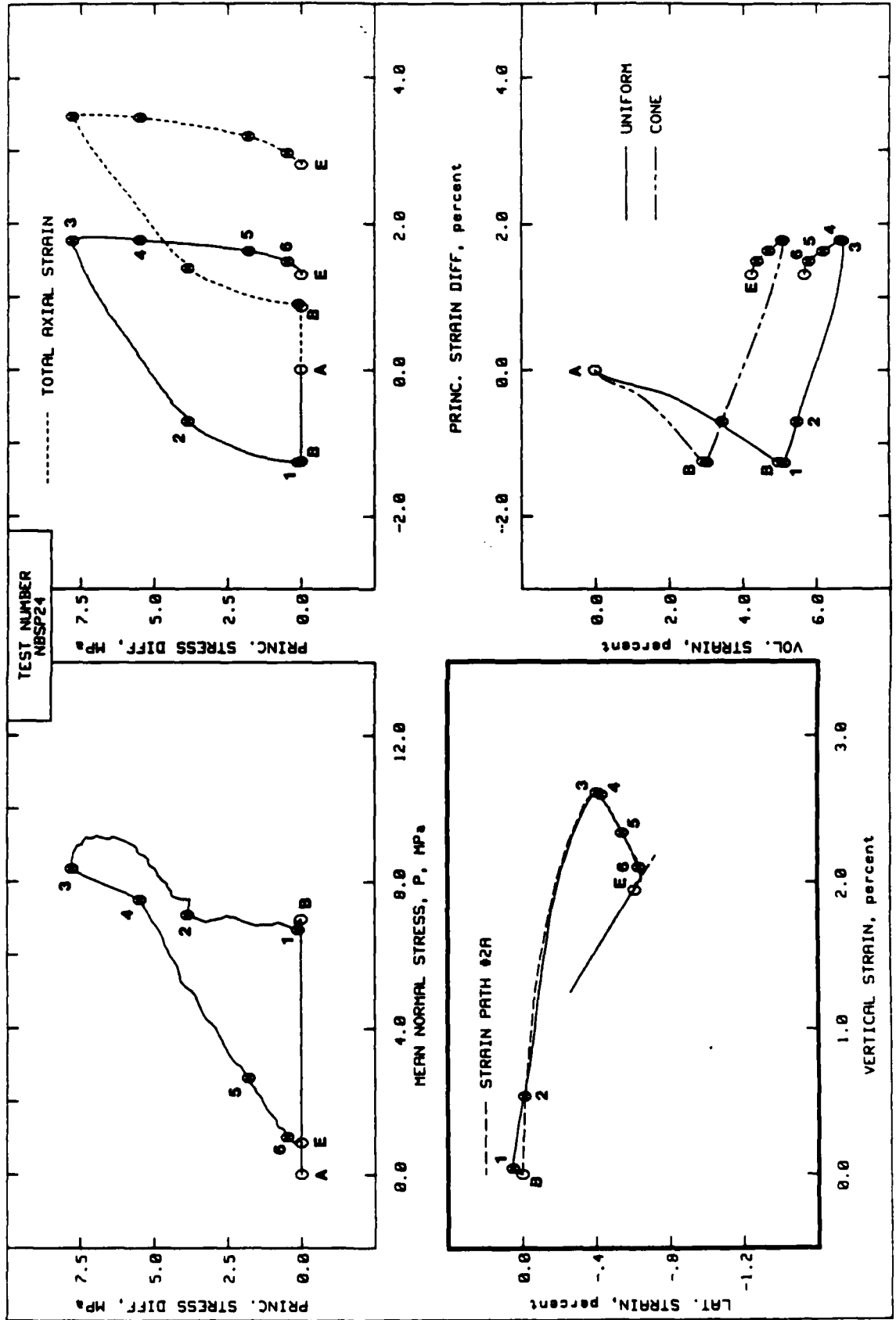
NELLIS BASELINE SAND



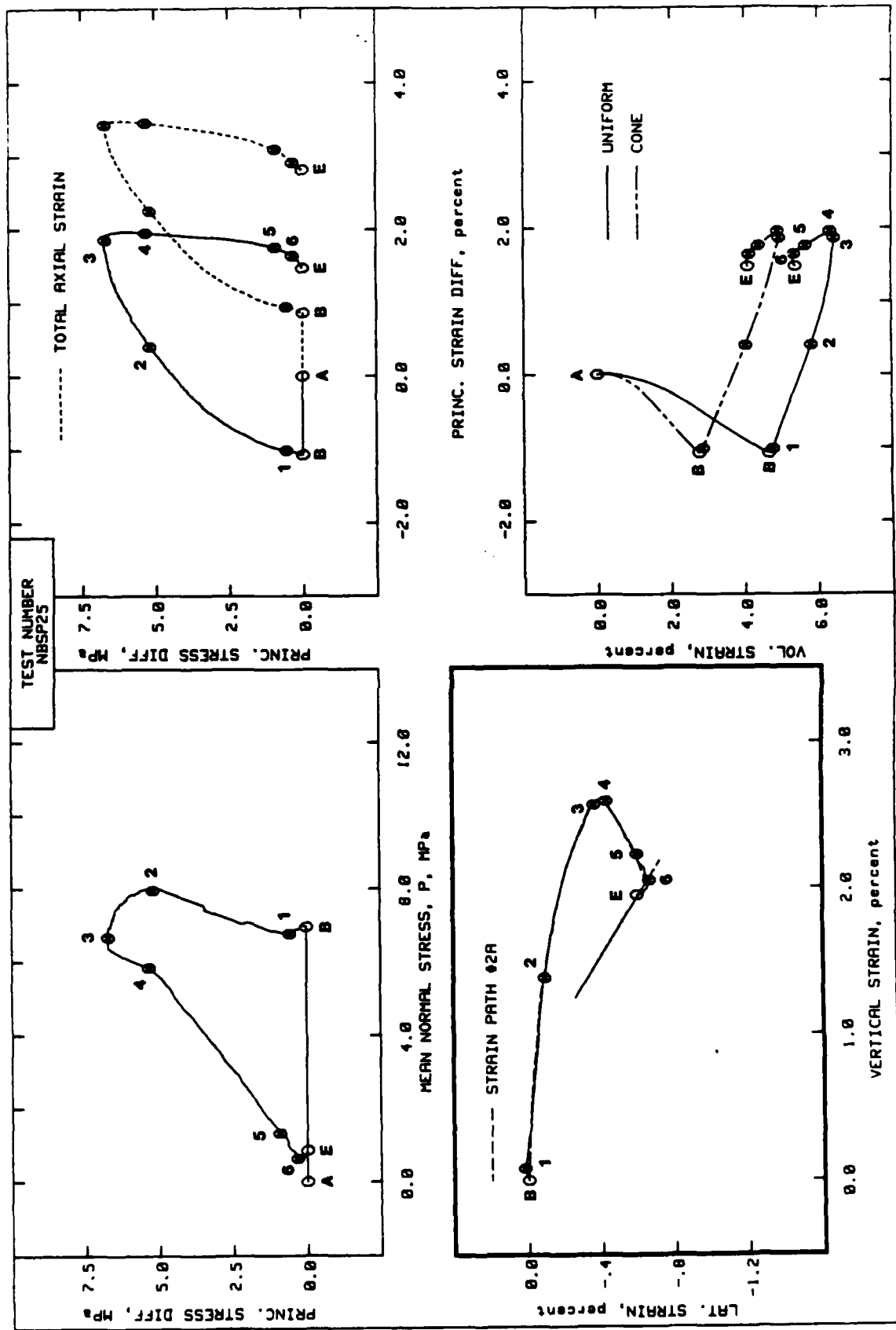
NELLIS BASELINE SAND



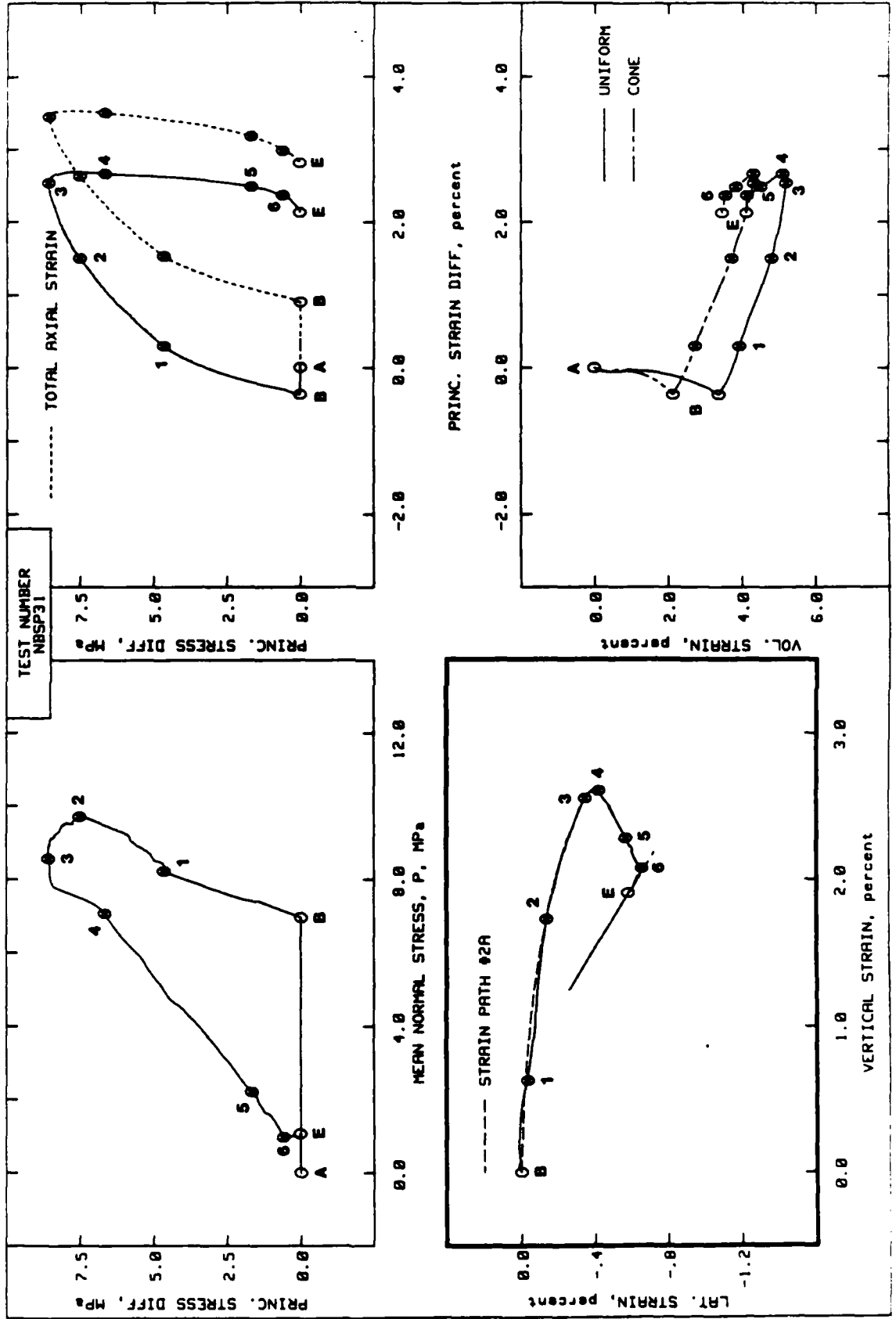
NELLIS BASELINE SAND



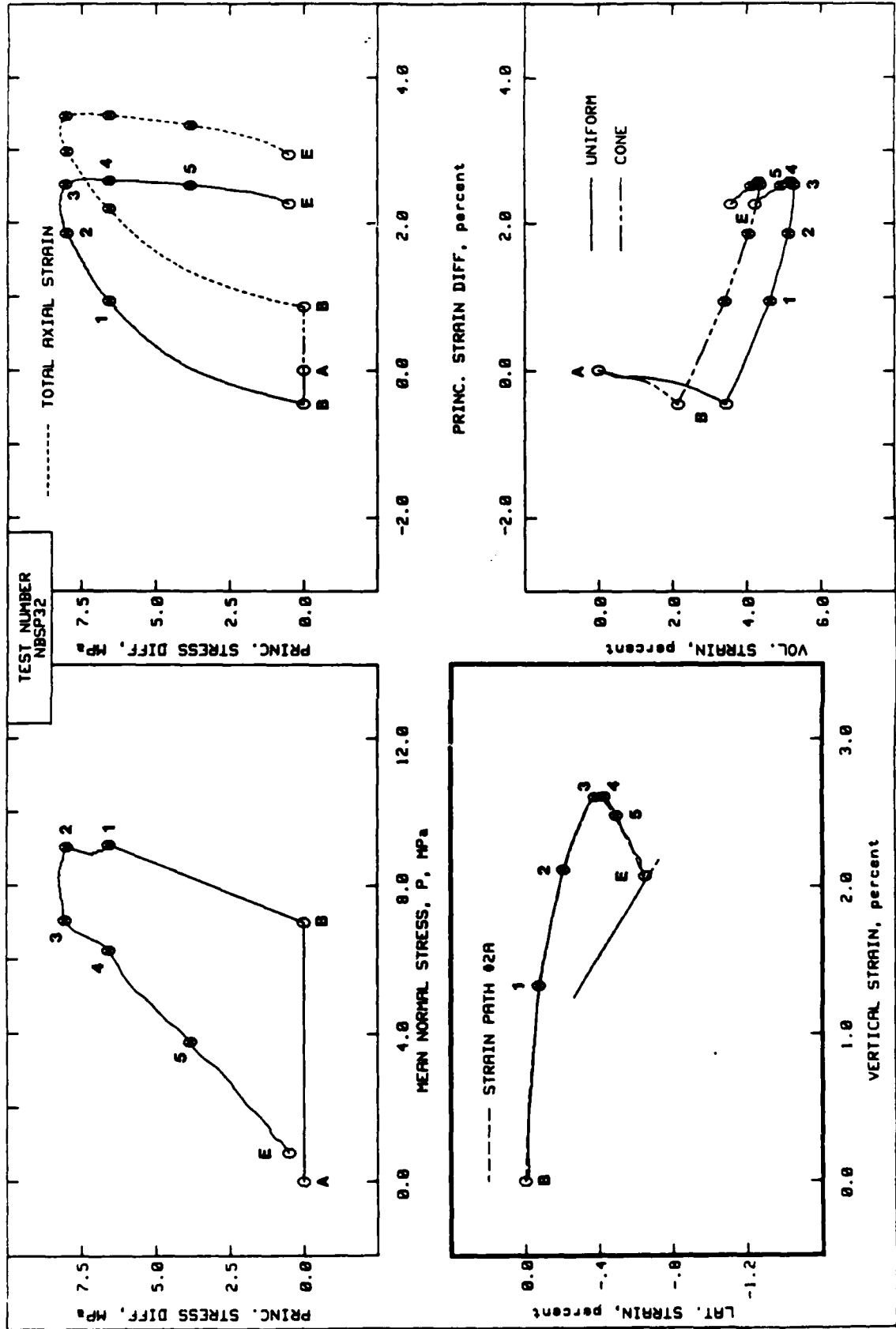
NELLIS BASELINE SAND



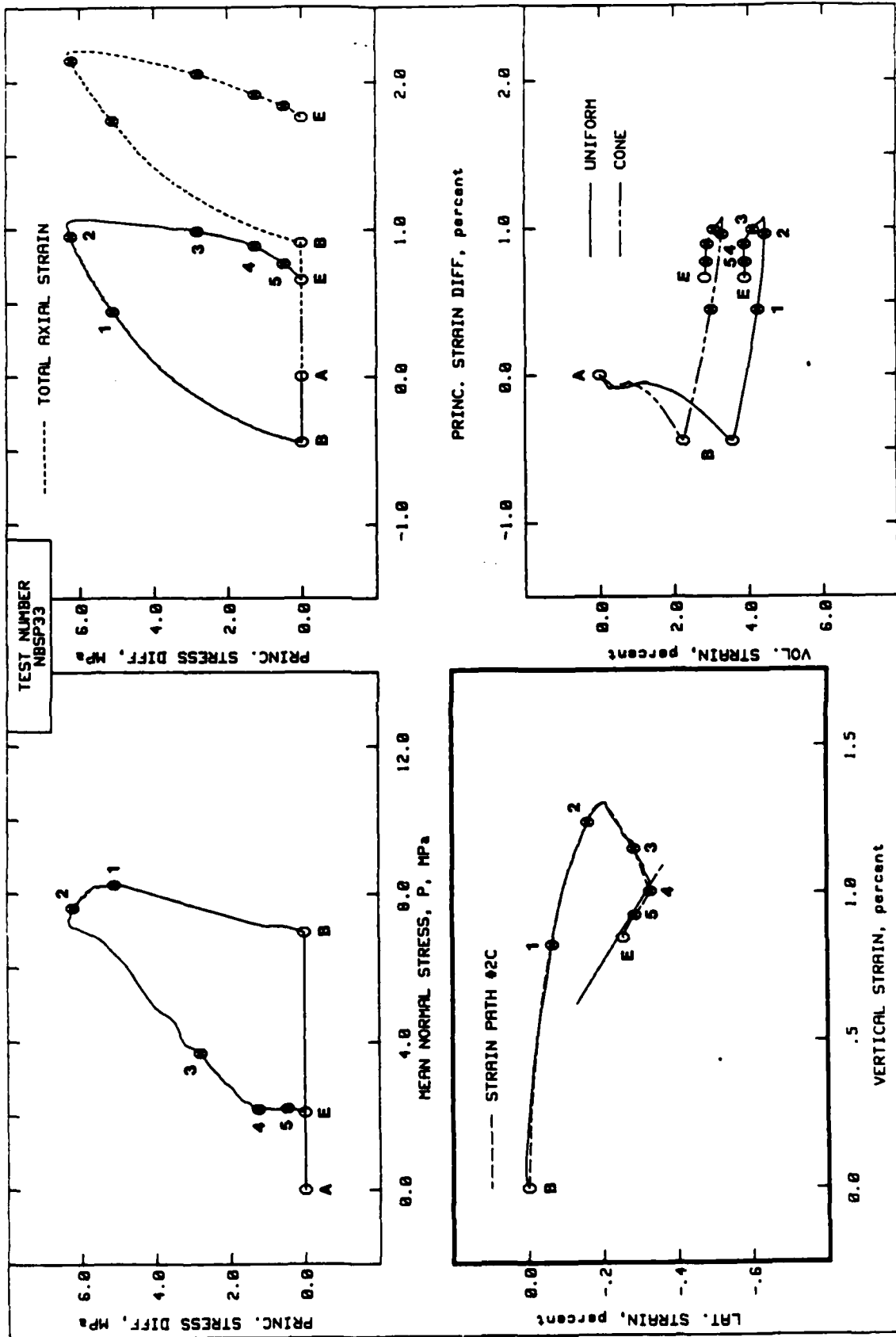
NELLIS BASELINE SAND



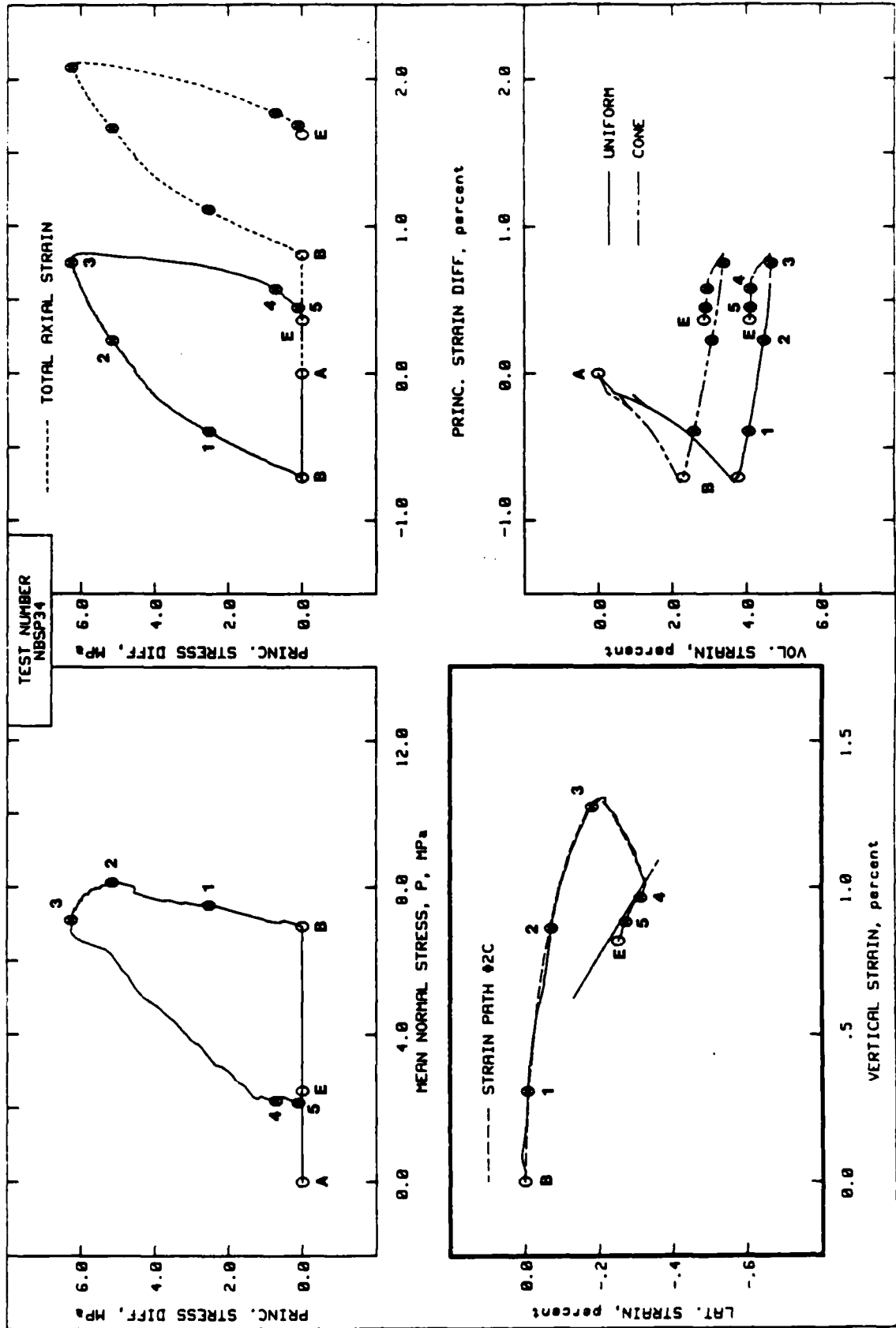
NELLIS BASELINE SAND



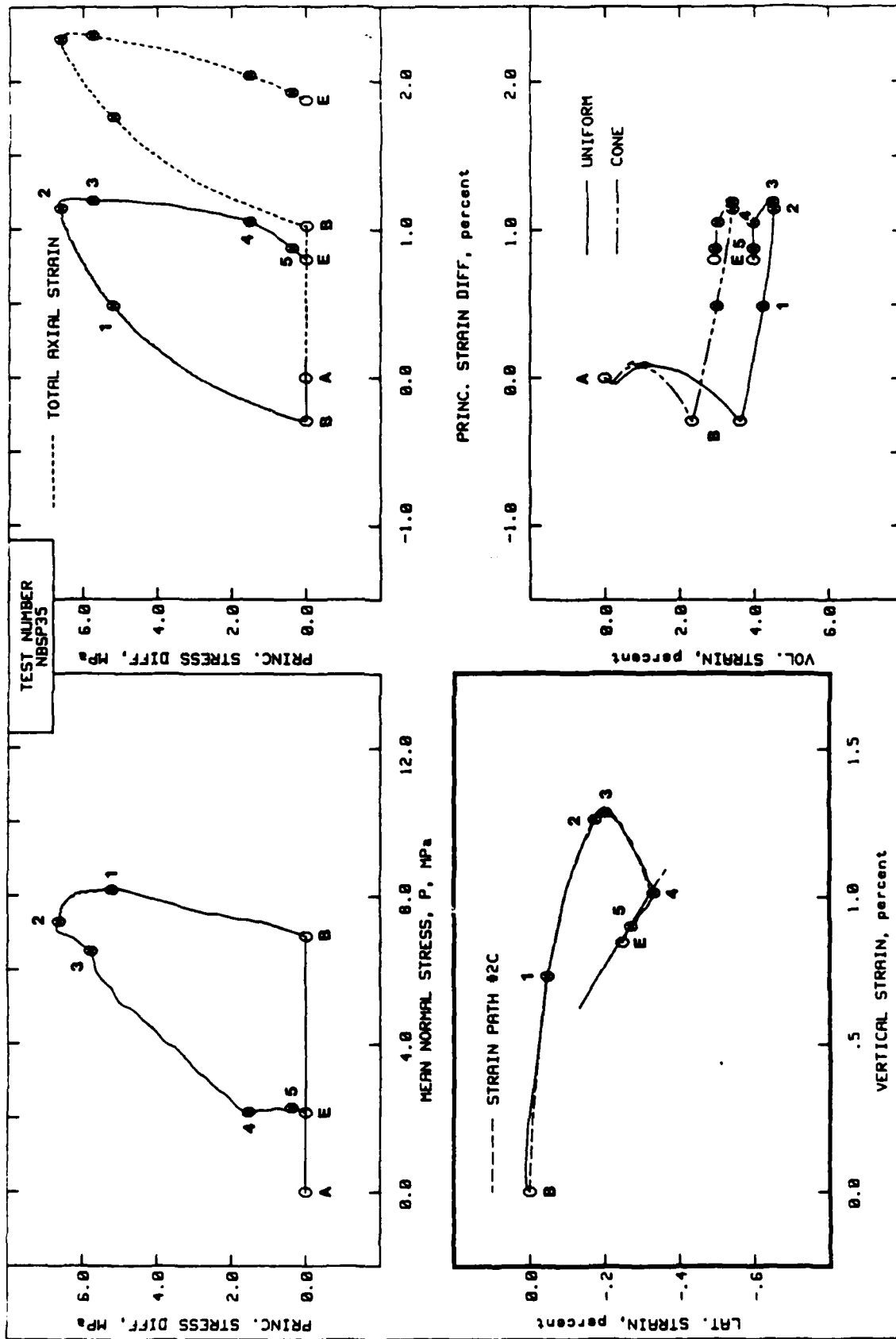
NELLIS BASELINE SAND



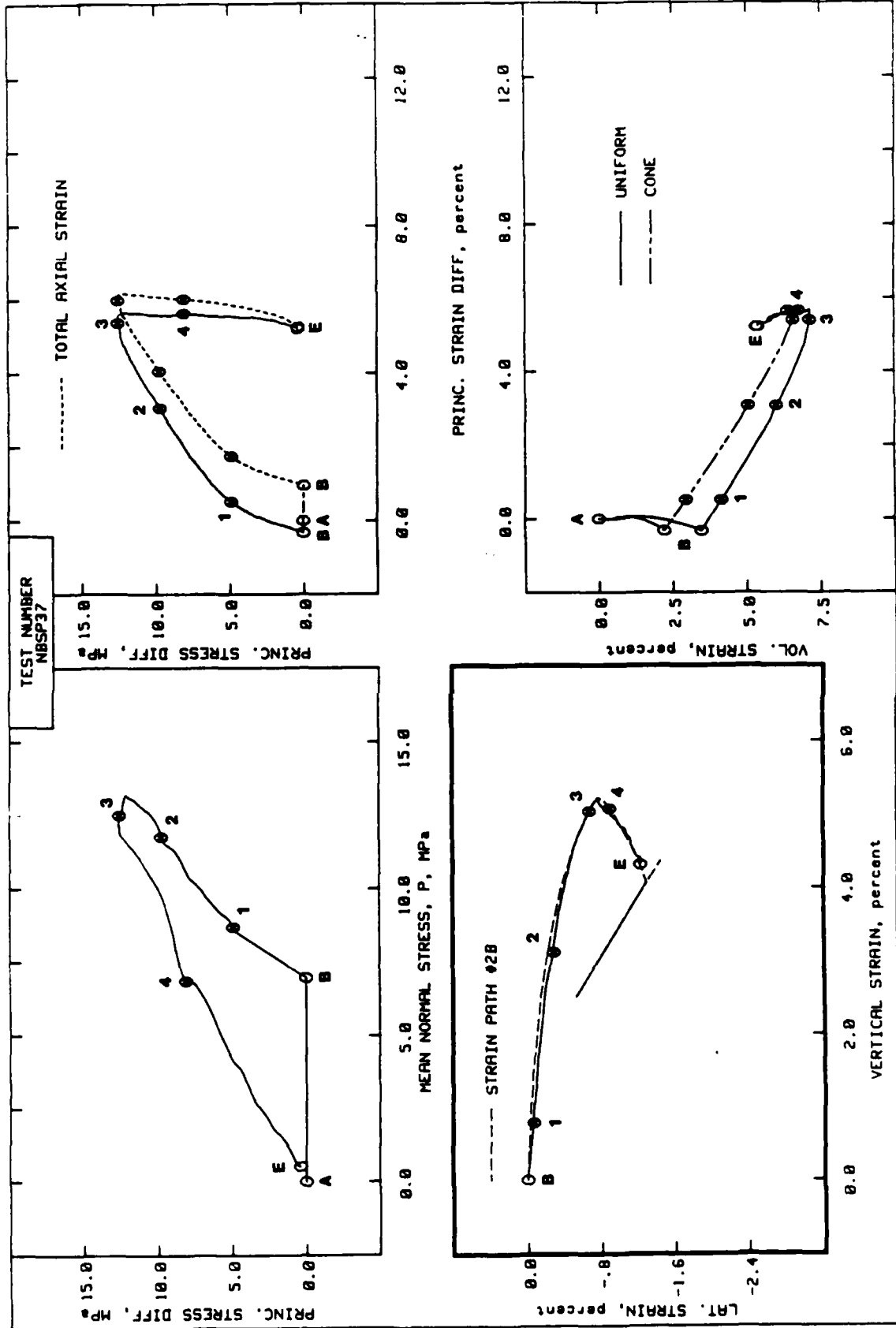
NELLIS BASELINE SAND



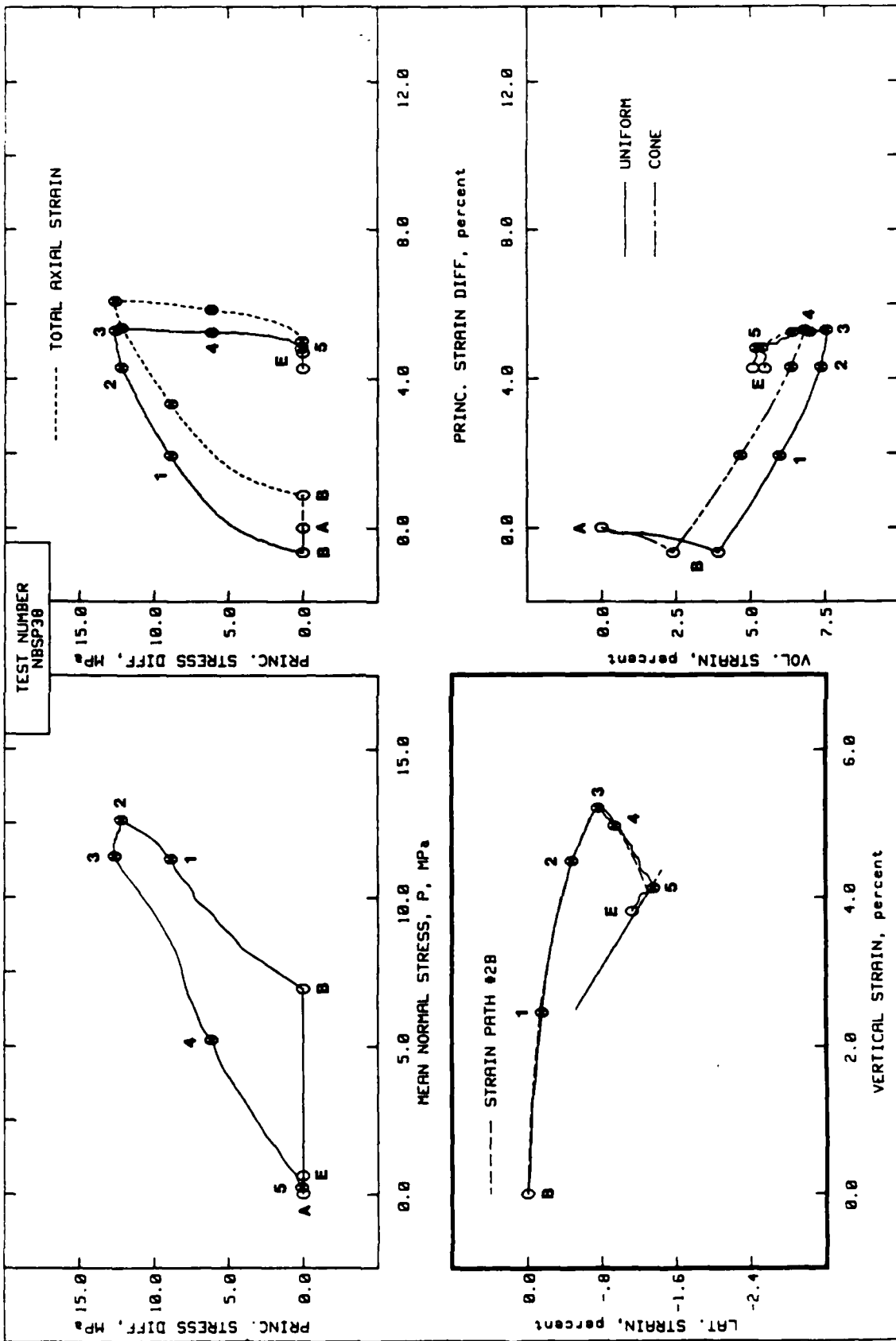
NELLIS BASELINE SAND



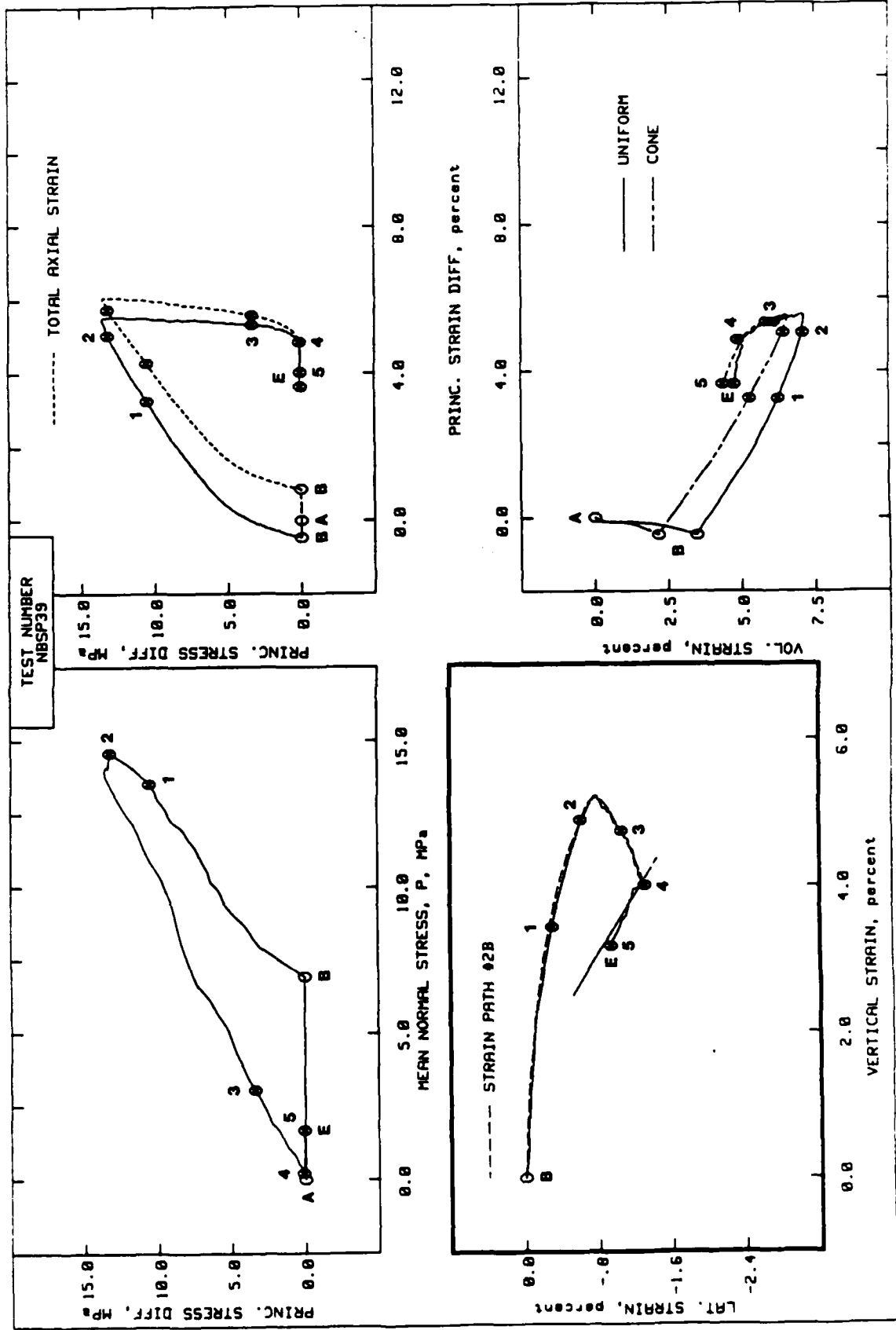
NELLIS BASELINE SAND



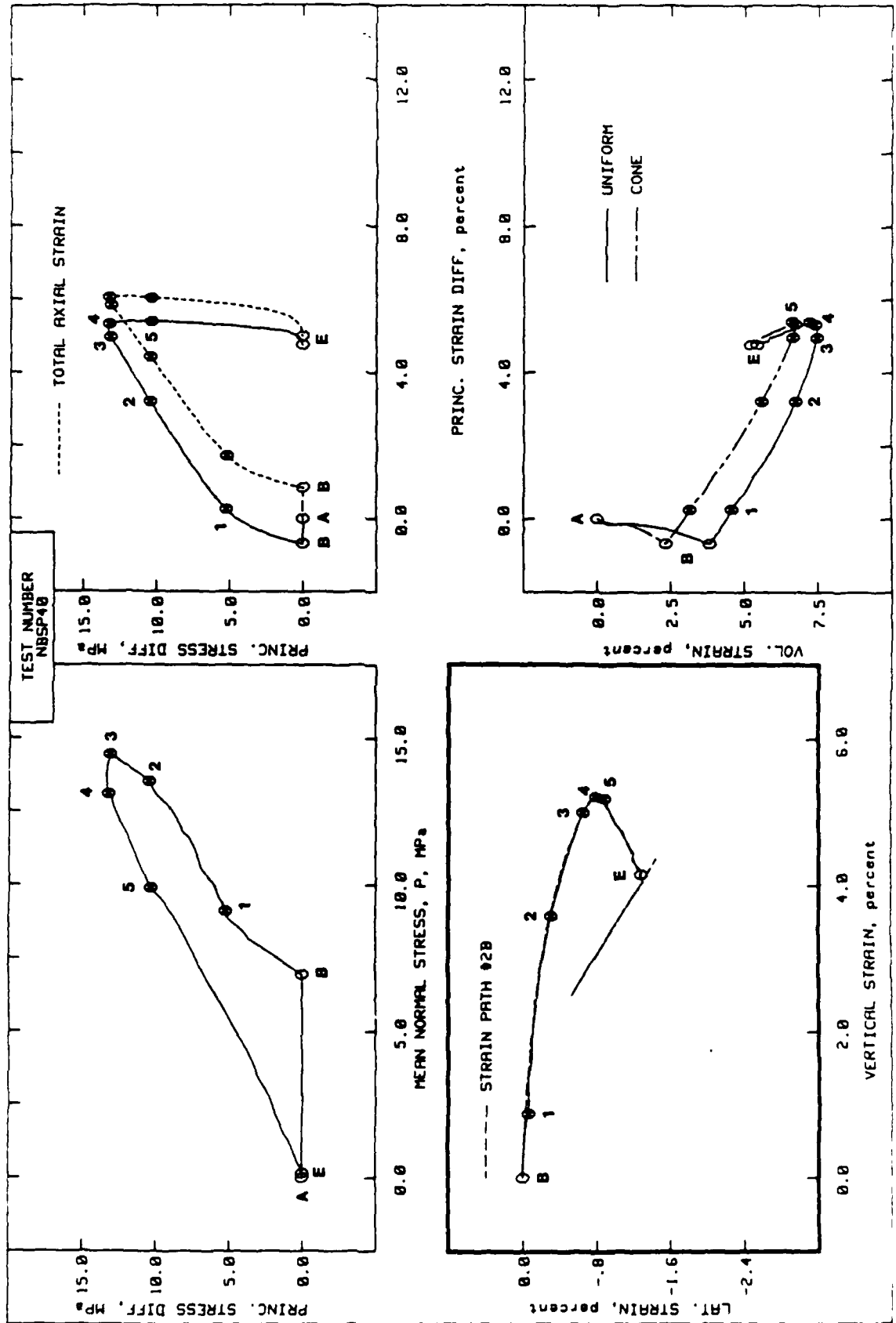
NELLIS BASELINE SAND



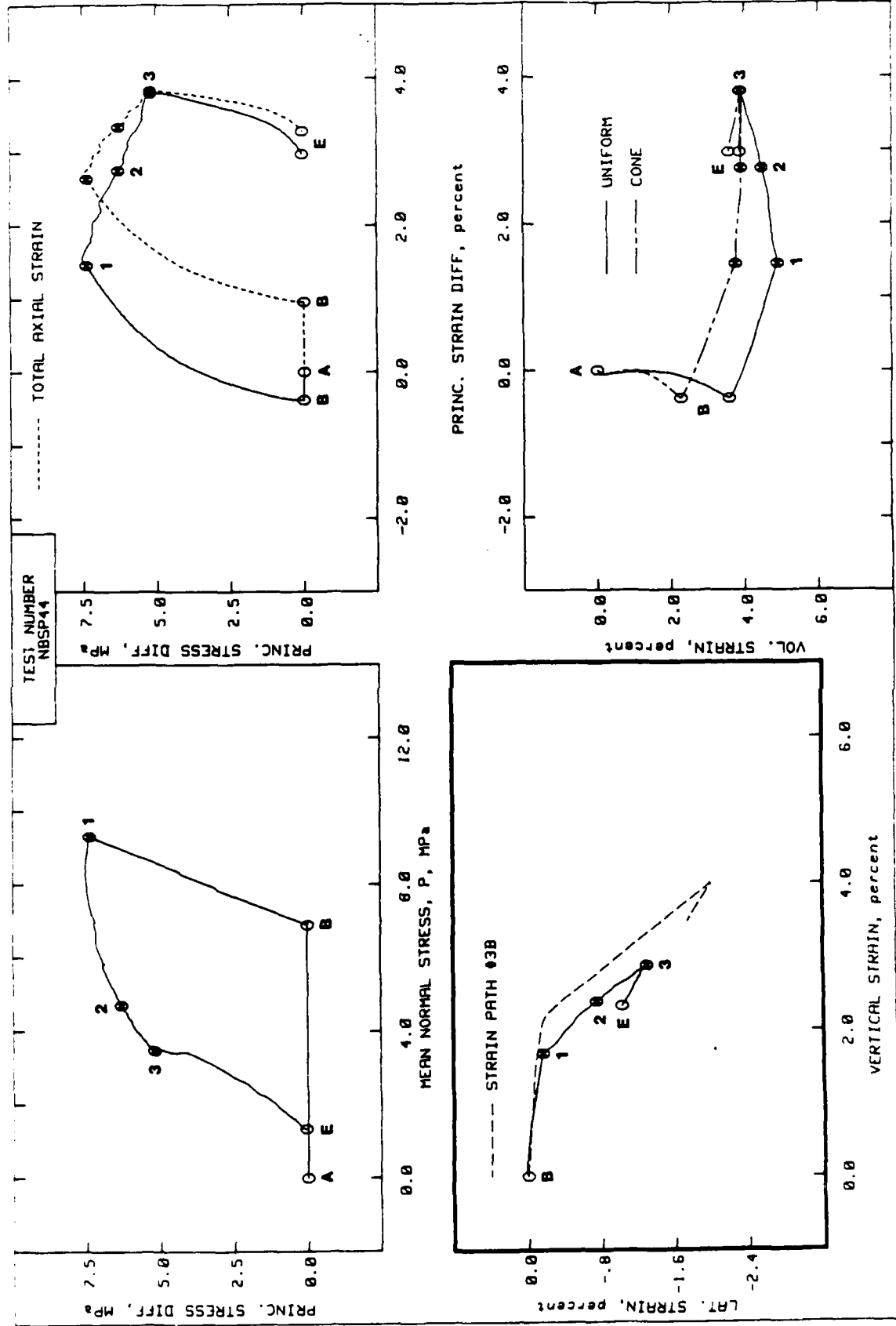
NELLIS BASELINE SAND



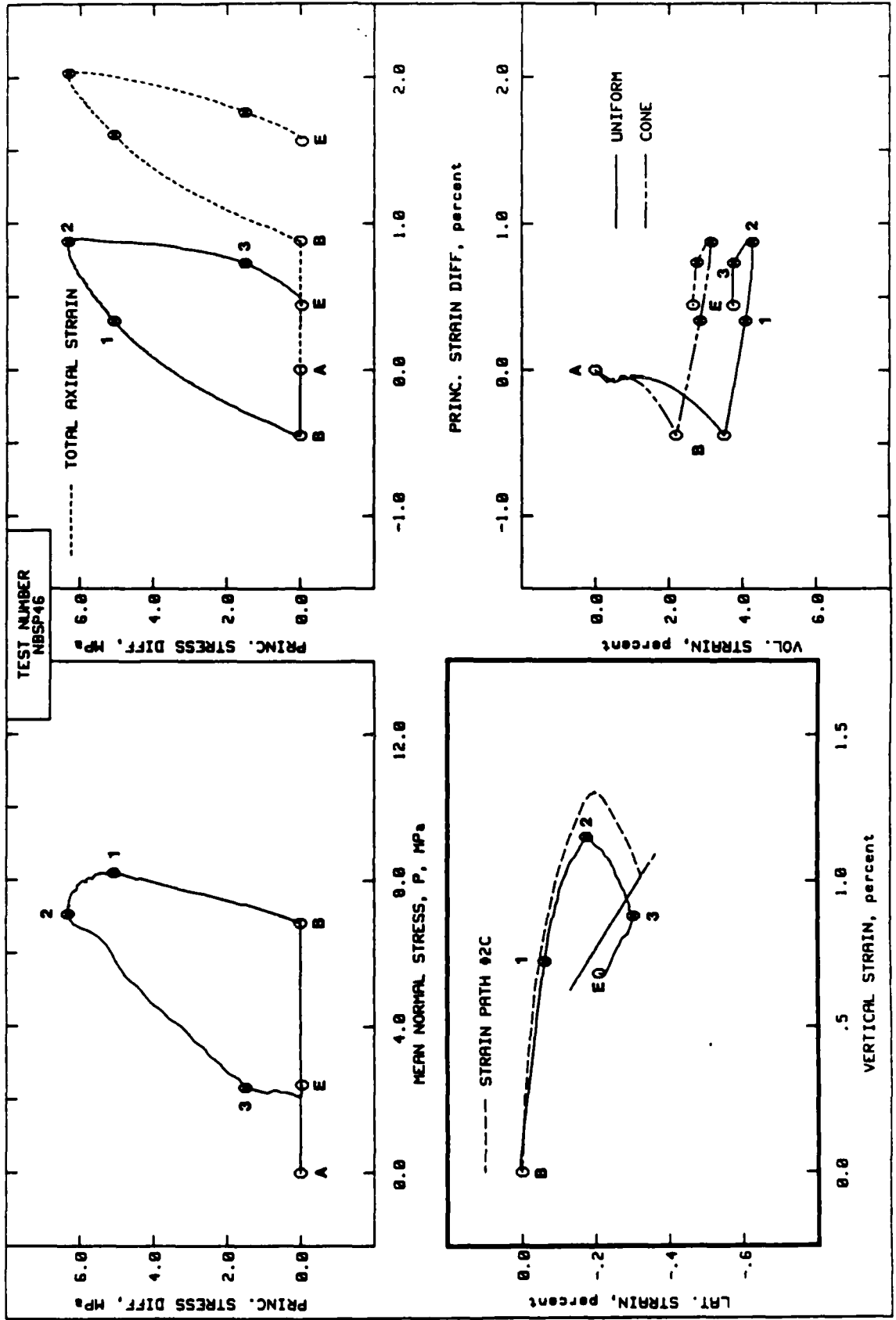
NELLIS BASELINE SAND



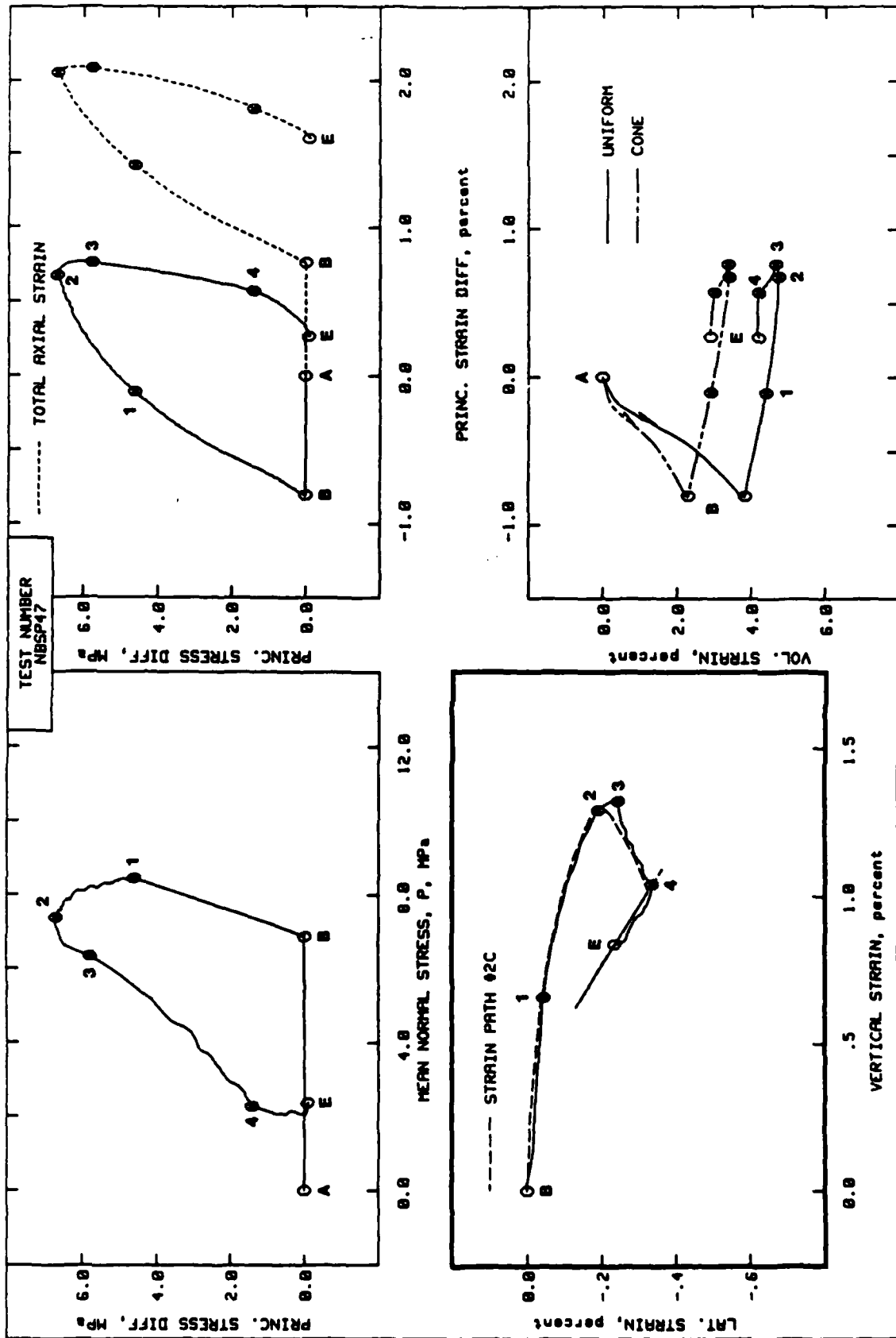
NELLIS BASELINE SAND



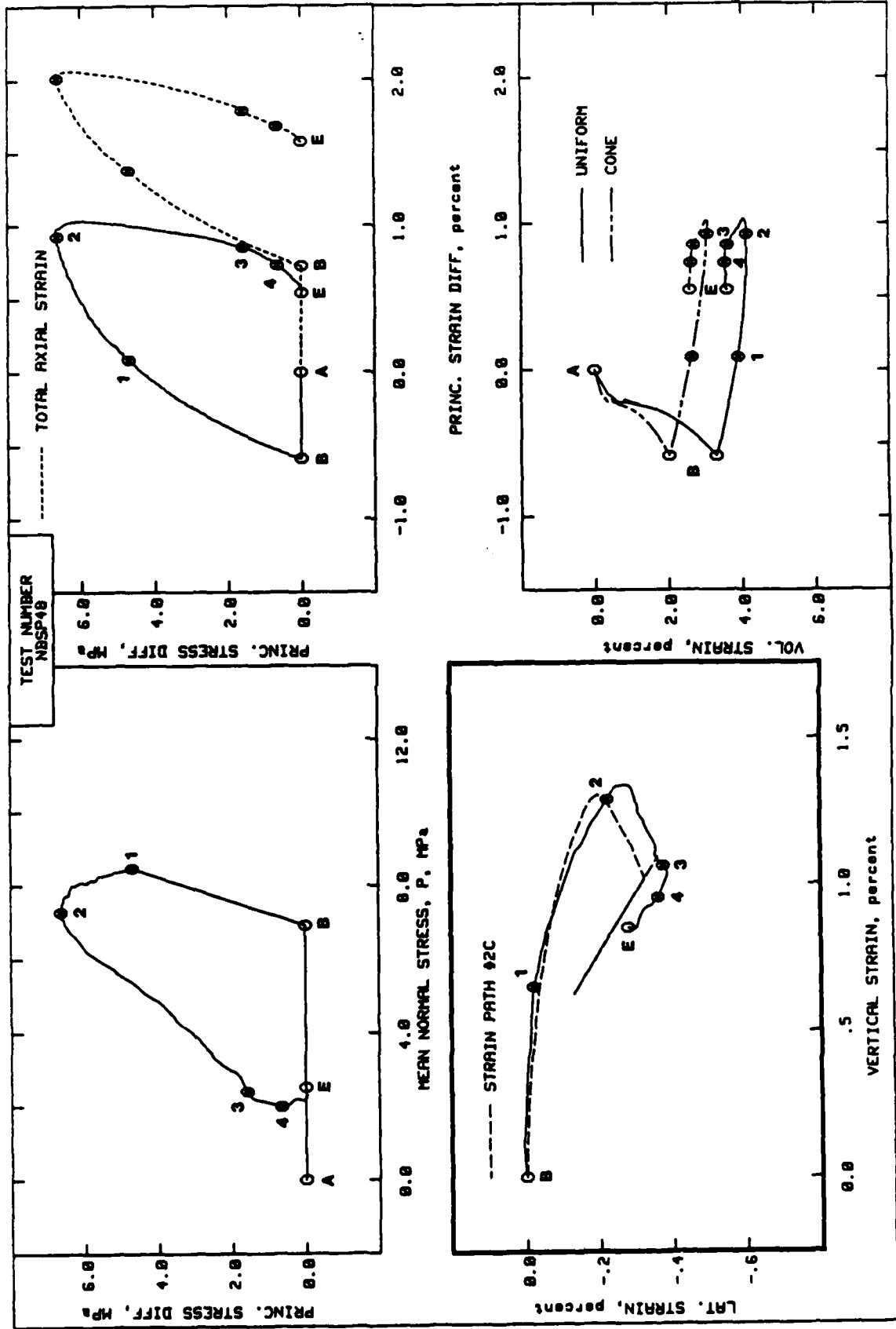
NELLIS BASELINE SAND



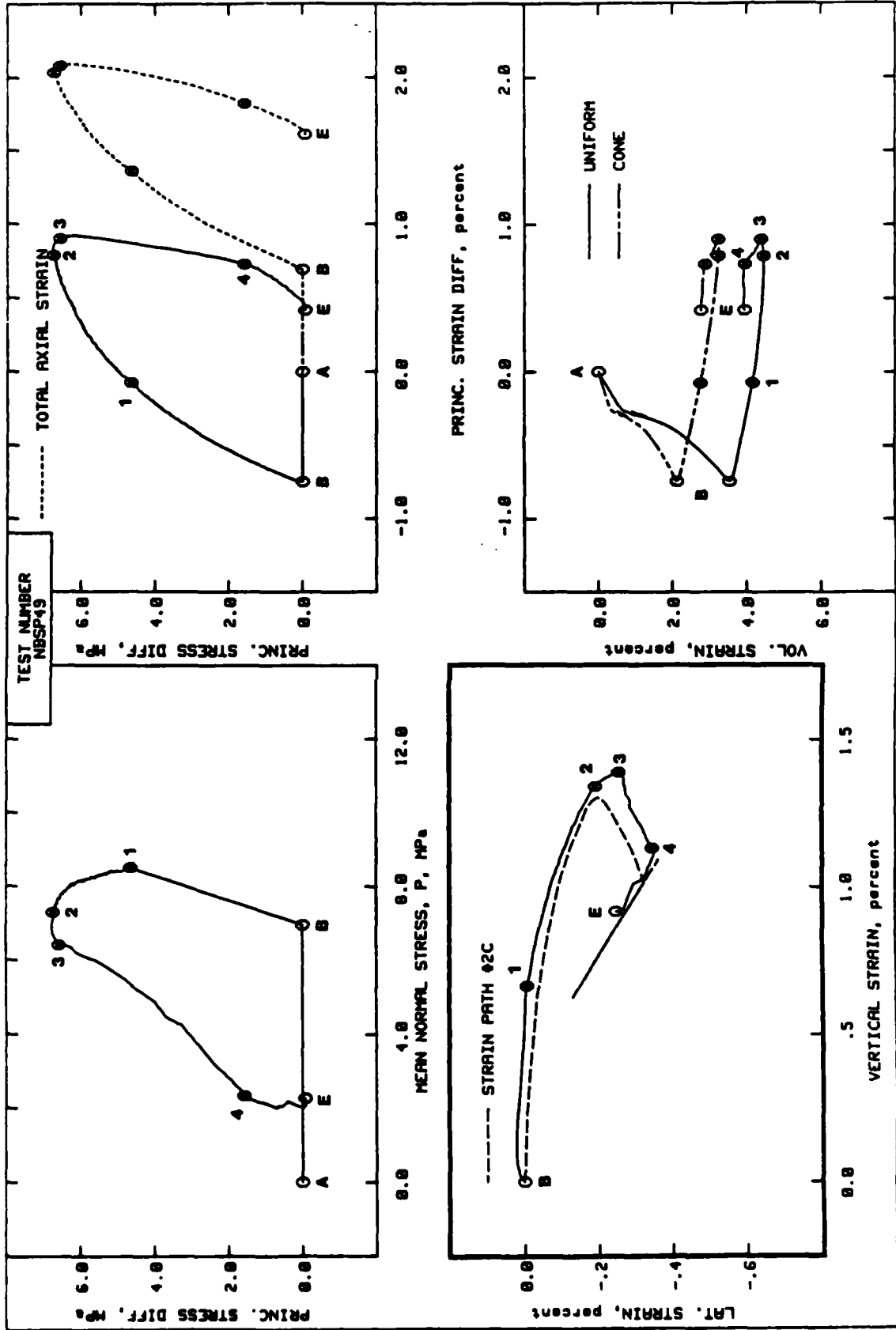
NELLIS BASELINE SAND



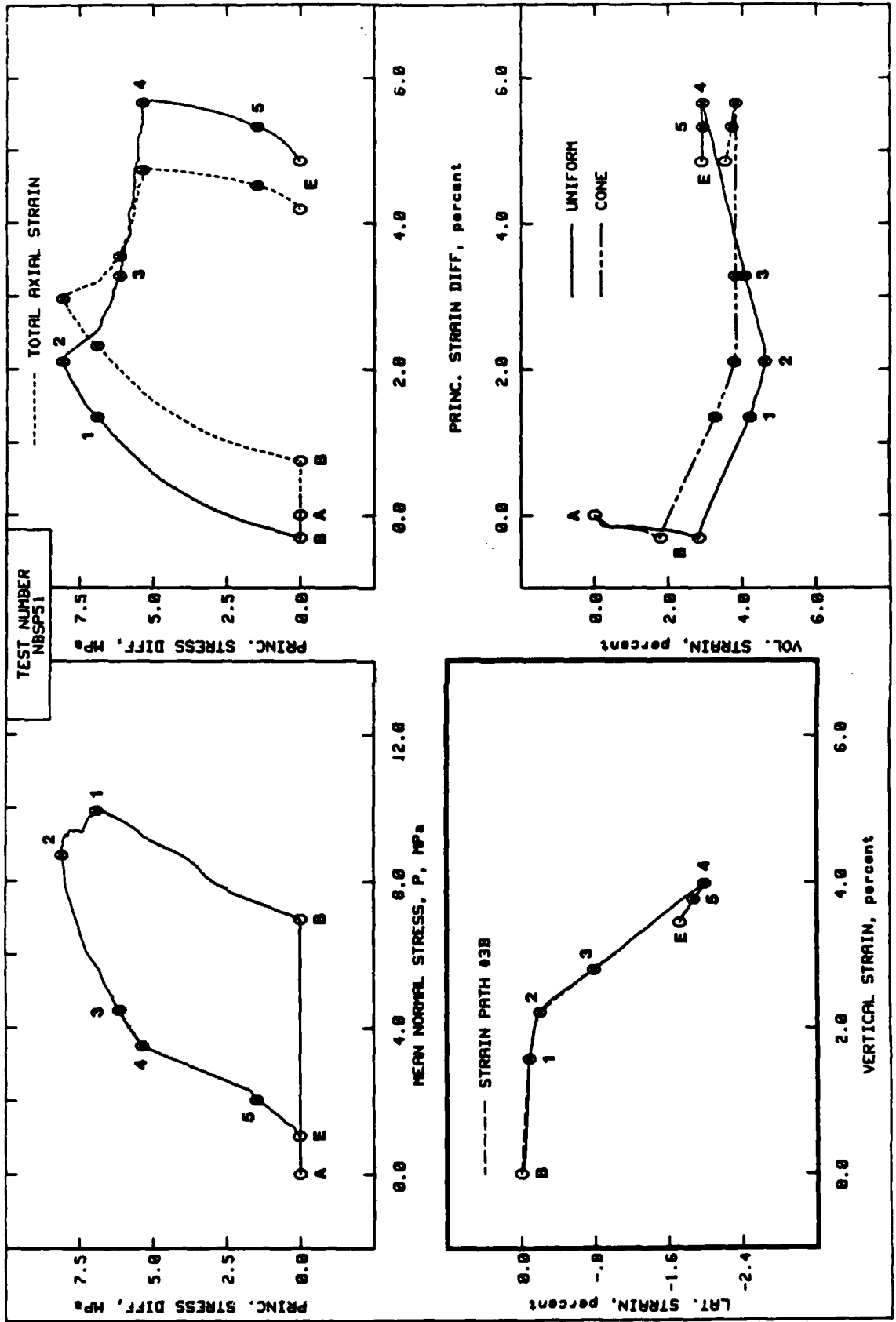
NELLIS BASELINE SAND



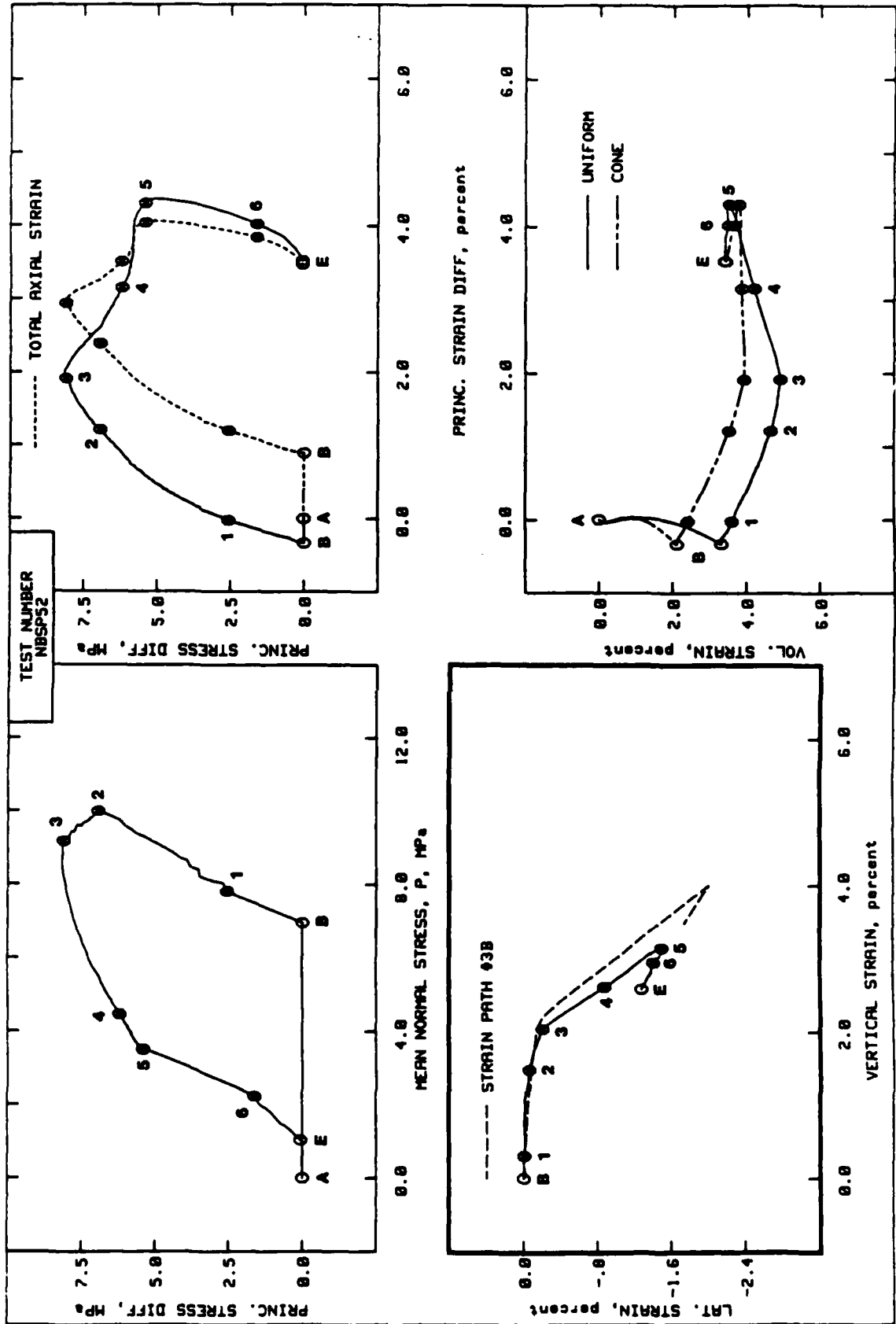
NELLIS BASELINE SAND



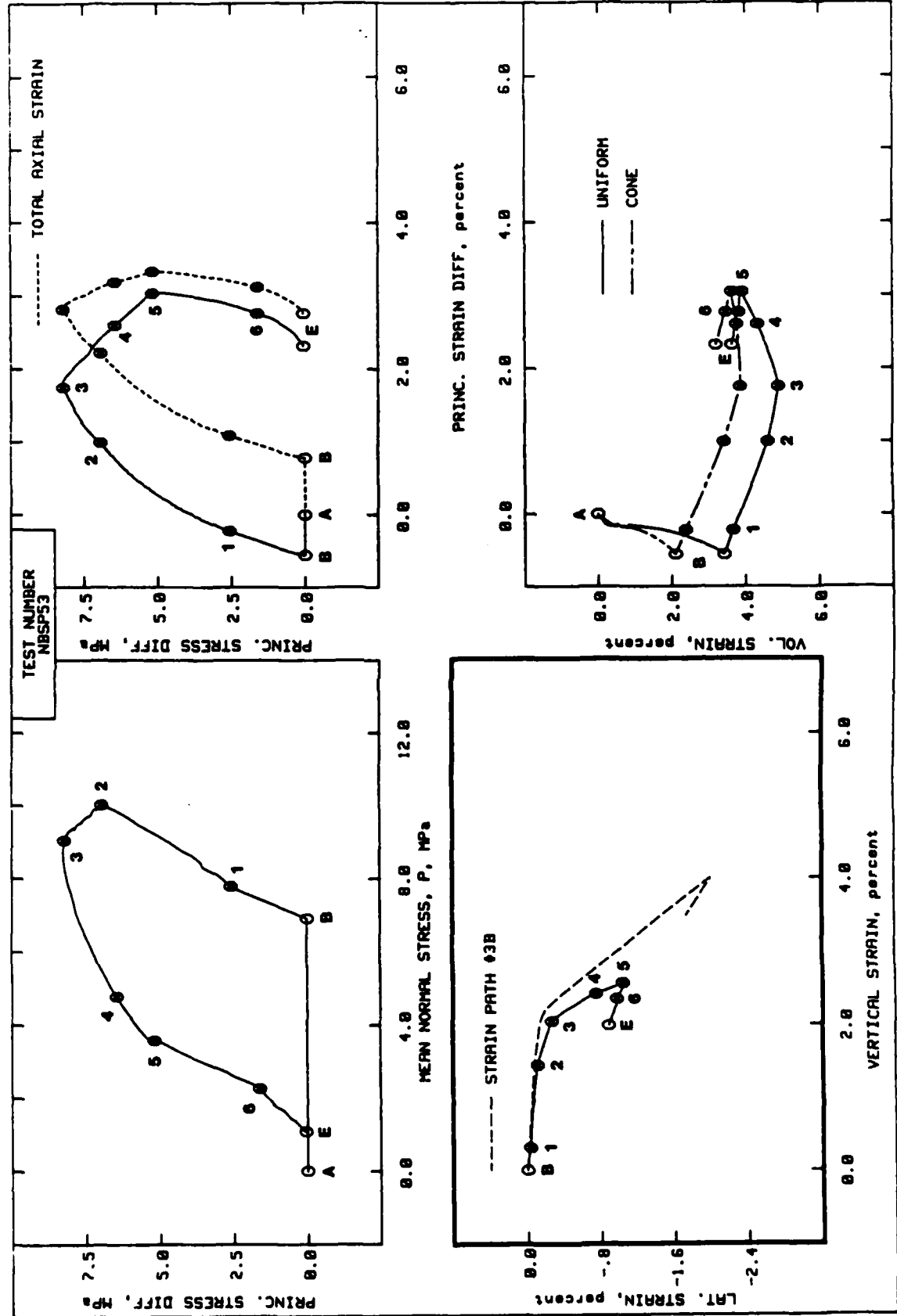
NELLIS BASELINE SAND



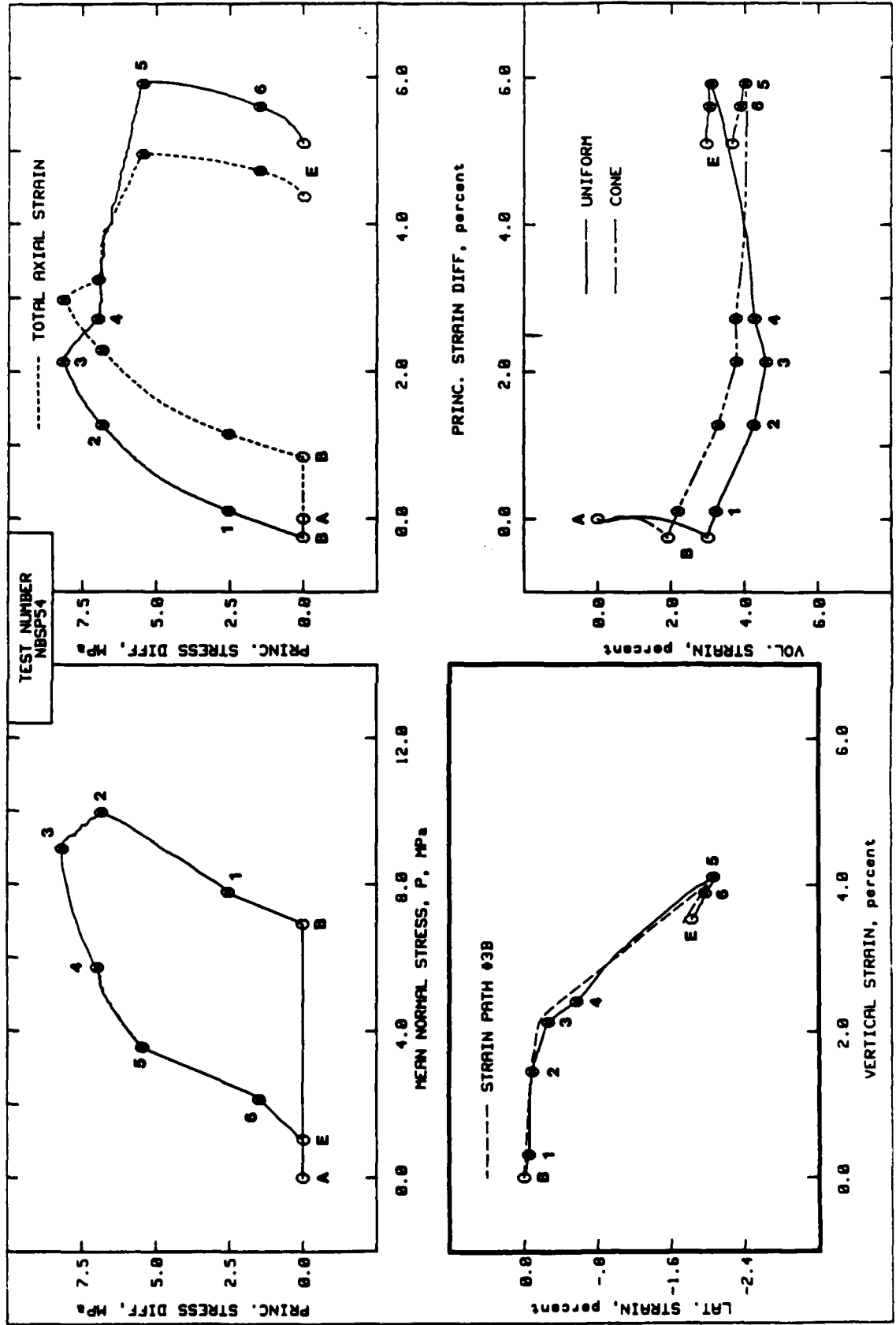
NELLIS BASELINE SAND



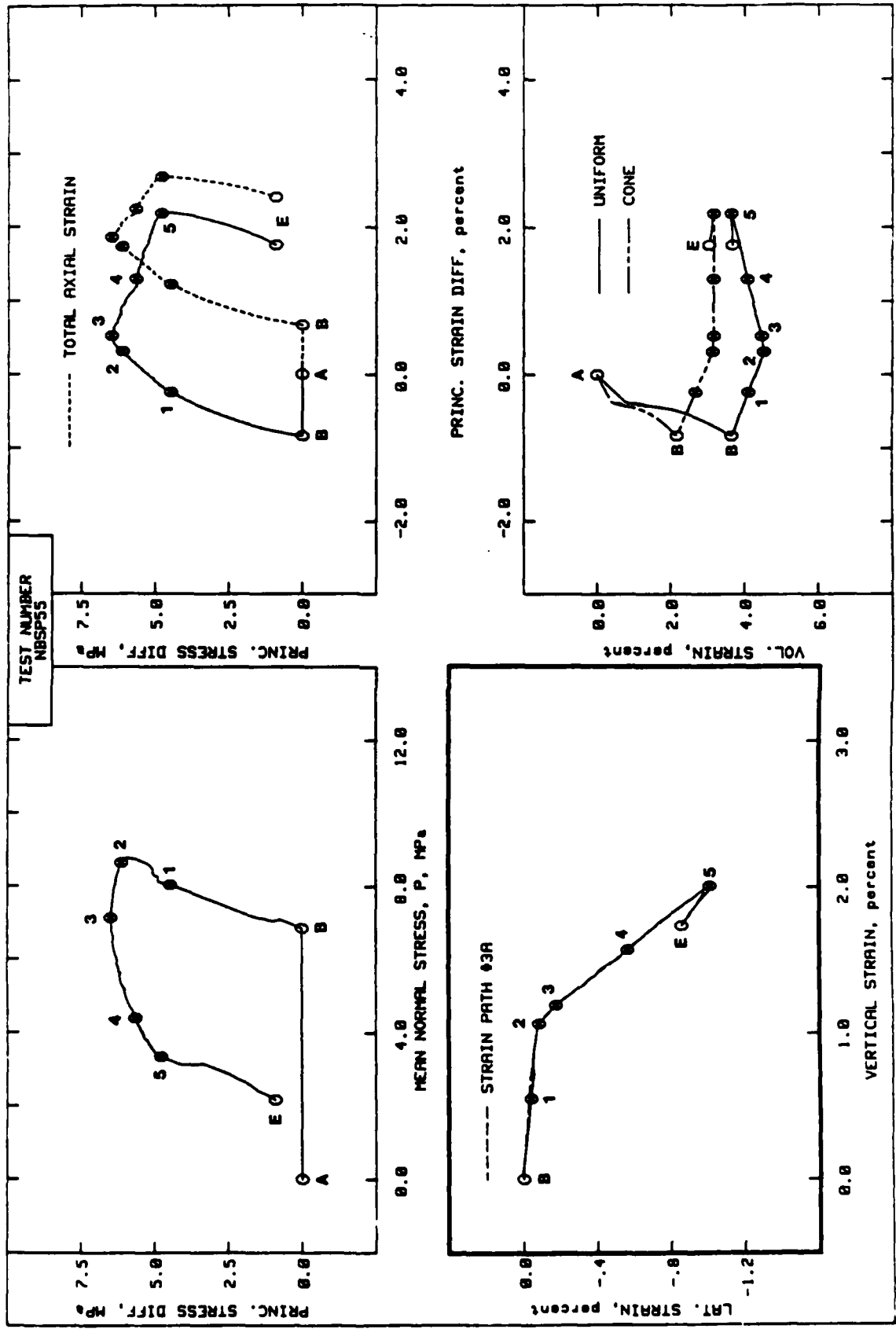
NELLIS BASELINE SAND



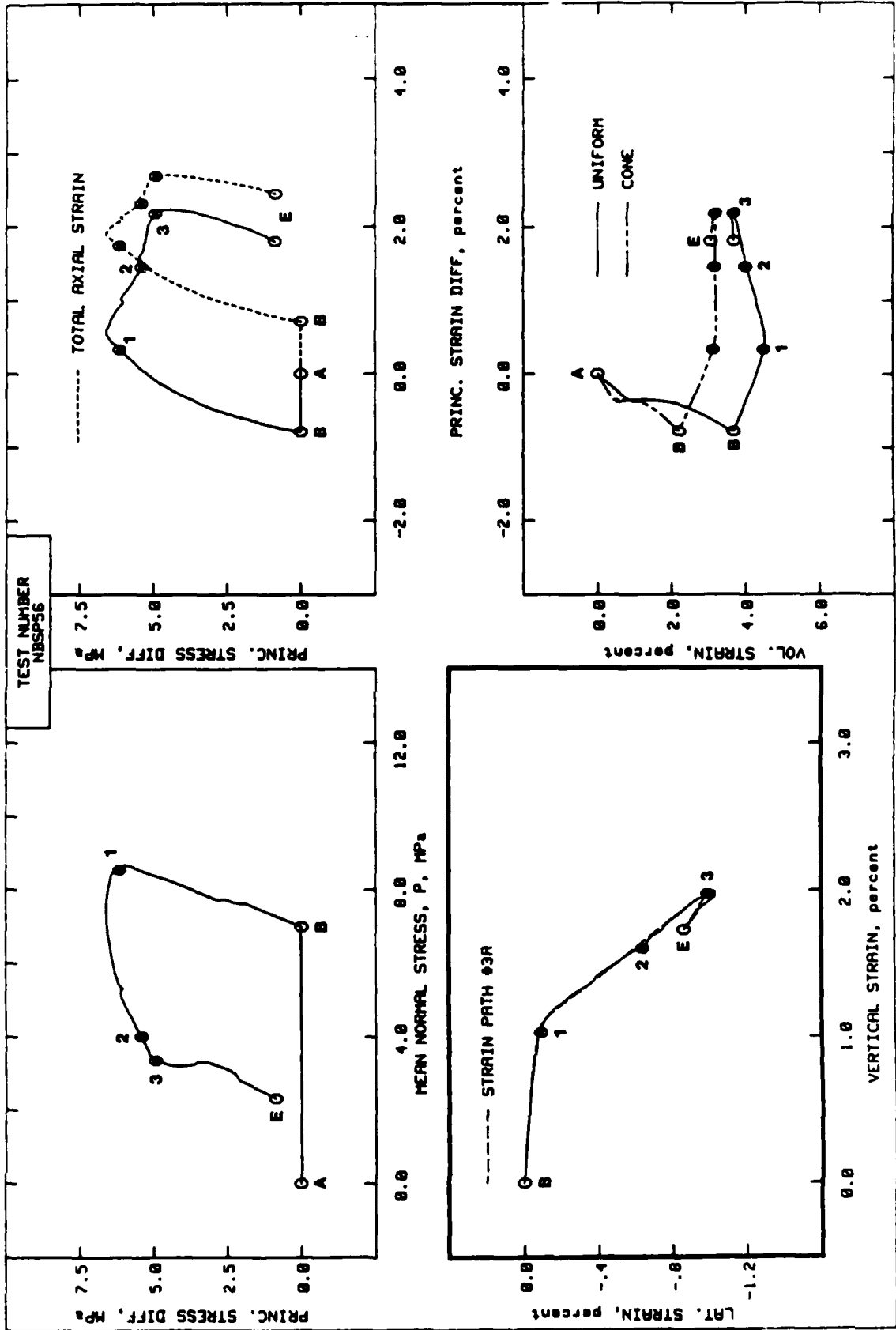
NELLIS BASELINE SAND



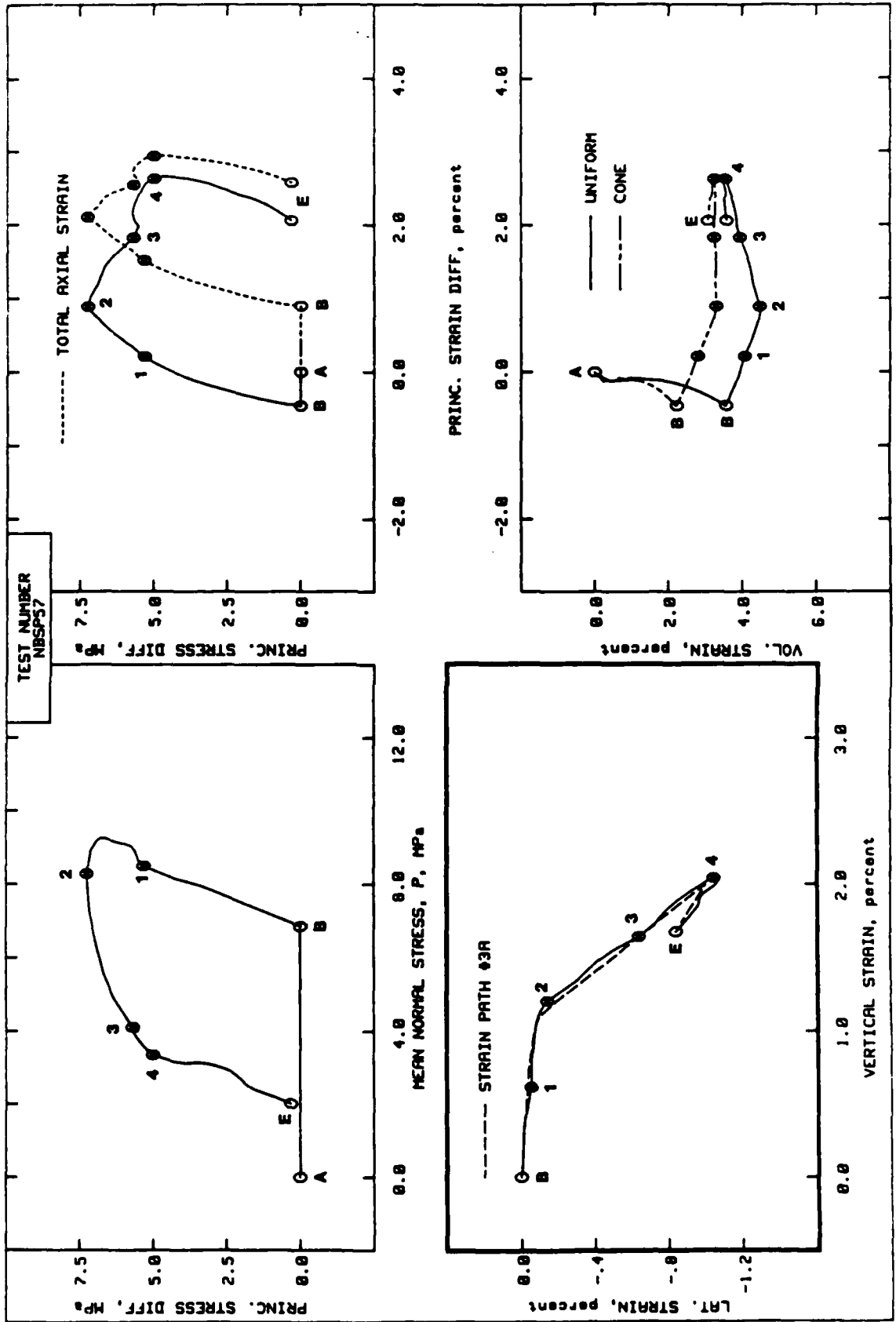
NELLIS BASELINE SAND



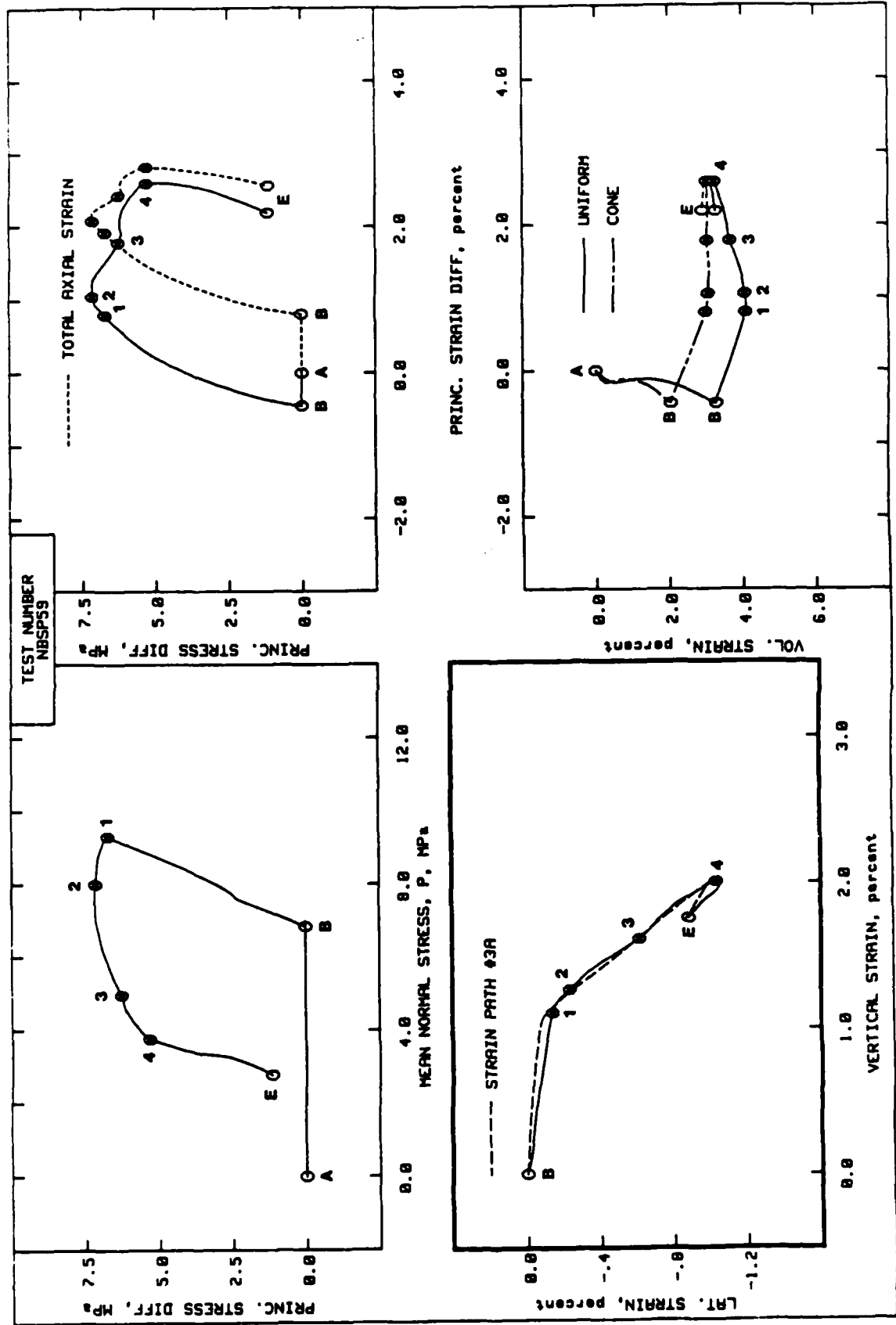
NELLIS BASELINE SAND



NELLIS BASELINE SAND



NELLIS BASELINE SAND



NELLIS BASELINE SAND

